

# The Institute of Paper Chemistry

Appleton, Wisconsin

## Doctor's Dissertation

**The Vapor Phase Adsorption of  
Decanoic Acid on Cellulose**

**F. Joseph Ehrhardt, Jr.**

**June, 1984**

## TABLE OF CONTENTS

	Page
ABSTRACT	1
INTRODUCTION	3
BACKGROUND OF THE THESIS PROBLEM	5
The Solid Surface	5
The Solid-Gas Interface	6
Classification of Isotherms	8
Thermodynamics of Adsorption	10
BET Theory	14
Two-dimensional Condensation	18
Fatty Acid Adsorption	23
Adsorption from Solution - Radiotracer Work	25
Adsorption from Solution - Infrared Work	27
Adsorption from the Vapor Phase	29
Summary	30
Fatty Acid Adsorption on Cellulose	31
Adsorption of Other Organics on Cellulose	33
Effect of Relative Humidity on Fatty Acid Adsorption	35
PRESENTATION OF THE PROBLEM AND THESIS OBJECTIVES	38
EXPERIMENTAL APPROACH	39
EXPERIMENTAL APPARATUS, MATERIALS AND PROCEDURE	41
Experimental Apparatus	41
Pumping System	41
Manifold Section	42
Oven Chamber	42
Cahn Electromagnetic Balance	45

Calibration of the Balance	47
Adsorbent	47
Preparation	47
Surface Area	49
Adsorbate	52
Purity	52
Variation of Adsorbate Pressure	52
Vapor Pressure	54
Adsorption	55
EXPERIMENTAL RESULTS	58
Preliminary Work	58
Effect of Impurities (Blank Runs)	58
Adsorption on the Balance	59
Effect of Heat and Vacuum on Cellulose	60
Effect of Water on Chemisorption	63
Adsorption Data	66
DISCUSSION OF RESULTS	70
Isotherm Analysis	70
Adsorption Isotherms - Qualitative Information	70
Thermodynamics of the Adsorption Process	74
Heat of Adsorption	74
Entropy of Adsorption	79
Two-dimensional Condensation	82
Orientation of Acid on Cellulose Surface	83
BET Analysis	84
Film Pressure - Area Analysis	88
Conclusions on Adsorbed Acid Orientation	90

Adsorbed Acid Mobility	92
Characteristic Adsorption Curves	92
SUMMARY OF CONCLUSIONS	96
SUGGESTIONS FOR FUTURE RESEARCH	98
NOMENCLATURE	99
ACKNOWLEDGMENTS	101
LITERATURE CITED	102
APPENDIX I. ESTIMATION OF THE MEAN FREE PATH OF DECANOIC ACID AT PRESSURES USED DURING ADSORPTION EXPERIMENTS	107
APPENDIX II. DECANOIC ACID MONOMER/DIMER EQUILIBRIUM IN VAPOR PHASE	109
APPENDIX III. DECANOIC ACID MOLECULAR AREA	110
APPENDIX IV. COMPUTER PROGRAM BET	111

## ABSTRACT

It is known that fatty acids can physically adsorb on the surface of cellulose from the vapor phase and chemically react with the cellulose hydroxyl groups through an esterification reaction. The higher molecular weight fatty acids are then a very efficient sizing agent. The objective of this study was to investigate the physical adsorption process which precedes this chemical reaction.

The adsorption data were collected by gravimetrically determining the quantity of acid adsorbed on cellulose at different acid pressures. Whatman No. 40 filter paper, an ashless cotton cellulose was used as the adsorbent. Decanoic acid was the adsorbate selected as a model compound for the fatty acids. The adsorption experiments were performed over a temperature range of 70 to 80°C in the absence of water. Under these conditions, decanoic acid would physically adsorb on the cellulose surface but chemisorption was inhibited.

BET analysis and film-pressure/area curves showed that decanoic acid adsorbs on cellulose with its major axis parallel to the surface. This conclusion supports previous work which found that physically adsorbed acid does not participate in sizing. The orientation of the fatty acid suggests that the interaction of the acid carboxyl group with the cellulose surface is not strong enough to overcome the van der Waals interaction of the fatty acid tails with the surface and other adsorbed acid molecules.

A thermodynamic analysis of the adsorption process in the submonolayer region showed a distinct variation in the isosteric heat and differential entropy of adsorption as a function of surface coverage. At all acid pressures used in this investigation, decanoic acid exists primarily as a monomer in the vapor phase and thus adsorbs as a monomer. Interpretation of the heat and entropy of adsorption as a function of surface coverage indicated that up to approximately

0.7 monolayers the acid exists on the surface as a monomer or in some monomer/dimer equilibrium. At the lowest coverages, the heat of adsorption suggests that hydrogen bonding with the cellulose is possible. When the fractional coverage approaches 0.7, two-dimensional condensation begins in discrete patches across the cellulose surface. This is exhibited by an increase in the heat of adsorption. Two-dimensional condensation releases energy primarily due to the acid dimerization ( $\sim 7$  kcal/mol). Increased lateral interaction of the hydrocarbon tails is also probable. The differential entropy decreases at the onset of two-dimensional condensation. The decline in differential entropy is primarily due to a decrease in the number of particles on the surface when dimerization occurs. At monolayer completion, the heat and entropy of adsorption indicate that the adsorbed fatty acid is highly dimerized. The thermodynamic properties of the adsorbed phase can then be approximated by those of liquid decanoic acid.

## INTRODUCTION

Paper, a cellulose product, if left untreated is very hydrophilic. In some paper products, such as tissue, this natural hydrophilicity is a desired property, while in others, such as writing paper, a certain amount of hydrophobicity (sizing) is needed in the final product.

The hydrophilic nature of cellulose results from hydroxyl groups on the cellulose surface. When paper is sized, its surface free energy is reduced by adsorbing a hydrophobic sizing agent which blocks these hydroxyl groups. Two widely used methods of sizing paper are internal sizing and surface sizing. With internal sizing, the sizing material is added to the pulp slurry prior to sheet formation and cellulose fibers throughout the sheet are sized. Surface sizing involves applying size after the sheet has been formed and only sizes the surface of the sheet.

Theoretically, less than a monolayer of sizing agent is needed to highly size a sheet of paper. Both of the primary methods of sizing use considerably more size than is necessary. Also, chemical losses to effluent are incurred in the sizing processes. An alternative method of sizing would be to adsorb the sizing agent from the vapor phase. Using this method, only a monolayer of size need be adsorbed on the paper surface and the paper could be highly sized throughout the sheet.

Fatty acids could be used as inexpensive sizing agents in a vapor phase sizing process. The fatty acids are capable of lowering the surface energy of cellulose through esterification with the cellulose hydroxyl groups. Once esterified, the fatty acid is firmly anchored to the cellulose surface and the long hydrocarbon tail lowers the cellulose surface energy. A difficulty with

this process is that the esterification reaction appears to be very slow. Further investigation into the adsorption process of fatty acids on cellulose could lead to methods of increasing the esterification reaction rate. Vapor phase sizing might then be a very feasible and desirable method of sizing paper.

Sizing of the cellulose is to be avoided when absorbency is a needed property in the final paper product. A problem encountered in the manufacture of some absorbent paper products is a gradual loss of absorbency as the product ages. Corrugated board manufacturers also encounter this problem which causes adhesion difficulties during the corrugating operation. This phenomenon, called self-sizing, is believed to be caused by the vapor phase distribution of resinous and fatty acid materials from colloidal extractive particles within the sheet to the paper surface. Presumably, a small fraction of this material, which chemically bonds to the fiber surface, is responsible for the sizing. Clarifying the mechanism of this vapor-phase adsorption process may lead to steps in the direction of inhibiting self-sizing.

Understanding the adsorption process of fatty acids on cellulose is of value whether inhibition or development of sizing is the area of interest. Based on this need for further investigation of the fatty acid adsorption process, this work is a study, on a fundamental level, of the physical adsorption process of decanoic acid on cellulose.

## BACKGROUND OF THE THESIS PROBLEM

The following background material is presented as a review of some of the fundamental aspects of adsorption phenomena. A section on adsorption thermodynamics defines the isosteric heat and differential entropy of adsorption. These thermodynamic quantities are later used when analyzing decanoic acid adsorption data. The BET and Hill equations, which interpret adsorption as localized and mobile, respectively, are discussed. These equations are used in the interpretation of decanoic acid adsorption isotherms. Finally, a review of the literature pertinent to fatty acid adsorption and adsorption on cellulose is presented.

### THE SOLID SURFACE

Unlike an atom within the body of a solid which is exposed to equal forces in all directions, an atom in the plane of a solid surface is subject to an unbalanced inward attraction. Therefore, analogous to a liquid, a solid has surface tension which tends to decrease the solid surface area. The surface tension in solids is much higher than that in liquids, since the inward attraction on a solid surface is much greater than that on a liquid surface.

The surface of a solid is not physically homogeneous. The solid surface is extremely rough, since the surface particles are essentially immobile. This surface roughness is one reason for the significant physical heterogeneity evidenced on solid surfaces (1). Other causes of physical heterogeneity could be defects in the crystalline surface structure such as lattice vacancies or the presence of interstitial atoms.

The complexity of solid surfaces is further increased by heterogeneity which may be chemical or induced. Chemical heterogeneity may arise from

impurities adsorbed on the solid surface after the surface is formed or from impurities present during the formation of the solid. Induced heterogeneity results from an adsorbed layer partially covering the surface. Other than the ability of adsorbed molecules to mask surface properties (2), the first molecules adsorbed can affect the energy with which succeeding molecules are adsorbed (3).

Physical and chemical heterogeneity result in a surface which is energetically heterogeneous. The surface has been described as a distribution of energetically homogeneous 'patches' which adsorb independently of each other (4).

#### THE SOLID-GAS INTERFACE

The concentration of gas molecules in the immediate vicinity of a solid surface is found to be greater than the concentration in the bulk gas phase. The process by which this surface excess is formed is known as adsorption. The gas or vapor is called the adsorbate, and the solid the adsorbent.

The molecules which constitute a solid surface are under the influence of unbalanced forces. Any process which can relieve these unbalanced forces will occur spontaneously. A molecule adsorbed by the solid reduces some of this dissymmetry, thereby decreasing the surface tension (surface free energy) of a heterogeneous (solid-gas) system.

The forces involved in the adsorption of gases and vapors by solids may be nonspecific (van der Waals) forces or stronger, specific forces, such as those which are operative in the formation of chemical bonds. The former are responsible for physical adsorption and the latter, for chemisorption. Only physical adsorption is possible after monolayer coverage of the surface since chemisorbed molecules must be in intimate contact with the adsorbent surface.

When adsorption takes place, there is a decrease in entropy due to the restriction of adsorbed gas molecules to two-dimensional motion. Adsorption is a spontaneous process, so there is also a decrease in free energy. Consequently, the thermodynamic relationship

$$\Delta G = \Delta H - T\Delta S$$

indicates that adsorption of gases is always exothermic. The heats of physical adsorption of gases are usually similar to their heats of liquefaction, whereas the heats of chemisorption are generally much greater. For example, the heat of physisorption of nitrogen on an iron surface is ca. -2.4 kcal/mol compared to ca. -36 kcal/mol for chemisorption (5).

Due to surface heterogeneity and interaction between adsorbed molecules, the heat of adsorption will vary with surface coverage (6). Surface heterogeneity implies that the surface has some adsorption sites which are more active than others. Adsorption will occur on the more active sites first, resulting in a high heat of adsorption. As the surface coverage increases, molecules are forced to adsorb on less active sites with lower heats of adsorption. Therefore, the heat of adsorption will decrease with increasing surface coverage due to surface heterogeneity if all other effects are small.

In physical adsorption, adsorbate-adsorbate van der Waals interactions will increase with increasing surface coverage. On an energetically homogeneous surface, this effect will cause an increase in the heat of adsorption with increasing surface coverage. This increase in the heat of adsorption is also noticeable with adsorption on low energy heterogeneous surfaces where the heat of interaction is a significant fraction of the total heat of adsorption.

In chemical adsorption, the attractive van der Waals forces from adsorbate-adsorbate interactions are relatively weak in comparison to chemisorption energies and have little influence on the overall heat of adsorption. In this case, two kinds of repulsion effects may be more important (7). First, if chemisorption sites are very close together, there may be a short range repulsion between the electron clouds of adjacent adsorbed molecules. Second, if adsorption bond formation strongly orients an existing dipole, or polarizes the adsorbate, the adsorbed layer will consist of similarly aligned dipoles. The resulting interaction should show both a short-range repulsion due to adjacent dipoles and a long-range repulsion due to the dipole field of the adsorbed phase.

As a monolayer is completed, the heat of adsorption generally approaches the heat of liquefaction. This indicates that the nature of the adsorbate is approaching that of the liquid state. As with enthalpies of adsorption, the entropies of adsorption generally approach the entropy of liquefaction with multimolecular layer formation. The differential entropy of the adsorbed phase usually goes through a minimum at or near monolayer coverage where restrictions on molecular motion are at a maximum.

#### CLASSIFICATION OF ISOTHERMS

Gas adsorption techniques are often used to study the thermodynamics of an adsorption process through the experimental measurement of adsorption isotherms. An adsorption isotherm shows the variation of the amount adsorbed,  $w$ , as a function of pressure at constant temperature:

$$w = f(p)_T$$

The isotherm shape can yield qualitative information about the adsorption process.

Brunauer (8) classified adsorption isotherms according to five types (Fig. 1). Type I is often referred to as the Langmuir type. It corresponds to monolayer adsorption as predicted by the Langmuir equation. This contour is characteristic of chemisorption phenomena in which a monolayer completes the significant interaction of adsorbent and adsorbate. The Type I isotherm is also found in adsorption of gases on solids which contain micropores (pores which are no more than a few molecular diameters in width). In the micropores the potential fields from neighboring walls will overlap and the interaction of the solid with a gas molecule will be correspondingly enhanced. This will result in increased adsorption at low relative pressures. If the majority of the adsorbent surface area is in the pores, then as the pores fill at low relative pressures the isotherm will level off.

Types II and IV are the result of multilayer adsorption. Type II indicates physical adsorption on nonporous solids and is the most common isotherm shape. Type IV is similar to Type II except that a limited pore volume is indicated by a horizontal approach to the  $P_0$  line.

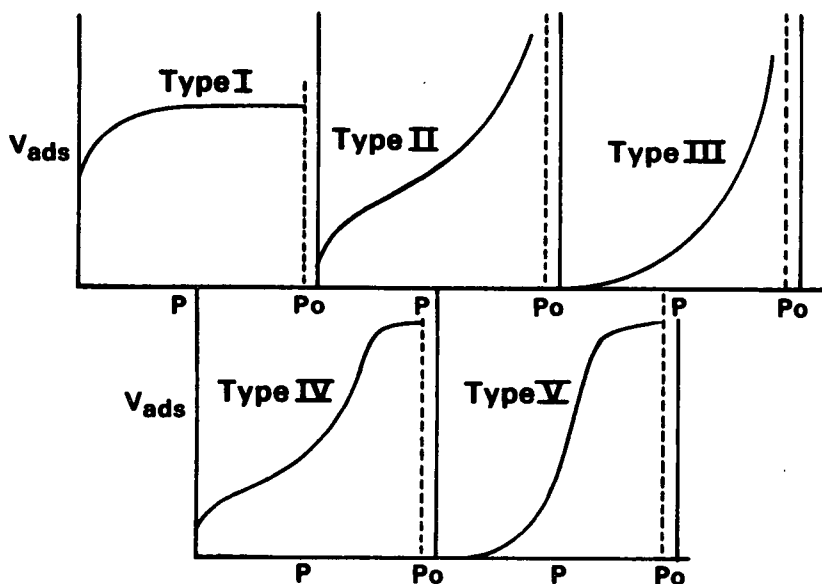


Figure 1. Brunauer classification of isotherms (8).  $P_0$  = saturation vapor pressure.

Types III and V are characterized by convexity toward the relative pressure axis, commencing at the origin. They are characteristic of weak gas-solid interactions. The weakness of the adsorbent-adsorbate forces results in little adsorption at low relative pressures. However, once a molecule is adsorbed, the adsorbate-adsorbate interaction promotes the adsorption of further molecules so that the isotherms are convex to the pressure axis. In the higher relative pressure regime, isotherm Types III and V are analogous to Types II and IV, respectively.

#### THERMODYNAMICS OF ADSORPTION

From a series of adsorption isotherms at different temperatures, heats and entropies of adsorption as a function of surface coverage can be calculated. Specifically, these terms are called the isosteric heat of adsorption and the differential entropy of adsorption. The following derivation of these thermodynamic quantities is from Clark (9), Aveyard and Haydon (10) and Young and Crowell (11).

If it is assumed that the solid remains unchanged by adsorption and that it simply provides a potential field which causes adsorption, the energy change for the surface on adsorption can be described:

$$dE_s = TdS_s - pdV_s - \pi dA + \mu_s dn_s \quad (1)$$

This equation is identical to that calculated in ordinary three-dimensional thermodynamics, except for the additional work term,  $\pi dA$ . In the above equation the surface area of the adsorbent,  $A$ , is proportional to the number of moles of adsorbent in the system,  $n_a$ . The pressure,  $p$ , is the pressure of the gas over the solid (provided there is not a second nonadsorbing gas present). The two dimensional surface pressure,  $\pi$ , is analogous to  $p$  in a one-component, three-dimensional phase.

It is often termed the 'spreading pressure'.  $\pi$  is equal to  $\gamma_0 - \gamma_s$ , where  $\gamma_0$  is the surface energy of the clean surface and  $\gamma_s$  is the surface energy of the surface with adsorbate.  $E_s$  is the energy of  $n_s$  moles of adsorbed molecules in the potential field of the surface of the adsorbent.  $S_s$ , and  $V_s$  are analogously defined.

From the definition of Gibbs' free energy,

$$G_s = E_s + pV_s - TS_s \quad (2)$$

and Eq. (1), the differential free energy is:

$$dG_s = -S_s dT + V_s dp - \pi dA + \mu_s dn_s \quad (3)$$

From Eq. (3), it follows (9) that:

$$d\mu_s = -\bar{s}_s dT + \bar{v}_s dp - \left(\frac{\partial \pi}{\partial n_s}\right)_{p,T,A} dA + \left(\frac{\partial \mu_s}{\partial n_s}\right)_{p,T,A} dn_s \quad (4)$$

since  $\mu_s = (\partial G_s / \partial n_s)_{p,T,A}$ . The differential molar quantities are defined as:

$$\bar{s}_s = (\partial S_s / \partial n_s)_{p,T,A} \text{ and } \bar{v}_s = (\partial V_s / \partial n_s)_{p,T,A}$$

Utilizing adsorption isosteres (variation of  $p$  with  $T$  at constant  $n_s$ ), Eq. (4) can be rewritten assuming  $dA=0$ :

$$d\mu_s = -\bar{s}_s dT + \bar{v}_s dp \quad (5)$$

For the gas in equilibrium with the adsorbed phase:

$$d\mu_G = -\bar{s}_G dT + \bar{v}_G dp \quad (6)$$

where  $s_G$  and  $v_G$  are molar quantities for the unadsorbed gas. At equilibrium,  $d\mu_s = d\mu_G$ , therefore:

$$-\bar{s}_s dT + \bar{v}_s dp = -s_G dT + v_G dp \quad (7)$$

or

$$(dp/dT)_{n_s,A} = (s_G - \bar{s}_s) / (v_G - \bar{v}_s) \quad (8)$$

Assuming that  $\bar{v}_s$  is negligible compared to  $v_G$  and that the gas is ideal:

$$(d \ln p / dT)_{n_s,A} = (s_G - \bar{s}_s) / RT \quad (9)$$

Separating and integrating Eq. (9):

$$\ln p = (s_G - \bar{s}_s) \ln T / R + \text{constant} \quad (10)$$

Thus the quantity  $(s_G - \bar{s}_s)$  can be calculated from adsorption isosteres, i.e., the plot of  $\ln p$  versus  $\ln T$  at constant mass adsorbed.

The quantity  $s_G - \bar{s}_s$  corresponds to the entropy difference between one mole of gas at equilibrium pressure,  $p$ , and one mole of adsorbed gas in equilibrium with that pressure. Both  $s_G$  and  $\bar{s}_s$  are functions of pressure. Consequently, it is often convenient to obtain the difference between  $\bar{s}_s$  and some reference state. If the reference state is chosen to be the pure liquid adsorbate at temperature  $T$ , where the molar entropy of the liquid is  $s_l$ , then (10):

$$s_l - \bar{s}_s = (s_G - \bar{s}_s) + R \ln(p/p_0) - \Delta H_{vap} / T \quad (11)$$

where  $\Delta H_{vap}$  is the molar heat of vaporization of the adsorbate and  $p_0$  is the saturated vapor pressure, both at temperature  $T$ .

The differential entropy,  $\bar{s}_s$  is defined as

$$\bar{s}_s = (\partial S_s / \partial n_s)_{p,T,A} = (\partial n_s s_s / \partial n_s)_{p,T,A} = n_s (\partial s_s / \partial n_s)_{p,T,A} + s_s \quad (12)$$

where  $S_s$  is the entropy of the adsorbed phase and  $s_s$  is the molar entropy of the adsorbed phase. As the surface coverage approaches a monolayer, the adsorbed

phase is usually approximated thermodynamically by a liquid state. Therefore, at monolayer coverage the molar entropy of the adsorbed phase will approximate the molar entropy of the liquid state of the adsorbate. Any additionally adsorbed material will not significantly alter the molar entropy of the adsorbed phase. Therefore, as a monolayer approaches completion, it is generally found that  $\bar{s}_g$  approaches  $s_l$ , as indicated by Eq. (12).

At equilibrium,

$$T(s_G - \bar{s}_S) = (h_G - \bar{h}_S) \quad (13)$$

Using Eq. (9),

$$(\partial \ln p / \partial T)_{n_S, A} = (h_G - \bar{h}_S) / RT^2 \quad (14)$$

Separating and integrating Eq. (14),

$$\ln p = -(h_G - \bar{h}_S) / RT + \text{constant} \quad (15)$$

The quantity  $(h_G - \bar{h}_S)$  is called the isosteric heat of adsorption,  $q_{st}$ . It can be calculated from a series of adsorption isotherms using Eq. (15). The isosteric heat can be conceptualized as the heat involved in the process of desorbing one mole of gas on a surface of infinite extent having the specific properties of the adsorbed gas plus adsorbent (12).

Analogous to the definition of the differential entropy,  $\bar{h}_S$  is defined:

$$\bar{h}_S = (\partial H_S / \partial n_S)_{p, T, A} = n_S (\partial h_S / \partial n_S)_{p, T, A} + h_S \quad (16)$$

where  $H_S$  and  $h_S$  are the total enthalpy and molar enthalpy of the adsorbed phase respectively. As the adsorbed phase approaches a monolayer,

$$\bar{h}_s \sim h_s \sim h_g \quad (17)$$

Eq. (17) implies that the isosteric heat will generally approach the heat of vaporization of the adsorbate.

The isosteric heat of adsorption, calculated from a series of adsorption isotherms, is the differential heat involved in the transfer of gas at constant temperature and pressure from the adsorbed phase to the gas phase. This is the heat of adsorption that is referred to throughout this thesis. Another differential heat, called the calorimetric heat is obtained from a constant volume, constant temperature process. The calorimetric heat is approximated using the isosteric heat by

$$q_d = q_{st} - RT \quad (18)$$

where  $q_d$  is the calorimetric heat.

#### BET THEORY

There have been many theories developed to model adsorption isotherms. Probably the most widely used model is the BET equation developed by Brunauer, Emmett and Teller (13). It is an easily used model from which surface areas can be calculated.

The BET treatment is based on a kinetic model of the adsorption process proposed by Langmuir (14). In this model the surface of the solid is regarded as an array of sites available for localized adsorption. The rate of adsorption is dependent on the rate at which the adsorbate molecules collide with an available site on the surface. The rate of desorption is dependent on an adsorbed molecule gaining enough energy to overcome the heat of adsorption.

In the derivation of the BET equation a number of assumptions were made. First, to apply the Langmuir treatment to multilayer adsorption, it was assumed that the heat of adsorption in the second and succeeding layers is equivalent to the heat of liquefaction. The heat of adsorption in the first layer, while not equal to the heat of liquefaction, is considered to be constant. The model assumes that gas is adsorbed through vertical interactions only, neglecting any adsorbate-adsorbate horizontal interactions. The adsorbed phase can be described as a number of noninteracting molecular piles.

Brunauer (15) states that it is reasonable that the increase in heat of adsorption from adsorbate-adsorbate interactions will compensate for the decrease in heat of adsorption due to surface heterogeneity. Consequently, the overall heat of adsorption should remain relatively constant for submonomolecular surface coverage. Experimentally obtained curves of the heat of adsorption as a function of surface coverage demonstrate that in most cases the heat of adsorption will vary significantly in the submonolayer region. Halsey (16) noted that the BET theory is based on "the quite untenable hypothesis that an adsorbed molecule can adsorb a second molecule on top, yielding the full energy of liquefaction, and that in turn the second molecule can adsorb a third, and so on." Generally, it is recognized that, theoretically, the assumptions in the BET theory are open to criticism. However, empirically, the model has been widely used with success.

Due to surface heterogeneity, i.e., the high adsorption energies at low surface coverages, the BET theory usually predicts too little adsorption in the relative pressure,  $p/p_0$ , region less than about 0.05. At higher relative pressures (greater than about 0.35) the BET theory predicts too much adsorption.

One reason for this breakdown is the assumption that as the relative pressure approaches 1.0, the number of adsorbed layers approaches infinity. On a porous solid this prediction will not hold since the number of layers adsorbed will be restricted by the pore diameter. Halsey (17) pointed out that the combinatorial entropy term associated with the random molecular piles is another reason why the BET theory predicts too large adsorption at the higher relative pressures.

Using the aforementioned assumptions, the BET equation has been derived from both a kinetic (13) and statistical thermodynamic (18) viewpoint. The isotherm equation can be presented in the linear form:

$$p/[w(p_0-p)] = 1/w_m c + [(c-1)/w_m c](p/p_0) \quad (19)$$

where

$w$  = mass adsorbed,  $\mu\text{g}$  adsorbate/g adsorbent

$p$  = pressure

$p_0$  = vapor pressure of the gas at the adsorbent temperature

$w_m$  = monolayer mass,  $\mu\text{g}$  adsorbate/g adsorbent

$c$  = constant related to the heat of adsorption,  $\sim \exp[(Q_1-Q_L)RT]$

$R$  = gas constant

$Q_1$  = heat of adsorption in first layer

$Q_L$  = heat of liquefaction of the liquid adsorbate at the adsorbent temperature.

If the function  $p/[w(p_0-p)]$  is plotted against the relative pressure,  $p/p_0$ , a straight line is usually obtained between the relative pressures of 0.05 and 0.35. The inverse of the sum of the slope and intercept equals the monolayer mass:

$$w_m = 1/(\text{slope} + \text{intercept}) \quad (20)$$

The specific surface area of a solid adsorbent can then be determined, using an approximate molecular cross-sectional area of the adsorbate, by the equation:

$$\sum_{\text{BET}} = w_m N \sigma_o 10^{-20} / M \quad (21)$$

where,

$\sum_{\text{BET}}$  = BET surface area,  $\text{m}^2/\text{g}$

$w_m$  = monolayer mass of adsorbate,  $\mu\text{g adsorbate}/\text{g adsorbent}$

$N$  = Avogadro's number

$\sigma_o$  = adsorbate molecular cross-sectional area,  $\text{\AA}^2/\text{molecule}$

$M$  = molecular weight of adsorbate,  $\mu\text{g}/\text{mol}$ .

Although the physical significance of the BET equation has been highly criticized, it is still widely used in the determination of surface areas. It should be noted that the surface area calculated using this theory is referenced as a BET surface area and is useful when compared to the BET surface area of other materials. It should be distinguished from surface areas calculated using any other methods. The absolute value of the surface area is very often dependent on the technique used to calculate the area. For example, Barber (19) used the Ross and Olivier theory (20), which treats the adsorbed material as a two-dimensional gas on a heterogeneous surface, to determine surface areas. He showed that the BET equation predicts surface areas which are considerably lower than the Ross and Olivier areas on some cellulosic adsorbents.

Supporting evidence for the validity of the BET surface area is afforded by curves of the heat of adsorption as a function of surface coverage. With surfaces which are energetically homogeneous, a distinct drop in the heat of adsorption as the BET monolayer mass is approached is noticed. The heat of adsorption drops and approaches the heat of vaporization, indicating inception of

a multilayer. This effect is masked by an energetically heterogeneous surface. The variation in the entropy of the adsorbed phase as a function of surface coverage also supports the validity of the BET monolayer mass. A minimum in this curve is often found at monolayer completion corresponding to a minimum in the configurational entropy of the adsorbed phase.

#### TWO-DIMENSIONAL CONDENSATION

The BET model of adsorption theorizes the adsorption process as localized. An alternative procedure is to consider the adsorbed material as a two-dimensional phase. This is analogous to the treatment of monolayers on liquid substrates, and therefore many different phases might be expected. As examples, Ross and Olivier (20) developed an adsorption model which treats the adsorbed phase as a two-dimensional gas using the DeBoer equation (the two-dimensional analog of the van der Waals equation). Volmer (21) developed an adsorption model which uses the two-dimensional ideal gas law modified with a covolume term. And Harkins and Jura (22) considered the adsorbed phase as a two-dimensional condensed film. Without stipulating the two-dimensional phase, the following discussion describes a method of determining the two-dimensional surface pressure of an adsorbed material. The surface pressure as a function of surface coverage can be used to follow any two-dimensional phase changes.

One of the fundamental equations of surface chemistry is Gibbs' Eq. (22):

$$d\gamma = - \Gamma RT d \ln a \quad (22)$$

which relates the change in surface tension,  $d\gamma$ , to the surface excess,  $\Gamma$ . Assuming ideality, the activity,  $a$ , in Eq. (22) is often set equal to the adsorbate

pressure. Hill (24) has shown that Gibbs' equation can be manipulated so the film pressure,  $\pi$ , of the adsorbed phase can be calculated from the equation:

$$\pi_{at\ p} = \frac{1000RT}{M\sum} \int_0^p w d \ln p \quad (23)$$

where,

$\pi$  = film pressure, dyne/cm

R = gas constant, 8.314 J/K·mol

T = temperature, K

M = molecular weight of adsorbate,  $\mu\text{g/mol}$

$\sum$  = specific surface area,  $\text{m}^2/\text{g}$

w = mass adsorbed,  $\mu\text{g adsorbate/g adsorbent}$

p = pressure, torr.

If Eq. (23) is rearranged (25):

$$\pi_{at\ p_1} = \frac{1000RT}{M\sum} \left[ \int_{p/w \text{ as } w \rightarrow 0}^{p_1/w_1} w d \ln(p/w) + w_{at\ p_1} \right] \quad (24)$$

the surface pressure can be determined graphically. In the low relative pressure regions where data are often difficult to obtain, Henry's law region may be reached. In this region,  $p/w$  is constant and the integral in Eq. (23) will equal zero. Thus, if it is assumed that the adsorption follows Henry's law, accurate data in the low relative pressure region are unnecessary. A phase diagram for the adsorbed material can be constructed by evaluating Eq. (23) at different surface coverages.

Analogous to adsorption on liquid substrates, material adsorbed on a solid substrate can go through phase changes. Figure 2 is an adsorption isotherm of Kr adsorbed on NaBr (26).  $\theta$  is the fractional BET monolayer coverage and is

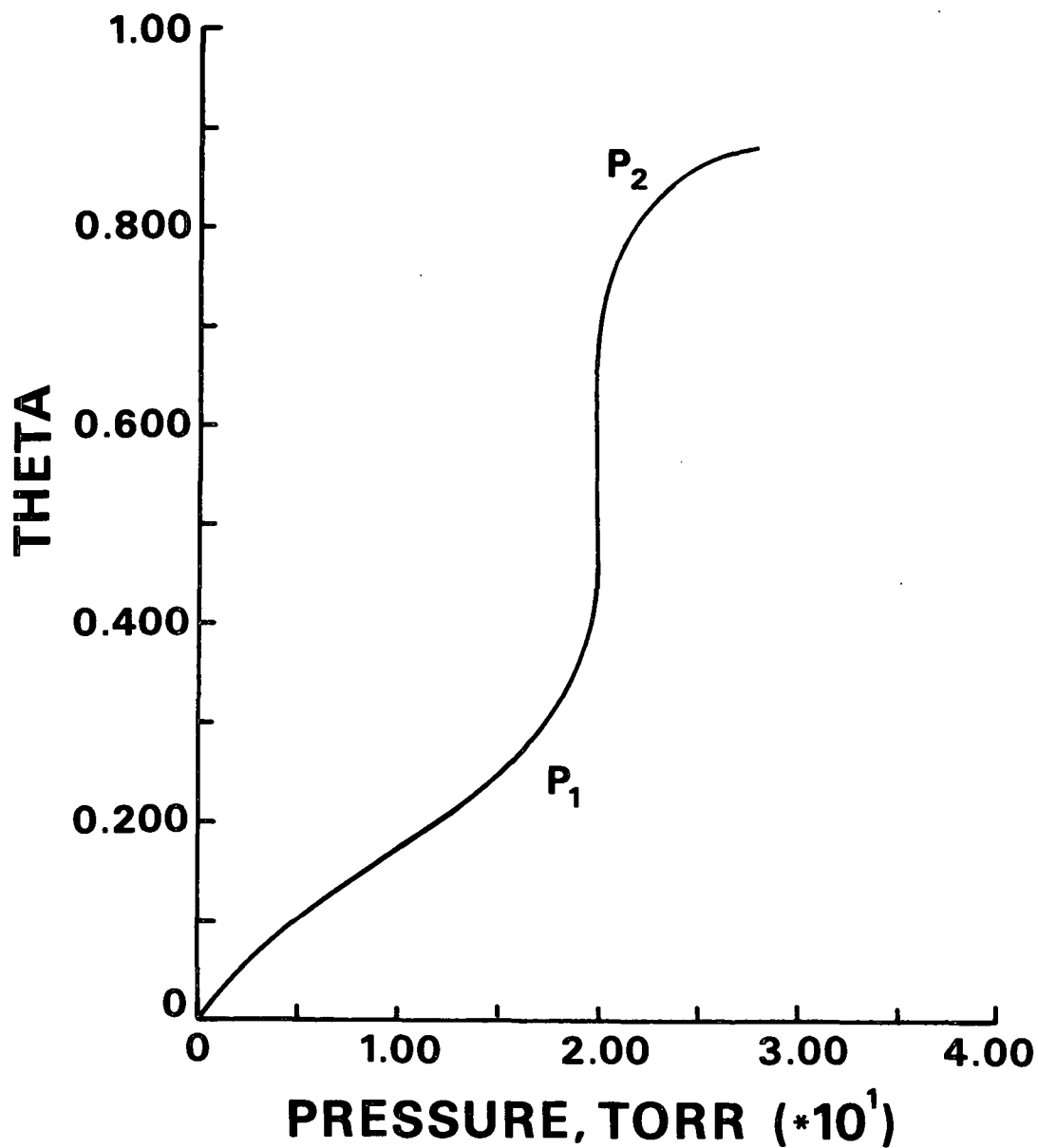


Figure 2. Adsorption isotherm of Krypton on NaBr (26).

proportional to the mass adsorbed. At  $\theta$  equal to 1.0, a mass corresponding to the BET monolayer mass has adsorbed on the surface. As  $\theta$  increases, the area available per molecule,  $\sigma$ , decreases. Using Eq. (23),  $\pi$  can be related to the area below the isotherm. It is apparent that as the pressure increases from  $p_1$  to  $p_2$ , there is only a slight increase in  $\pi$ . Thus at the step in the isotherm,

a very small increase in film pressure causes a large decrease in area available per molecule. This is what occurs in the transition from the gas phase to the liquid phase in bulk condensation. Thus a step in an adsorption isotherm in the submonolayer region is attributed to two-dimensional condensation.

A step in the adsorption isotherm is usually only apparent with low energy adsorption on homogeneous surfaces. Low energy adsorption shows this condensation phenomenon because the heat of condensation is a significant part of the total heat of adsorption. This may not be the case with adsorption on a high energy surface. On a homogeneous surface, the surface film pressure is equal across the surface and corresponds to a specific adsorbate pressure. However, on a heterogeneous surface, the film pressure varies across the surface. Thus, condensation is occurring in patches over a range of adsorbate pressures not at a specific adsorbate pressure as with Kr on NaBr. Condensation in a patchwise manner causes a "smearing" of the vertical step. The more heterogeneous the surface the more pronounced the smearing, i.e., the less pronounced the step. A typical Type II isotherm does not necessarily indicate that condensation is not occurring. Possibly, the surface is highly heterogeneous and condensation is occurring (27).

Although a step in the isotherm is often evident with adsorption of non-polar adsorbates on homogeneous adsorbents (e.g., Kr on NaBr), this phenomenon is not as common when following the adsorption of polar adsorbates. However, two-dimensional condensation has been followed during the adsorption of water on oxides (28-33). Recently, a step in the isotherm of alcohols adsorbed on NaF has been observed (34).

Kittaka, *et al.* (29) followed the adsorption of water on Cr<sub>2</sub>O<sub>3</sub>-I which had been calcined at different temperatures. Their results are shown in Fig. 3. As

the calcination temperature is increased to 1373 K, the particle size of the  $\text{Cr}_2\text{O}_3\text{-I}$  increases, accompanied by the growth of crystal planes. The surface should become more homogeneous with crystal growth. This increase in homogeneity is evident when examining the adsorption isotherms, since, as the calcination temperature is increased, the isotherm step becomes more dramatic (less "smeared"). The 1573 K treated  $\text{Cr}_2\text{O}_3\text{-I}$  sample should be heterogeneous because of lattice defects and/or dislocations caused by the very high calcination temperature. This increase in the heterogeneity is responsible for the disappearance of the step in the isotherm.

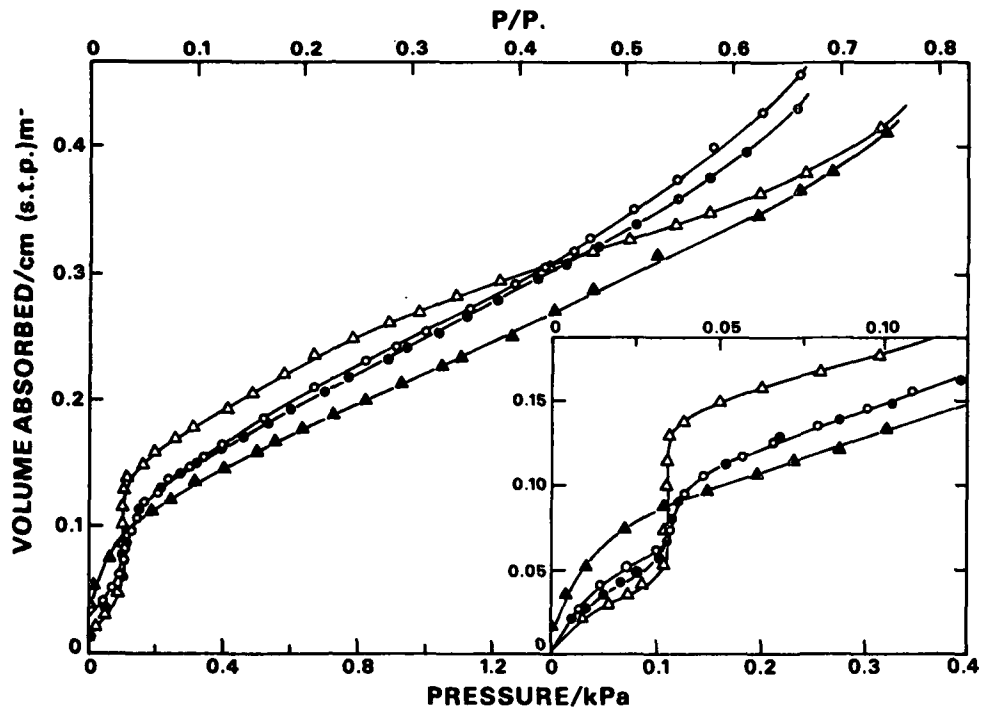


Figure 3. Adsorption isotherms of water on  $\text{Cr}_2\text{O}_3\text{-I}$  at 293 K. Calcination temperature (K): 0, 973; 0, 1173;  $\Delta$ , 1373;  $\Delta$ , 1573 (29).

If the heat of adsorption as a function of surface coverage is examined, two-dimensional condensation is evident as a minimum in the heat curve. At the minimum, condensation is beginning to occur and the heat of adsorption is

increasing because of the added heat of condensation. In the example of water on Cr<sub>2</sub>O<sub>3</sub>-II (Fig. 4) (29), two minima in the heat of adsorption curve are evident. (Note that Fig. 3 and 4 do not involve the same adsorbent.) Kittaka et al. proposed that this indicated the presence of two kinds of homogeneous planes with different adsorption energies. Therefore, two-dimensional condensation occurs at different surface coverages.

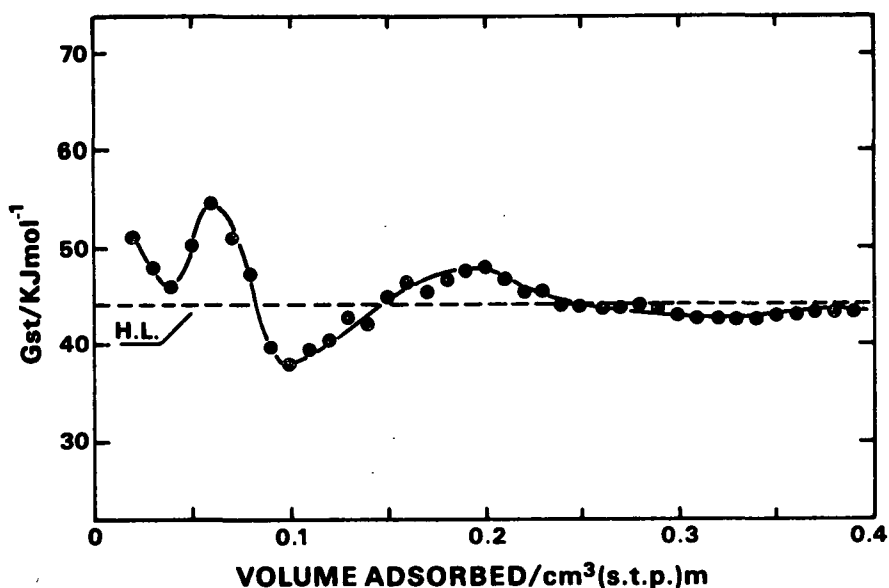


Figure 4. Isosteric heat of adsorption of water on Cr<sub>2</sub>O<sub>3</sub>-II at 298.2 K (29). Dashed line represents heat of liquefaction at 298.2 K.

#### FATTY ACID ADSORPTION

Only an adsorbed monolayer is necessary to alter the surface properties of an adsorbent. Langmuir (2) first reported this effect when he studied the wetting and frictional properties of solids with an adsorbed monolayer of polar organic molecules. He proposed that only those atoms at the interface between the solid and liquid controlled the wettability of the system. Bennett and Zisman (35) presented an example of this effect when they demonstrated that

water adsorption lowered the surface energy of the adsorbent to the same value for fourteen types of metals.

Rideal and Tadayan (36) showed that the surface layer of crystalline stearic acid has the ability to overturn, burying the polar end of the molecule in the medium of higher dielectric constant. This explains the decrease in the water contact angle with time on crystalline stearic acid. Yiannos (37) showed that 50% of the molecules in the top molecular layer of a long-chain fatty acid would reorient themselves. The shorter chain acids attained equilibrium faster than longer chain acids.

The adsorption of fatty acids from solution and from the vapor phase has been studied. The adsorption of long chain fatty acids on metals from solution has been investigated by many workers. The majority of work on the vapor phase adsorption of fatty acids has been completed using the lower molecular weight acids, acetic and formic. Hasegawa and Low (38) have studied the vapor phase adsorption of decanoic acid on magnesia.

The major difference between the two adsorption processes (from solution or vapor) is the competitive effect of the solvent molecules in adsorption from solution. Cook and Ries (39) studied the adsorption of radio-tagged stearic acid on iron and gold from n-hexadecane. They found that the solvent molecules had a significant effect on the adsorption of the stearic acid. The first acid molecules, adsorbed individually and widely scattered, are immediately surrounded by six of the more plentiful n-hexadecane solvent molecules. These solvent molecules in contact with an adsorbed stearic acid molecule are less easily displaced than other adsorbed solvent molecules, which inhibits further adsorption of stearic acid.

The process of adsorption from solution has been followed using two techniques: radioactively tagged acid and infrared analysis. Typically, infrared analysis follows the adsorption process in situ. The radiotracer technique usually determines the quantity of adsorbed material after the adsorbent has been removed from the solution.

#### Adsorption from Solution - Radiotracer Work

Young (40), using the Langmuir-Blodgett adsorption technique, found that on unreactive surfaces such as platinum or quartz glass, stearic acid is only weakly adsorbed (physical adsorption). On copper and calcium the existence of a stearate bond (chemisorption) was proposed. Young also demonstrated that under favorable conditions, material can desorb from one part of a surface and re-adsorb elsewhere after movement over considerable distances in the vapor phase. If this vapor phase transport was suppressed, no evidence of true surface diffusion over macroscopic distances on the adsorbents used could be found.

Smith and Allen (41) found that n-nonadecanoic acid chemisorbs on metal oxides but not on clean (no oxide) metal surfaces. In the discussion of their results, they assumed that the acid adsorbed perpendicular to the surface with a cross-sectional area of  $20.5 \text{ \AA}^2$ .

Timmons (42,43) looked at stearic acid adsorption on metals and the contact angle as a function of surface coverage. A solution retraction technique was used in this work. Timmons proposed that the rate of loss of radioactivity in both desorption and exchange experiments suggests two different forms of bonding between stearic acid and substrate. This indicated that there was both chemically and physically adsorbed material on the surface.

Kipling and Wright (44-46) studied the adsorption of higher molecular weight fatty acids on metal oxides and carbon blacks. They found that on oxides of the more electropositive elements (alumina, titania) stearic acid would adsorb with its major axis perpendicular to the surface. However, on silica and carbon blacks, the major axis is parallel to the surface. The difference in orientation was attributed to small differences in energies of adsorption. For perpendicular orientation, the heat of adsorption has to be substantial to overcome the heat of interaction available in the parallel orientation. On most surfaces, sites for adsorption will not be spaced closely enough to provide significant lateral interaction of the perpendicularly adsorbed fatty acids.

It is interesting to compare Kipling and Wright's results to adsorption on aqueous substrates where fatty acids can adsorb in the perpendicular orientation. Unlike adsorption sites on a solid, which are fixed, the aqueous adsorption sites (hydroxyl groups) are mobile and can reorient until the adsorbed fatty acid close-packs in a perpendicular orientation with lateral interaction.

On the less electropositive surfaces, Kipling and Wright (44,46) proposed that stearic acid is adsorbed as a dimer. Using Kipling and Wright's data, the surface area covered per dimeric molecule on carbon blacks can be calculated using Eq. (25):

$$\text{Area, } \text{\AA}^2 = (11.15)n + 26.44. \quad (25)$$

where  $n$  is the number of carbon atoms in the monomer. This equation is based on work using stearic, palmitic, lauric and octanoic acids.

Rahman et al. (47) studied the adsorption of stearic acid on oxides from solution. The stearic acid was primarily chemically adsorbed, covering an area

between 60 and 70 Å<sup>2</sup> per molecule. Using paraffins as a model, they proposed that the acid should cover approximately 100 Å<sup>2</sup> if it is oriented parallel to the surface (47). Rahman et al. concluded that the acid orientation was between perpendicular and parallel to the surface.

Dacre et al. (48,49) studied the adsorption of linoleic and dilinoleic acid on metal surfaces from nonaqueous solutions. Based on this work and a modification of Langmuir kinetics, they were able to derive a general rate equation. Adsorption followed Langmuir kinetics, but an activation energy which was a function of surface coverage was needed to explain desorption.

#### Adsorption from Solution - Infrared Work

Carboxylic acids normally exist in dimeric form with very strong hydrogen bridges between the carbonyl and hydroxyl groups of the two molecules (Fig. 5). This association persists to some extent even in the vapor phase (50). In the liquid or solid state only dimers have been found (51).

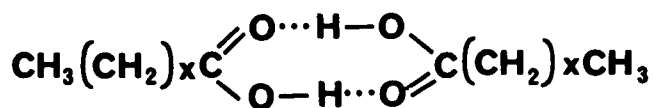


Figure 5. Fatty acid dimer.

When a carboxylic acid dimerizes, the frequency of the carbonyl absorption changes. A number of lower molecular weight acids in the vapor phase have been studied. The results indicate that the carbonyl absorption shifts from 1785 cm<sup>-1</sup> to near 1735 cm<sup>-1</sup> when the acid dimerizes (52-54). In solution, the carbonyl absorption shift is from 1768 cm<sup>-1</sup> to 1719 cm<sup>-1</sup> when the acid dimerizes (55). A shift from 1760 cm<sup>-1</sup> to 1708 cm<sup>-1</sup> has also been cited (51).

Upon dimerization, the O-H stretching absorption also shifts. In the monomer, the O-H stretch absorbs near  $3550\text{ cm}^{-1}$ . In the dimeric form there is a broad absorption region between  $3000\text{ cm}^{-1}$  and  $3500\text{ cm}^{-1}$  (51). The shifts in both the carbonyl and hydroxyl stretches have been used to study the monomer/dimer equilibrium of adsorbed fatty acids.

Hasegawa and Low (56) have studied the adsorption of stearic acid on various materials using an infrared transmission technique. The stearic acid molecules adsorbed predominantly as monomers at low surface concentrations and dimers formed at higher surface concentrations. The surface coverage was not determined. At higher solution concentrations the acid was in the dimer form and thus could adsorb as a dimer. Adsorption in the dimeric form is weak and readily reversible, while adsorbed monomers are more tightly held (carbonyl interaction with the surface) and more difficult to desorb. The dimeric hydrogen bond is weaker in the adsorbed acid than in the acid in solution due to interaction with the surface. Only physical adsorption occurred on silica, whereas chemisorption occurred on alumina. On silica, the dimer carbonyl absorbed at  $1710\text{ cm}^{-1}$  and the monomer carbonyl at  $1735\text{ cm}^{-1}$ .

Marshall and Rochester (57) studied the adsorption of oleic and linolenic acid on the surface of silica immersed in carbon tetrachloride. They proposed three distinct modes of adsorption. At the lowest coverage, pairs of adjacent interacting surface hydroxyl groups hydrogen bond to the acid carboxyl group. As the coverage increases, the acid hydrogen bonds to isolated silanol groups. Finally, at the highest surface concentrations, the acid dimerizes. The adsorbed molecules are oriented so that the alkene groups and the carboxyl group interact with the oxide surface simultaneously. The alkene interaction is weak.

Yang et al. (58) studied the adsorption of stearic acid on germanium from carbon tetrachloride, using polarized radiation. The implications of this work were that the adsorbed molecules were oriented randomly as hydrogen-bonded dimers and/or multimers on the germanium surface.

Jakobsen (59) studied the chemical reaction of stearic acid with thallium-bromide. Approximately 1.4 molecular layers adsorbed from solution, assuming the acid oriented with its major axis perpendicular to the surface. Apparently, the acid adsorbs as a dimer and then converts to the metal salt without first dissociating to the monomeric form. Further evidence indicated that the stearic acid molecular layer next to the crystal is a hydrogen bonded polymer, not the single dimer. The reaction to form the metal salt would involve the end groups of this polymer and would be similar to the "unzipping of a polymer chain".

#### Adsorption from the Vapor Phase

Most studies of the vapor phase adsorption of carboxylic acids have used the lower molecular weight fatty acids (formic, acetic, propionic). Studies of the adsorption of acetic acid are the most common. The adsorption of these fatty acids has been studied on germania (60,61), goethite (62), haematite (63), rutile (64) and Spheron 6 (carbon black) (65). In all cases, monomer was not found on the surface. The acid was either adsorbed as a weakly bonded dimer or as an ester. The chemical reaction was the common adsorption process in almost all systems.

Hasegawa and Low (56) studied the adsorption of decanoic acid on magnesia from both solution and the vapor phase. In adsorption from the vapor phase, they found that weakly adsorbed dimers are randomly oriented on the surface. No

evidence of the monomer could be found. In adsorption from solution, the orientation of the adsorbed dimers was fairly regular, similar to that of solid decanoic acid. Adsorption from solution promoted stronger interaction with the surface than adsorption from the vapor phase, probably due to the large polarizing effect of the solvent.

### Summary

It has been established that fatty acids chemically and physically adsorb on a variety of adsorbents. These processes occur in both adsorption from the vapor phase and adsorption from solution.

Workers using radiotracer techniques to follow adsorption from solution have attempted to establish the orientation of the adsorbed acid. In general, the orientation is dependent upon the adsorbate-adsorbent interaction and the spacing of adsorption sites. A range of orientations, from parallel to perpendicular have been proposed.

Infrared work on adsorption from solution shows that fatty acids adsorb as monomers at lower surface coverages. At higher coverages the acid dimerizes. Unfortunately, these coverages were not quantified. With adsorption from the vapor phase, only dimers have been found. However, this might be an effect of surface coverage, not the process.

Hasegawa and Low's (56) work has established that the acid-adsorbent interaction is somewhat dependent upon the adsorption process (solution or vapor). This implies that adsorption from solution work can not be applied to vapor phase adsorption studies without qualification.

## FATTY ACID ADSORPTION ON CELLULOSE

J. Swanson and Cordingly (66), while studying the mechanism of the "self-sizing" of paper, found that certain extractives in the paper may undergo vapor phase transport from colloidal extractive particles within the sheet to neighboring fiber surfaces. Once adsorbed, the extractive material lowers the average free surface energy of the fiber, causing loss of absorbency.

Using stearic acid as a model compound for the extractives in pulp, J. Swanson and Cordingly (66) found that the fatty acid could adsorb from the vapor phase on the cellulose surface and produce sizing. Exposure of paper to methyl stearate did not produce sizing.

Buchanan et al. (67) found that on oven aging of handsheets, the higher molecular weight fatty acids would self-size more efficiently than the lower molecular weight fatty acids. Linoleic acid was more effective than stearic and oleic acid.

Sinclair et al. (68) studied the vapor phase adsorption of fatty acids on cellulose as an alternative method of sizing. The sizing effect of the fatty acids could not be removed by extraction with solvents such as ethyl alcohol and ethyl ether. After treatment of the sized cellulose with hot alcoholic NaOH the sizing effect was lost. Sinclair proposed that the fatty acids may have formed an ester with the surface.

J. Swanson (69) reported that a handsheet treated with stearic acid vapor and then extracted with boiling benzene is still highly sized. The boiling benzene removed all but 6% of a perpendicularly oriented monolayer of stearic acid from the surface. Apparently, the extraction procedure removed any physically adsorbed stearic acid but left behind any acid chemically bonded to the surface.

Takeyama and Gray (70) studied the vapor phase adsorption process of stearic acid on cellulose using ESCA (Electron Spectroscopy for Chemical Analysis). Their findings supported J. Swanson's work (69) on the chemisorption of fatty acids on cellulose.

R. Swanson (71,72) proposed that the high sizing ability of small quantities of chemisorbed molecules is due to the hydrocarbon tails of the chemisorbed molecules sweeping out an area far greater than their cross-sectional area.

R. Swanson (71) also studied the attenuated total reflectance (ATR) infrared spectrum of adsorbed stearic acid on cellulose film. The existence of chemisorbed acid was demonstrated by comparing a methyl stearate ATR spectrum with that of cellulose film which was treated with stearic acid vapor and then extracted in boiling benzene. The carbonyl absorption frequencies in the two spectra correlated well. Swanson also acquired an ATR spectrum of the sample prior to benzene extraction, finding that physically adsorbed acid was highly dimerized. No absorption peak corresponding to the acid monomer could be found.

Ferris (73) concluded that the vapor phase adsorption process of stearic acid on cellulose can increase the water repellency of cellulose film in a predictable manner. Ferris postulated that a monomer of acid in the vapor phase could adsorb on an active site of the cellulose, quickly dimerize, and dissociate again to the monomer in some equilibrium. Any monomer on the surface could then slowly chemisorb by esterification with the cellulose hydroxyl groups. Ferris also concluded that sizing is entirely due to the chemisorbed acid.

Other studies have investigated the effect of external conditions and additives on the self-sizing process. Becher (74,75) studied the self-sizing process at different temperatures and pressures. He found that the process was much

slower at lower temperatures and/or lower pressures. Soteland and Loras (76) found that the self-sizing rate was pH dependent. The most favorable pH range for inhibiting self-sizing is between pH 7 and 8. If a buffer was added to the pulp to keep the pH within this range, no sizing occurred. J. Swanson and Cordingly (66), using stearic acid vapors, noted that a sheet containing alum would self-size better and faster. Presumably an aluminum stearate bond is formed which helps anchor the hydrophilic end of the acid to the cellulose, inhibiting molecular overturning.

To summarize, as with adsorption on a variety of adsorbents, fatty acids are able to physically and chemically adsorb on cellulose. The majority of evidence indicates that the chemisorption process is an esterification reaction of the fatty acid with the cellulose hydroxyl groups. Once chemisorbed, the fatty acid is a very efficient sizing agent.

#### ADSORPTION OF OTHER ORGANICS ON CELLULOSE

Tremaine and Gray (77) studied the adsorption of n-decane, 1,4-dioxan and a number of alcohols on cotton and ramie fibers. They used the gas chromatographic "peak-maxima" elution method. The alcohols interacted strongly with the cellulose. Both hexanol and butanol showed a minimum in entropy and a maximum in isosteric heat at 0.3 BET monolayers ( $\theta = 0.3$ ). This indicated that energetically preferred sites appear at this coverage. Tremaine and Gray speculated that the first molecules adsorbed create more energetic sites on which later molecules can adsorb and form sorbate-sorbate hydrogen bonds.

Mazurak (78) studied the adsorption of n-decane and n-hexanol on cellulose which had varying amounts of stearic acid chemisorbed on its surface. Mazurak also used the gas chromatographic "peak-maxima" method to obtain adsorption

data. Similar to Tremaine and Gray (77), Mazurak found a maximum in the heat of adsorption and the corresponding minimum in entropy at  $\theta = 0.5$ . After the fiber surfaces are about half covered with stearic acid, the maximum in the heat of adsorption curve disappears. Presumably, at the higher stearic acid coverages the decane-decane interactions are inhibited by the adsorbed stearic acid. Mazurak also proposed that physically adsorbed acid dimers are oriented in a "standing up" configuration.

Dorris and Gray (79) studied the adsorption of n-alkanes on cotton cellulose and on thermomechanical pulp (TMP). All of the isotherms were of the BET Type II classification with very indistinct knees. The indistinct knee of the isotherm indicated that the interaction between the adsorbent and adsorbate was weak. The area per molecule in a BET monolayer was calculated on the two adsorbents by setting the BET surface area equal to that determined using nitrogen as the adsorbate. The calculated molecular areas indicated that the alkanes are adsorbed with their major axis parallel to the surface in a "relatively compact packing". All of the isotherms were well described by the BET equation.

Katz and Gray (80) studied the adsorption of a series of n-alkanes on cellulose film. Analogous to that of n-alkanes on cotton cellulose and TMP, their data indicated that the n-alkanes are weakly adsorbed with the major axis parallel to the cellulose film surface. Low isosteric heats of adsorption at very low coverages indicated that the cellulose film appears to be energetically homogeneous with respect to n-alkanes.

Columbo et al. (81) studied the adsorption of benzene, methanol, and N,N'-dimethylformamide on cellulose using the gravimetric method of measuring gas adsorption. From this work it appears that adsorption of these vapors involves hydrogen bond formation. In the case of methanol and DMF, the hydrogen

bond formation extends over a wide range of coverage, while for benzene the hydrogen bonding decreases rapidly after monolayer completion. These results were obtained using heat of adsorption data which had been extrapolated back to zero surface coverage.

The adsorption of organics on cellulose has shown that cellulose has a relatively low surface energy as indicated by weak-kneed BET Type II isotherms. With adsorbates which are capable of it, hydrogen bond formation has been proposed. Adsorption of n-alkanes indicates that they adsorb with the major axis parallel to the surface, allowing maximum van der Waals interaction with the surface.

#### EFFECT OF RELATIVE HUMIDITY ON FATTY ACID ADSORPTION

The presence of moisture is always important in any surface study, since the water can easily adsorb on the surface of the adsorbent, masking its surface properties. Walker and Ries (82) showed that adsorption of stearic acid on gold and iron in the absence of moisture was generally consistent with the relative reactivities of the adsorbents. When moisture was present, the adsorption properties of the two metals were nearly equal.

Tremaine *et al.* (83) showed that as the water content of cellulose increased the BET parameter  $c$  decreased for n-decane adsorption. Dorris and Gray (84) noted that as the water content of cotton cellulose increased, the adsorption isotherm of n-decane transformed from a BET Type II to a BET Type III classification. This transformation is indicative of a decrease in the BET  $c$  constant.

Campbell (85) concluded that in the presence of water vapor there is competition with the fatty acid for active surface sites. On reactive metals the acid could displace water; however, on glass the adsorbed water could not be displaced.

Young (40) found that desorption of stearic acid from metal surfaces is favored in the presence of water vapor. Timmons (42) concurred with this, postulating that water promotes the desorption of some of the chemically adsorbed species by hydrolyzing the acid-metal bond.

Wan and Haller (86) studied the effect of coadsorbed water on the surface transport of stearic acid on  $\alpha$ -Al<sub>2</sub>O<sub>3</sub>. At coverages below a monolayer of coadsorbed water the diffusion rate was dominated by the residence time on any given site. Since there is site competition as the water coverage increases, the residence time will decrease. The acid diffusion rate will then increase as the water coverage approaches a monolayer.

Ferris (73) studied the adsorption of stearic acid vapors on cellulose film preconditioned at 50% RH and 70°F. His work indicated that a significant amount of stearic acid penetrates into the bulk of the cellulose film. R. Swanson (71) proposed that the penetration was attributable to excess film moisture content causing swelling of the cellulose. When Swanson preconditioned the cellulose film at 32% RH and 70°C, penetration did not occur.

Hirst and Lancaster (87) studied the effect of water on the interaction between stearic acid and fine powders. On reactive powders (Cu, Cu<sub>2</sub>O, CuO and Zn), water initiates the chemical reaction between stearic acid and the powder. After initiation, the reaction proceeds autocatalytically. Under dry conditions the acid only physically adsorbs on the powder surface.

Ferris (73) proposed that the chemical reaction of stearic acid with the cellulose surface proceeds by one of the two acid-catalyzed mechanisms for esterification described by Ingold (88). Ferris considered the acid catalysis probably due to the presence of water in the system.

Closer examination of Ferris' (73) and R. Swanson's (71) data indicates that water has an effect on the reaction rate of stearic acid with cellulose film. Ferris conditioned the cellulose film at 50% RH, while Swanson's samples were conditioned at 32% RH. Table I shows the initial reaction rate in both Swanson's and Ferris' work. At both 85 and 105°C, the samples conditioned at 50% RH react with stearic acid more rapidly than those conditioned at 32% RH.

TABLE I

CHEMISORPTION REACTION RATE (MMOL/M<sup>2</sup> · HR) AS A FUNCTION OF MOISTURE CONTENT AND TEMPERATURE (71,73)

Temp. °C	85	105
50	0.0027	0.0080
32	0.0023	0.0058

Water affects fatty acid adsorption through its ability to mask the adsorbent surface and its effect on the chemisorption reaction. Of particular importance in this work is the effect on the chemisorption reaction. Hirst and Lancaster's work (87) indicates that under dry conditions the esterification reaction is inhibited. In apparent contradiction of this, Young (40) and Timmon's (42) work shows that water promotes the desorption of chemically adsorbed species. Therefore, it seems that there is an optimum water concentration for the esterification reaction to proceed.

## PRESENTATION OF THE PROBLEM AND THESIS OBJECTIVES

To ascertain more about the fatty acid vapor sizing process, the kinetics and thermodynamics of the vapor phase adsorption process need to be investigated. Previous workers in this area did not attempt to investigate the kinetics of the chemical reaction. Also, since all of the studies have adsorbed acid from an acid saturated atmosphere, implying nonequilibrium conditions, the thermodynamics of the process have not been investigated.

The physical adsorption process has to be studied on a more fundamental level before a thorough investigation of the kinetics of the chemisorption process can be accomplished. It might be expected that an acid monomer would react much differently with a cellulose hydroxyl group than would an acid dimer. Therefore, it would be difficult to accurately explain the kinetics of the chemisorption process if the physical adsorption process were not fully understood.

The objective of this thesis was to investigate the physical adsorption process of a fatty acid on cellulose. Specifically, it was to determine the following:

1. Orientation of the acid on the surface
2. Association of physically adsorbed acid (monomer/dimer equilibrium) as a function of surface coverage
3. Interaction of acid with cellulose surface as a function of surface coverage

### EXPERIMENTAL APPROACH

The analysis of the physical adsorption process of decanoic acid on cellulose primarily involved the interpretation of adsorption isotherms acquired at different temperatures. A BET analysis of the isotherms supplied clues concerning the orientation of the acid adsorbed on the cellulose surface. An analysis of the heat and entropy of adsorption as a function of surface coverage answered questions about the interaction of the acid with the cellulose surface and with other adsorbed acid molecules.

The adsorption data were collected by gravimetrically determining the quantity of acid adsorbed on the cellulose at different acid pressures. Prior to exposing the sample to the fatty acid vapor, the cellulose was outgassed under vacuum to remove water and other volatiles from the surface. After outgassing the sample, the cellulose was exposed to a known pressure of acid and the system was allowed to equilibrate to a constant weight. The observed weight gain was one point on an adsorption isotherm.

The objective of this work was to investigate the physical adsorption process of a fatty acid on cellulose. Ferris (73) suggested that water is the catalyst in the chemisorption process. Since the cellulose sample was under vacuum prior to the adsorption experiments, water was removed from the adsorption system and the chemisorption reaction inhibited. Chemisorption would have been apparent if, after the cellulose was exposed to acid vapor and reoutgassed, the sample weight was higher than the initial outgassed weight. Also, an infrared surface analysis of cellulose treated with decanoic acid at 0% and 32% RH elucidated the effect of water on the chemisorption reaction.

The adsorbent chosen in this investigation was Whatman No. 40 filter paper, an ashless cotton cellulose. Filter paper was selected because of its high specific surface area. The microbalance used was limited to a one gram sample. Therefore, a high specific surface area sample was needed to minimize the error in weight gain measurements at low surface coverages. Whatman No. 40 was chosen over other filter papers because of its low ash content.

Decanoic acid (a ten carbon, saturated, straight chain fatty acid) was the adsorbate selected. Although the acid chain length is too short to efficiently size paper, the chemical and physical interactions of the acid with the cellulose surface should be similar to the higher molecular weight fatty acids found in wood. Since double bonds or branches on the hydrocarbon chain could cause complications in the adsorption process, a straight chain, saturated acid was selected.

Decanoic acid was chosen, since it is the highest molecular weight fatty acid with a vapor pressure high enough to feasibly perform adsorption experiments. Lower molecular weight fatty acids, with higher vapor pressures, could possibly absorb into (swell) the cellulose. The higher molecular weight fatty acids, with lower vapor pressures, require high vacuums to be attained and held. Gases in the system (even on the order of 0.0001 torr) would significantly slow the diffusion of the higher molecular weight acids to the cellulose sample. A very slow diffusion rate (implying slow adsorption) could be mistaken as an equilibrium quantity of acid adsorbed on the cellulose sample.

The adsorption experiments were performed over an adsorbent temperature range of 70 to 80°C. This range was selected for experimental purposes. The temperature was low enough to minimize damage to the microbalance but high enough to keep the adsorption process (which was limited by diffusion) within a reasonable time frame.

## EXPERIMENTAL APPARATUS, MATERIALS AND PROCEDURE

The gravimetric method of measuring gas adsorption was selected to obtain data for the adsorption of decanoic acid on cellulose. The gravimetric method was chosen since it is suited to the low adsorption pressures used. To gravimetrically determine adsorption isotherm data, the mass of the gas adsorbed was measured using a microbalance.

### EXPERIMENTAL APPARATUS

A recording vacuum microbalance system was constructed for the collection of the necessary adsorption data. The major components were

1. Pumping system
2. Manifold section
3. Oven chamber containing microbalance
4. Microbalance control unit with recorder

#### Pumping System

The pumping system was composed of a CENCO Hyvac 7 mechanical forepump backing a three-stage mercury diffusion pump manufactured by Pope Scientific, Inc. The forepump is rated to  $1 \times 10^{-4}$  torr with a capacity of 79 liters/minute at atmospheric pressure. The diffusion pump is rated to  $1 \times 10^{-8}$  torr with a pumping speed of 35 liters/second. The diffusion pump was water cooled with a safety cutoff if the water stops flowing. The pumping system was isolated from the rest of the system by a 60 mm o.d. liquid nitrogen trap.

The ultimate vacuum attainable in the system was strongly dependent on the system temperature. At room temperature dynamic vacuums in the  $10^{-7}$  torr range could be obtained. At an oven temperature of  $80^{\circ}\text{C}$ , pressures in the  $10^{-5}$  torr range could be obtained.

### Manifold Section

Connected directly to the pumping system was a glass manifold manufactured by Pope Scientific (Fig. 6). The manifold had lower connections to a Bayard-Alpert ionization gage, a fatty acid reservoir, and a vent. It had upper connections to the pumping system and microbalance chamber.

All joints and stopcocks were lubricated with Apiezon H grease. This grease will withstand temperatures to 250°C without melting. At 80°C it has a vapor pressure of about  $6 \times 10^{-7}$  torr, which is the lowest of the Apiezon greases (89).

The manifold was wrapped with heating tape and insulated with fiberglass insulation. The stopcocks were wrapped with heating tape and then glass wool and enclosed in fiberglass-walled boxes. The temperature of the manifold was monitored in two places with dial thermometers and was held at about 130°C. Care was taken to assure that the entire manifold was hotter than the acid reservoir, since acid vapor would condense on any cold spots, lowering the acid pressure in the system.

The fatty acid reservoir was in a constant temperature ( $\pm 0.03^\circ\text{C}$ ) water bath. There was an outer sleeve on the reservoir which allowed the inner tube to be wrapped with heating tape below the water surface. This assured that there was no cold zone at the air/water interface. The bath temperature was monitored with a thermometer with divisions every  $0.2^\circ\text{C}$ .

### Oven Chamber

Connected directly to the manifold was the microbalance chamber, which was located inside a large air oven (Fig. 7). The oven was thermostatted to  $\pm 0.1^\circ\text{C}$  using a Model 252 Precision Temperature Controller manufactured by Bayley Instrument Company. A high temperature cutoff on the oven was set at  $100^\circ\text{C}$  to protect the electrobalance from temperatures exceeding this limit.

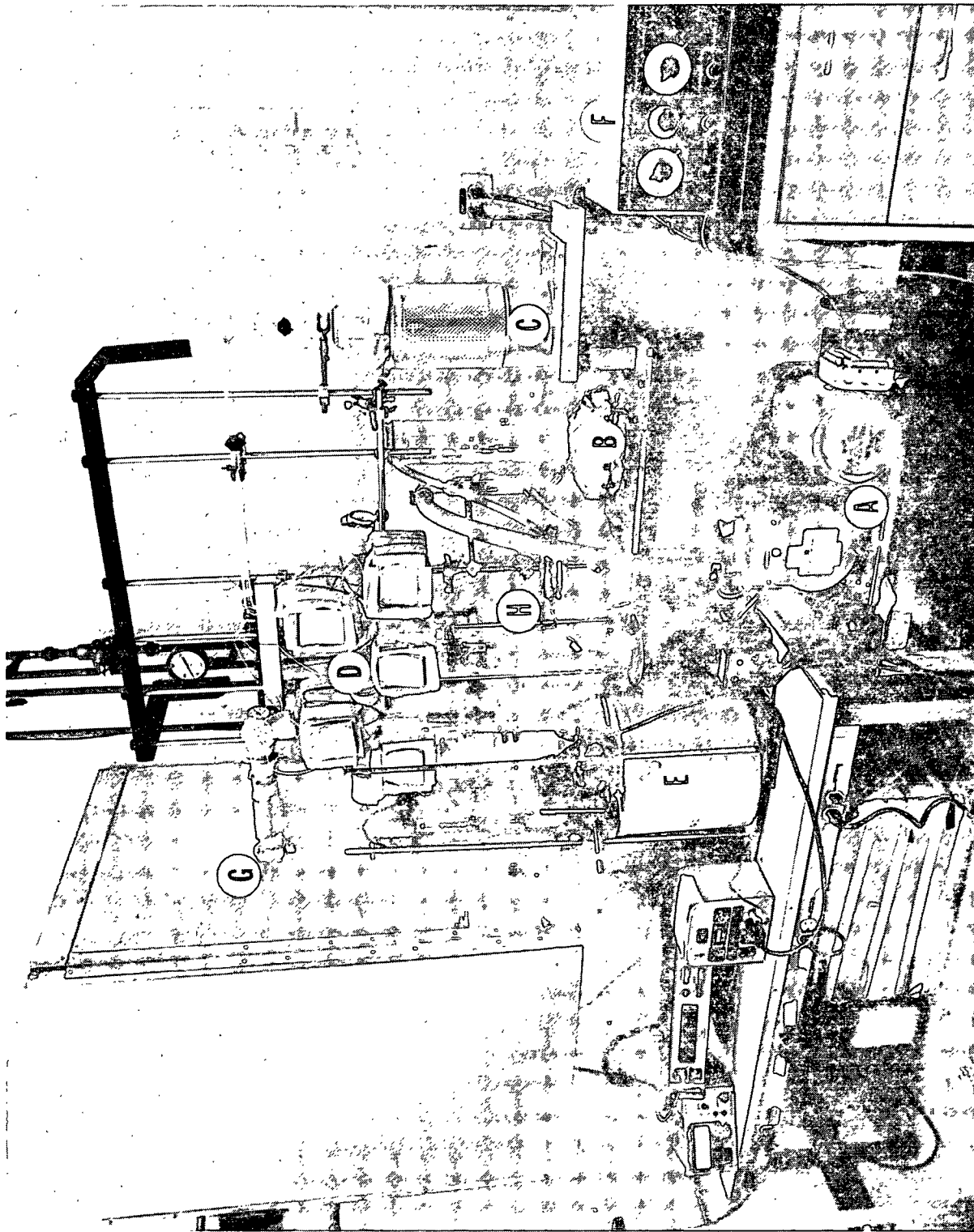


Figure 6. Manifold section of adsorption apparatus. (A) Mechanical forepump, (B) mercury diffusion pump, (C) cold trap, (D) manifold, (E) acid reservoir, (F) Cahn control unit, (G) connection to air over, (H) ionization gage.

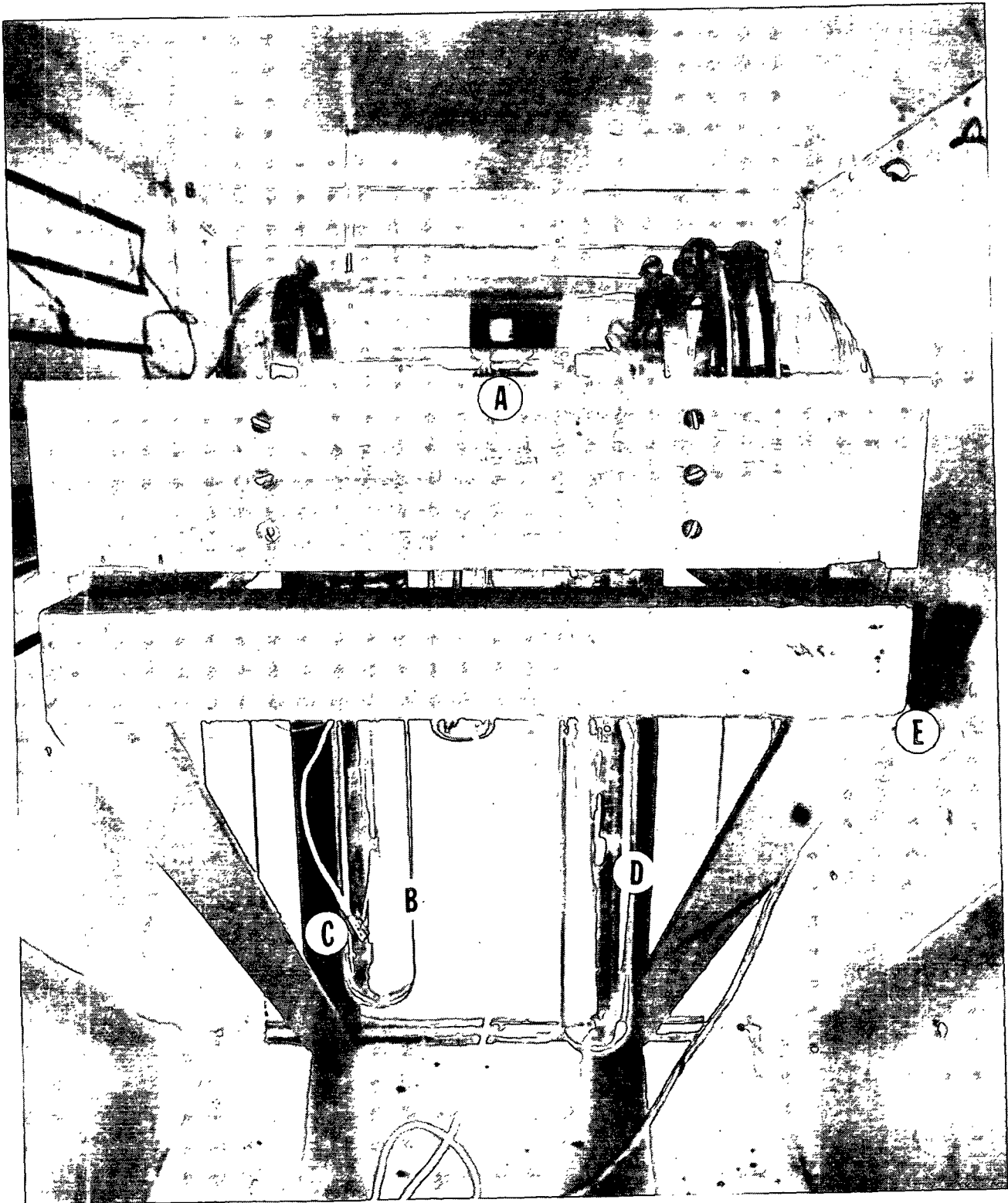


Figure 7. Air oven containing Cahn RG electrobalance. (A) Cahn balance inside vacuum chamber, (B) filter paper adsorbent, (C) quartz thermometer probe, (D) Teflon counterweight, (E) connection to manifold.

The oven temperature was monitored with a Hewlett-Packard Model 2801A quartz thermometer reading to two decimal places. The thermometer was calibrated using an ice bath as outlined in the thermometer operation manual. The quartz sensor was suspended as close as possible to the sample hangdown tube, at the height of the sample.

A standard mercury thermometer with markings every degree was positioned at the top of the oven. This was to determine whether there was an unnaturally large temperature gradient in the oven. Typically the temperature gradient between top and bottom in the oven was about 0.5°C.

#### Cahn Electromagnetic Balance

The microbalance used in this work was the Cahn RG Electrobalance (Fig. 8). The microbalance is a beam-type balance that works on the null-balance principle. When the sample weight changes, the beam deflects. The flag moves with the beam changing the amount of light to the phototube and therefore the phototube current. The phototube current is amplified in a 2-stage servo-amplifier and the amplified current is applied to a coil attached to the beam at the fulcrum. The coil is in a magnetic field. The current in the coil acts like a dc motor, exerting a force on the beam, restoring it toward the original balance position. The beam is always in dynamic equilibrium, but the restoring force is so powerful and fast that the beam appears visually to be locked in place.

According to Ampere's Law the electromagnetic restoring force is exactly proportional to the current that caused it. To convert this current to mass an accurately calibrated voltage is subtracted from the voltage across the coil by means of a potentiometer reading directly in milligrams. This excess voltage is also available for a previously calibrated recorder. By attenuating the

voltage, various weight ranges can be displayed on the control unit, the recorder, or a combination of the two.

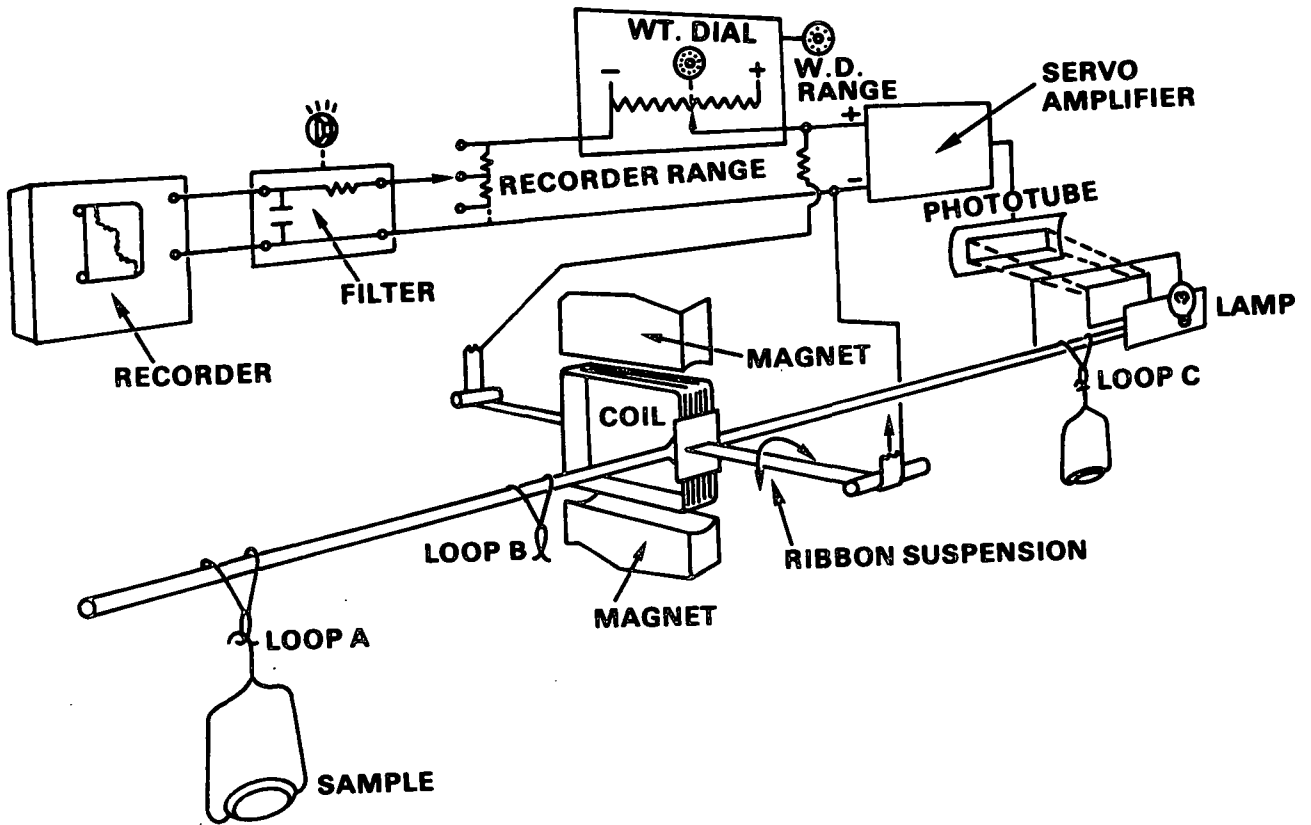


Figure 8. Cahn RG electrobalance.

Referring to Fig. 8, a sample was suspended from sample loop A and counterbalanced at loop C. With this positioning the coil exerts a force variation of 200 mg and the balance theoretically detects weight changes of 0.2 microgram.

The balance beam was mounted in a vacuum flask supplied by Cahn with the loops centered over two standard taper joints in the flask. The beam unit was connected to the control unit of the balance by wires sealed through the glass flask.

The sample and tare weights hung from the balance on 20 cm, 0.1 mm stainless steel wires. The wires hung down through the ground joints into Pyrex tubes 30 cm long with a 41 mm inside diameter. A tare weight, cut from Teflon stock, was suspended from loop C. A small piece of 0.1 mm SS wire was trimmed to bring the weight within the balance calibrating range.

A Cole-Parmer Model 261 recorder was used in conjunction with the Cahn Balance. A 1-mv span was used for the adsorption work so that full-scale on the recorder was typically 0.2 mg.

#### Calibration of the Balance

The balance and recorder were calibrated using the "Basic Method" instructions in the Cahn Balance Manual on the 0 to 10 mg scale. National Bureau of Standards class M weights were used as the calibrating weights. The balance was calibrated at the operating temperature and atmospheric pressure.

The mass of the calibrating weights and aluminum weighing pan was measured on a Mettler balance to be 675.4 mg. This mass corresponded to midrange on the electrobalance. Using the 0 to 10 mg mass dial range restricted the dry weight of the cellulose sample to be within  $\pm 5$  mg of the mass of the calibrating weights and weighing pan.

#### ADSORBENT

#### Preparation

Whatman No. 40 filter paper was used as the adsorbent. Whatman No. 40 has a medium filter speed and an ash content of 0.01%. Micrographs of the filter paper are presented in Fig. 9. Whatman No. 40 has been acid washed to obtain

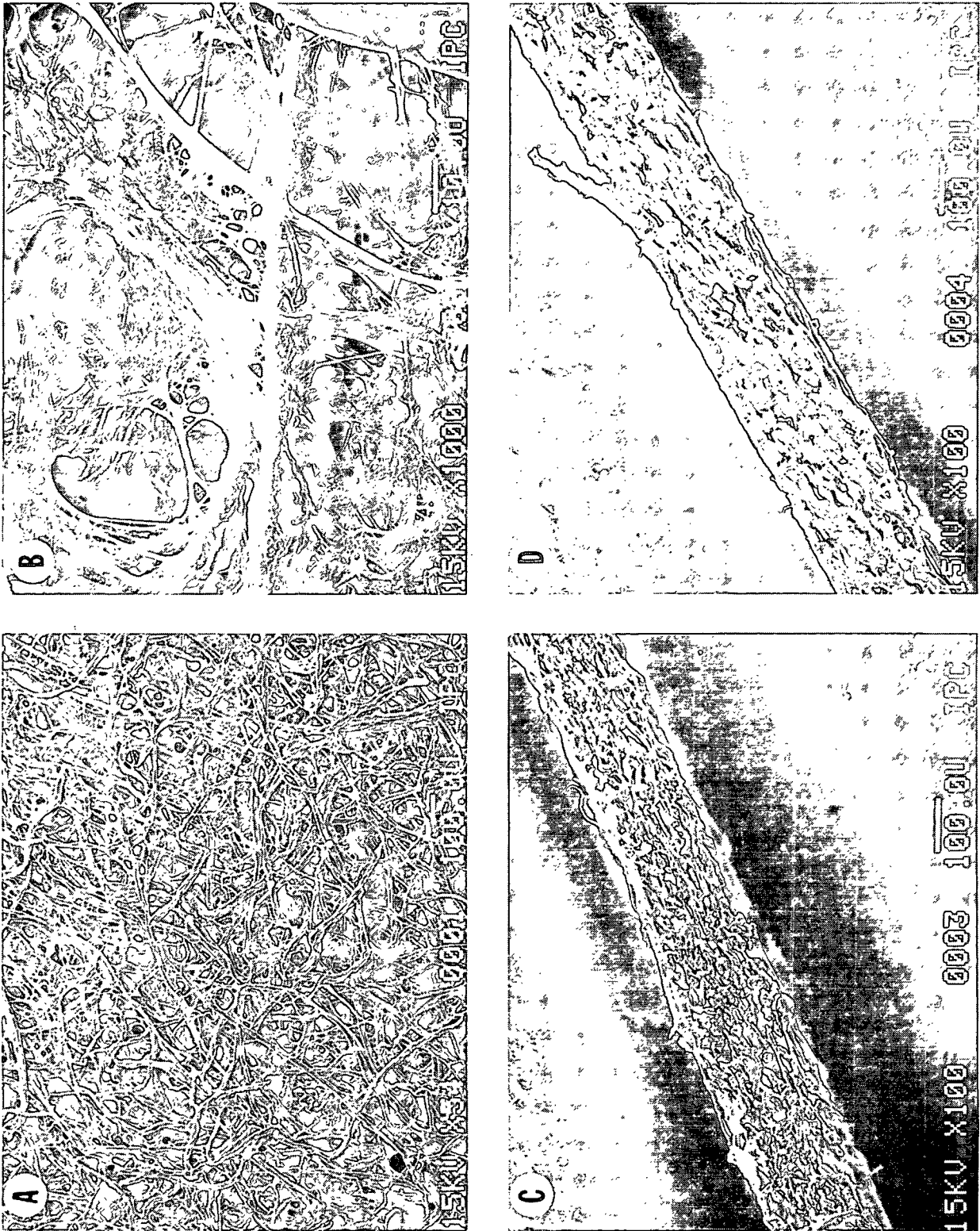


Figure 9. Electron micrographs of Whatman No. 40 filter paper. (A) Surface at 54X, (B) surface cut by freeze fracture technique, (C) cross-section cut with razor blade as for adsorption experiments.

the low ash content. This procedure might increase the number of carboxyl groups on the cellulose surface. However, infrared spectra (see Fig. 14) of the surface showed no absorption in the carbonyl stretching region ( $1700-1750\text{ cm}^{-1}$ ). Apparently, if the acid wash increased the carboxyl content of the filter paper, the increase was insignificant.

One x 5.2 cm strips of the filter paper were cut out with razor blades on top of a glass cutting surface. Thirteen strips constituted a sample weighing about 0.67 gram. The strips were conditioned over magnesium perchlorate in vacuo until a constant dry weight was obtained. The exact weight was recorded. This was the sample weight used in any subsequent calculations. Prior to use, the strips were bundled together and loosely sewn at the top of the bundle with 0.1 mm stainless steel wire. The glass cutting surface, razor blades, needle, and stainless steel wire were cleaned with ethanol before using. All data were acquired on filter paper from the same box.

#### Surface Area

The BET surface area of the Whatman filter paper was determined on a Micromeritics AccuSorb gas adsorption instrument. The Micromeritics instrument uses the volumetric method of measuring gas adsorption. The volumetric method measures the quantity of material adsorbed by determining the adsorbate pressure drop when a known volume of gas is opened to the adsorbent. Corrections are made for the pressure drop due to the increase in system volume (the dead space). The volume adsorbed at standard temperature and pressure is calculated using the ideal gas law. The Fortran program, BET, which performs these calculations, plots the data and computes the surface area, is listed in Appendix V. A sample of the program output is shown in Fig. 10.

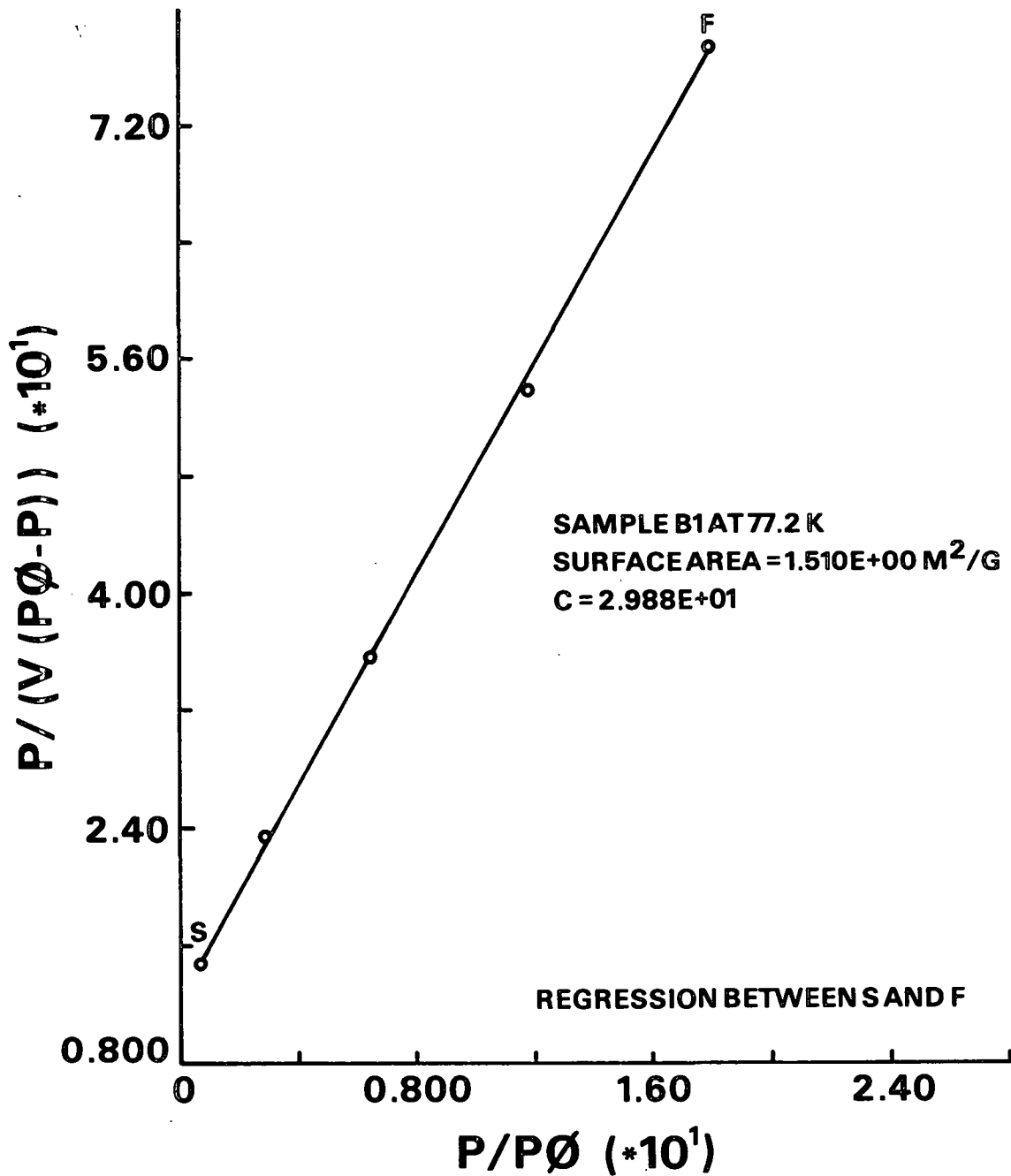


Figure 10. Program BET output for Krypton on Whatman No. 40 filter paper at 77.2 K.

Isotherm data were accumulated on samples of Whatman No. 40, Whatman No. 1, and a 10.3 m<sup>2</sup>/g TiO<sub>2</sub> standard. The results are presented in Table II. Whatman No. 1 has been used as a 1 m<sup>2</sup>/g standard (90). It was therefore used as a check

on the experimental method. Dorris and Gray (91) reported BET areas of 1.22 m<sup>2</sup>/g for Whatman No. 1 using a dynamic nitrogen adsorption method. Micromeritics (92) determined the surface area of Whatman No. 1 to be 1.23 m<sup>2</sup>/g using the Micromeritics instrument in their laboratory. Platt (93) calculated the surface area of Whatman No. 1 to be 1.40 m<sup>2</sup>/g using the Micromeritics instrument at The Institute of Paper Chemistry.

TABLE II  
BET SURFACE AREA

Sample No.	Sample	Adsorbate	Surface Area m <sup>2</sup> /g
A	Whatman No. 1	Kr	1.40
B	Whatman No. 1	Kr	1.40
B	Whatman No. 1	Kr	1.40
C	Whatman No. 1	Kr	1.45
D	Whatman No. 1	N <sub>2</sub>	1.40
1	Whatman No. 40	Kr	1.49
2	Whatman No. 40	Kr	1.53
3	Whatman No. 40	Kr	1.46
1	Whatman No. 40	Kr	1.51
1	Whatman No. 40	Kr	1.54
1	Whatman No. 40	Kr	1.52
1	Whatman No. 40	Kr	1.53
2	Whatman No. 40	Kr	1.60
10.3 m <sup>2</sup> /g TiO <sub>2</sub>	standard	N <sub>2</sub>	10.4

Average area of Whatman No. 40 = 1.51 ± 0.12 m<sup>2</sup>/g at 95% confidence limit.

Based on the consistency of the results using krypton and nitrogen as adsorbates and Whatman as the adsorbent, the experimental method appears to be correct even though the calculated surface area is significantly different from that determined elsewhere (91,92). The result for the TiO<sub>2</sub> standard also indicated that the experimental method was correct. Whatman No. 1, sample B, was repeated with results of 1.395 and 1.396 m<sup>2</sup>/g (rounded off in Table II) using the same dead space measurement for both experiments. This indicates that most

of the scatter in the surface area measurements was due to error in weighing the sample or in the dead space measurement.

The average surface area of Whatman No. 40 is  $1.51 \text{ m}^2/\text{g}$ . This is the value which will be used in all subsequent calculations in this work. The surface area is referenced as a BET surface area and is useful when comparing to BET surface areas of other adsorbents. Care should be taken when comparing this value (on an absolute scale) with surface areas determined using other techniques.

## ADSORBATE

### Purity

The fatty acid reservoir on the manifold system contained approximately 3 mL of 99.5+% decanoic acid purchased from Aldrich Chemical Company. A gas chromatographic analysis was performed on the decanoic acid using a 5% DEGS-PS column. Only one peak, corresponding to decanoic acid, was detected.

### Variation of Adsorbate Pressure

In typical gas adsorption work the sample chamber is dosed with varying volumes of adsorbate to achieve a range of relative pressures. To do this, the amount of gas in the system is determined using a pressure measuring device such as an ionization gage. This method assumes that the pressure in the system is due solely to the adsorbate. At higher adsorbate pressures (10-100 torr) this circumstance is easily achieved. When working with decanoic acid, at temperatures below  $80^\circ\text{C}$ , the adsorbate pressures are less than 0.1 torr. Obtaining and holding a good vacuum at the higher temperatures (ca.  $80^\circ\text{C}$ ) was very difficult. For this reason the assumption that the pressure in the system was due solely to the decanoic acid is unreliable.

An alternative to the dosing method would be to vary the vapor pressure of the acid in a reservoir by varying the temperature of the reservoir. If the reservoir temperature is lower than the rest of the system, the pressure of the acid in the system will equal the vapor pressure of the acid at the reservoir temperature. A range of relative pressures at the sample temperature can be obtained by varying the temperature of the acid reservoir. Whalen (94) has used this method to study the adsorption of water on teflon. The advantages of this method are

1. One need not worry about other gases in the system affecting the total pressure measured with an ionization gage, since the acid pressure can be determined from a vapor pressure curve.
2. There is no depletion of the vapor from adsorption on glass walls and balance parts, etc., since the sample is open to an infinite reservoir of acid.

There is one correction to consider when using this dosing method. When two chambers, A and B, are separated by a porous plug and at two different temperatures,  $T_A$  and  $T_B$ , thermal transpiration will occur until an equilibrium state is established. At equilibrium:

$$P_A/P_B = \sqrt{T_A/T_B} \quad (95) \quad (26)$$

The above equation is valid for two vessels connected by small-bore tubing if the diameter of the tubing is small compared to the mean free path of the gas. As the diameter increases with respect to the mean free path of the gas,  $P_A$  will approach  $P_B$  (95). The largest temperature difference in this work was 46°C.

Using Eq. (26), this is only a 7% difference in the pressures at the acid reservoir and balance. The mean free path of the decanoic acid is on the order of the tubing diameter (Appendix I), so the pressure difference was actually smaller than 7%. Since the greatest error in the pressure measurement was less than 7%, no pressure correction was made in the adsorption data. The manifold temperature has no effect on the pressure at the balance and acid reservoir.

### Vapor Pressure

To determine the pressure of acid in the balance chamber, the vapor pressure of the acid at the acid reservoir temperature had to be accurately known. Consequently, a review of the literature pertaining to decanoic acid vapor pressures in the temperature range of 20 to 80°C was completed. Data from higher temperature ranges extrapolated below 80°C were not used in this investigation.

Davies and Malpass (96) determined the vapor pressure of solid decanoic acid from 16.80 to 27.83°C using the Knudsen effusion method. They fitted their data to the Clausius-Clapeyron equation:

$$\ln(p, \text{ torr}) = 39.443 - 14089/T \quad (27)$$

In this temperature range the calculated heat of sublimation is  $28.0 \pm 0.4$  kcal/mol.

Spizzichino (97) determined the vapor pressure of various fatty acids and their methyl esters using the torsion effusion method. The vapor pressure of decanoic acid was determined in the temperature range of 36.5 to 79.0°C.

Spizzichino's data can be fitted to the following equation:

$$\ln(p, \text{ torr}) = 26.91 - 10280/T \quad (28)$$

De Kruif et al. (98) used both the torsion effusion method and mass-loss effusion techniques to determine the vapor pressure of various fatty acids in the pressure range of 0.1 to 1.0 Pa (.75 to 7.5 microns). The vapor pressure of decanoic acid was determined in the temperature range of 32 to 50°C. De Kruif et al. fitted their data to the Clausius-Clapeyron equation:

$$\ln(p, \text{ torr}) = 28.149 - 10656/T \quad (29)$$

The raw data were not presented. However, they claimed that the vapor pressures calculated from Eq. (29) are accurate within 10 percent.

Figure 11 is a Clausius-Clapeyron plot of Spizzichino's raw data (97) and De Kruif's calculated data (98). A linear regression of the data results in the following equation:

$$\ln(p, \text{ torr}) = 26.6021 - 10175/T \quad (30)$$

Using this data, error analysis shows that the vapor pressure calculated at a specific temperature is, at worst, precise within  $\pm 5\%$  at 95% confidence limits. The largest error occurs at the ends of the temperature range. This equation was used to determine the vapor pressure of decanoic acid above its freezing point (31.5°C). Davies and Malpass' equation was used to determine the vapor pressure below the freezing point. The heat of vaporization calculated using Eq. (30) is  $20.2 \pm 0.4$  kcal/mol.

#### ADSORPTION

To acquire isotherm data, the equilibrium quantity of acid adsorbed as a function of acid pressure had to be determined. Experimental acquisition of these data involved exposing a cellulose sample to a known pressure of acid vapor, allowing the system to come to equilibrium and noting the weight gain of the sample.

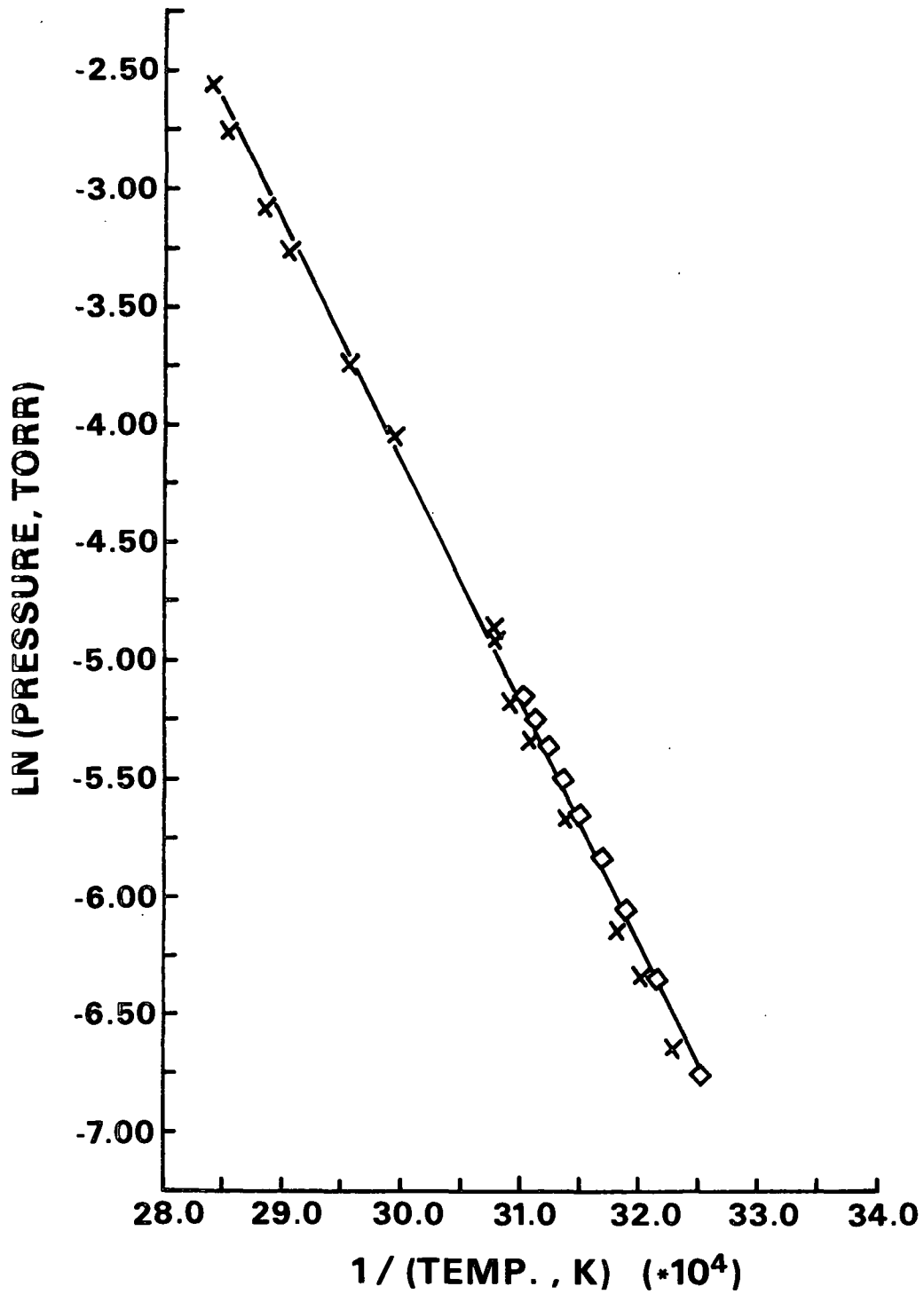


Figure 11. Clausius-Clapeyron plot of literature vapor pressure. X, Spizzichino (97);  $\diamond$ , De Kruijff, et al. (98).

After a cellulose sample was suspended from the balance it was outgassed to constant weight with the stopcock to the acid reservoir closed (Fig. 6). When the sample reached a constant weight, the stopcock to the oven chamber was closed and the acid reservoir was opened. The reservoir was outgassed for a few minutes and then the stopcock to the pumping system was closed (the entire system was then under a static vacuum). The stopcock to the oven chamber was then opened, allowing the acid to diffuse from the reservoir to the sample. Eventually, the acid pressure in the oven equaled the vapor pressure of the acid at the reservoir temperature. The acid reservoir vapor pressure was determined using Eq. (27) or (30).

Two different procedures were used to collect the adsorption data. The first procedure (method 1) was to outgas the sample to constant weight after each adsorption run. The acid pressure (acid reservoir temperature) was then changed and another point on the isotherm determined. The difference between the initial (outgassed) weight and final weight was used as the weight gain. Using this method, only one point could be determined per day. It takes about 14 hours for an equilibrium amount of acid to adsorb and overnight outgassing to reach a constant weight.

The second procedure (method 2) was to increase the pressure of acid in the system after equilibrium at a lower pressure had been established. The weight gain was calculated as the final weight minus the most recent outgassed weight. This method was used only when the pressure was increased, since the driving force to desorb acid by lowering the acid pressure is too small. The amount of acid adsorbed at a given pressure was not affected by the procedure used.

## EXPERIMENTAL RESULTS

The analysis of the physical adsorption process of decanoic acid on cellulose involved the interpretation of adsorption isotherms at different temperatures. An adsorption isotherm shows the variation of the amount adsorbed as a function of adsorbate pressure at constant temperature. The adsorption data were collected by gravimetrically determining the quantity of acid adsorbed on the cellulose surface at a specific acid pressure and temperature.

### PRELIMINARY WORK

Prior to the analysis of adsorption data, a number of experiments were completed to characterize the adsorption system. These experiments were to determine whether any correction of the experimental data was necessary and whether the conditions of the experiment effected any change in the surface of the cellulose sample.

#### Effect of Impurities (Blank Runs)

When the cellulose sample had been thoroughly outgassed, the total pressure in the system was on the order of 0.01 micron. When the vacuum pumps were closed off, leaving the sample under a static vacuum, the pressure slowly increased due to continued outgassing from components within the adsorption system. Therefore, when an adsorption experiment was started, the impurities in the system were a significant portion of the total pressure in the system.

Since the system was not free of impurities, it was necessary to determine if there was any apparent sample weight change without acid vapor present but with the sample under a static vacuum. Any weight change under these conditions would have been caused by adsorption of other gases within the system.

The results of this experiment showed that when the adsorption system was operating properly there was no weight gain. However, if the system was leaking, a weight gain, which did not reach an equilibrium value, was detected. This increase in weight could have been due to water vapor adsorption or perhaps an effect of thermomolecular flow. This experiment was performed often as a check on the system operation.

Adsorption on the Balance

To determine whether any weight change during an adsorption experiment could be attributed to adsorption on components of the system other than the cellulose sample, acid vapor adsorption experiments were performed using Teflon stock as the sample. Since the counterweight was Teflon stock, any adsorption on the Teflon sample was counterbalanced with adsorption on the counterweight.

The results from this experiment (Table III) show that when the microbalance had been recently cleaned, there was an apparent increase in the sample weight. Since the sample and counterweight were identical, this increase was due to adsorption on the balance, not to adsorption on the sample. However, as the adsorption experiments were repeated the magnitude of this increase diminished, eventually approaching zero.

TABLE III

ADSORPTION ON TEFLON SAMPLE

Run No.	Relative Pressure	Initial Wt., mg	Wt. Gain, $\mu$ g
1	0.166	676.968	72
2	0.166	677.001	35
3	0.426	676.998	84
4	0.029	676.994	0
5	0.129	676.994	12
6	0.082	676.754	0
7	0.493	676.754	14
8	0.185	676.764	0

The initial (outgassed) weight of the Teflon sample did not change significantly throughout the experiments, indicating that the decrease in the weight change was not due to irreversible adsorption on the sample or the sample side of the balance. (The decrease in initial weight of Runs No. 6-8 is due to the accidental switching of the sample and tare hangdown wires.) Irreversible adsorption was occurring on some other portion of the microbalance and the balance was being "conditioned" by the acid. After many adsorption experiments acid could be visually detected on the microbalance and this quantity of acid was not completely removed from the balance during outgassing of the system. Although the acid adsorbed on the balance might be construed as a reservoir of acid, the pressure of acid in the system was still regulated by the vapor pressure of the acid in the acid reservoir, which was always the coolest component in the adsorption system.

Figure 12 is an example of the anomalous weight gain observed when operating in a relatively clean system with a cellulose sample. The order in which the adsorption data were acquired is denoted by arrows along the curve. The solid upper curve (the first data acquired on sample 13) shows higher adsorption at a given pressure and could not be reproduced. The lower solid curve is data acquired on sample 13 after the system was "conditioned". The dashed curve shows data acquired after sample 13. It is reproducible as evidenced by the repeated runs. Also, it reproduces the later sample 13 data. Only the data in the lower curve were used in analysis.

#### Effect of Heat and Vacuum on Cellulose

Once a cellulose sample was mounted in the adsorption system, it was subjected to temperatures up to 85°C under high vacuum over an extended period of time. It is possible that these conditions could affect the surface composition or the surface area of the cellulose.

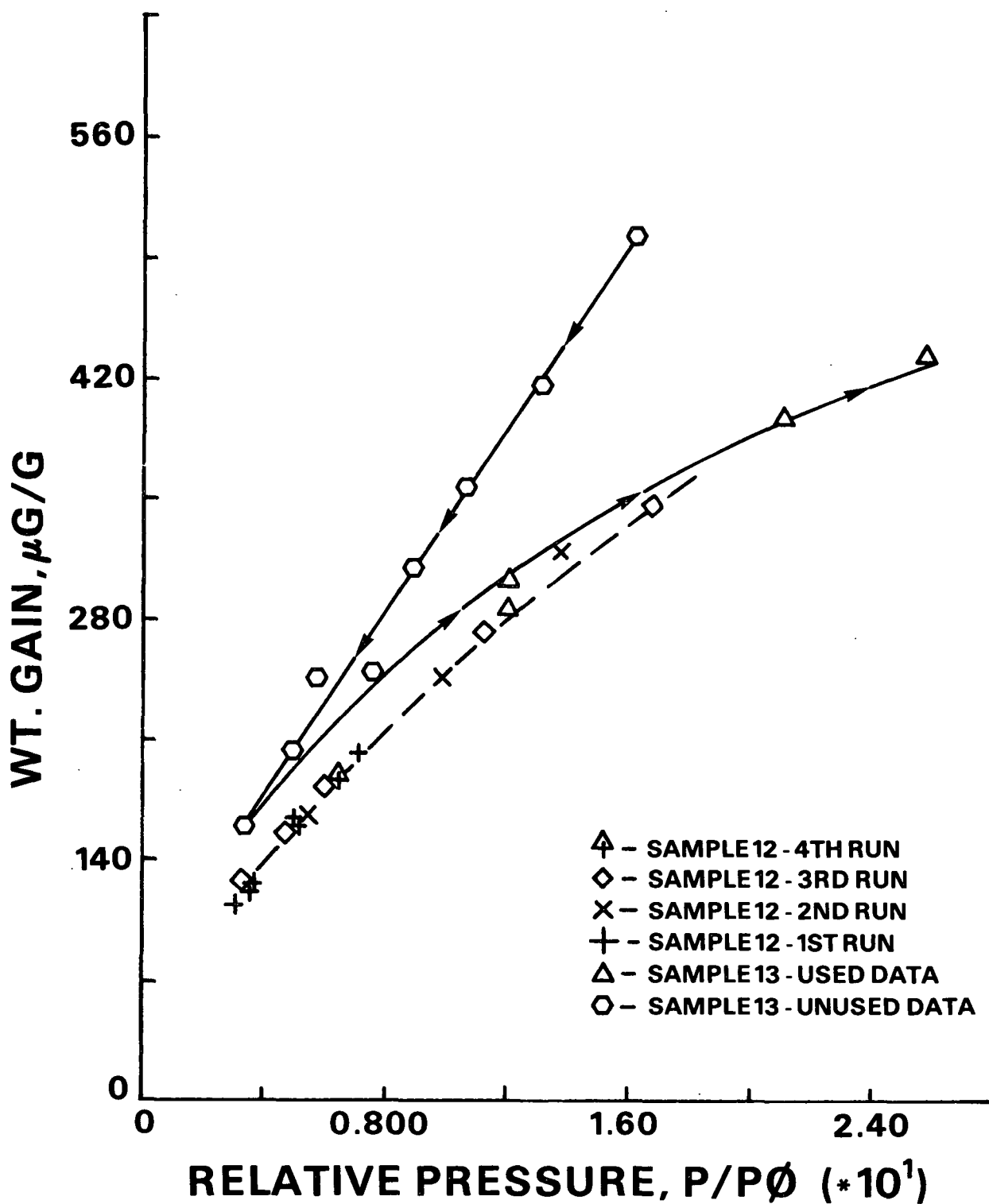


Figure 12. Example of anomalous weight gain during adsorption experiments.

To investigate the effect of heat and vacuum on the Whatman No. 40 filter paper, the surface area before and after treatment under these conditions was measured. The BET surface area was determined using a Micromeritics AccuSorb gas adsorption apparatus with krypton as the adsorbate. The cellulose sample was treated at 85°C under vacuum for a week on the Micromeritics instrument. It was not exposed to the atmosphere between surface area measurements. The results from this work are in Table IV. Based on the results in Table IV, it is apparent that exposing the cellulose to high temperature under vacuum does not alter its surface area.

Included in Table IV is a value for  $Q_1 - Q_L$  which is the difference between the heat of adsorption in the first layer and the heat of liquefaction of krypton at 77 K. This number is calculated from the BET c constant. The absolute value of this number is of little significance because the heat of adsorption in the first layer is not constant with surface coverage. However, the difference can be an indicator, on a relative scale, of the energetics of the adsorption process. The absence of change in the c constant after treatment of the cellulose under high temperature and vacuum indicates that the surface energy of the sample remained unchanged. In summary, the surface composition and the surface area of the cellulose sample remain unchanged during exposure to high temperature and vacuum over an extended period of time.

TABLE IV

EFFECT OF VACUUM AND HEAT ON WHATMAN NO. 40 SURFACE

Time at 85°C and 0.0001 torr	Surface Area, m <sup>2</sup> /g	$Q_1 - Q_L$ , cal/mol
0	1.60	542
2 days	1.59	543
1 week	1.61	544

### Effect of Water on Chemisorption

The objective of this work was to investigate the physical adsorption process of a fatty acid on cellulose. Ferris (73) suggested that water is a catalyst in the chemisorption process. Becher (94,95) found that self-sizing occurred more slowly at lower pressures. The inhibition of self-sizing at lower pressures was probably due to the lack of water in the system. Hirst and Lancaster (87) found that on reactive powders water initiated the chemical reaction between stearic acid and the powder. After initiation, the reaction proceeded autocatalytically.

In this investigation, the cellulose sample was under vacuum prior to the decanoic acid adsorption experiments. Consequently, water was removed from the adsorption system and the chemisorption (esterification) reaction should have been inhibited. Chemisorption would have been apparent if, after the cellulose was exposed to acid vapor, all of the adsorbed acid could not be removed by re-outgassing. Collection of adsorption data using the Cahn balance indicated that the chemical reaction was not occurring under these adsorption conditions.

To further elucidate the effect of water on the esterification reaction, an infrared analysis of cellulose which had been treated with decanoic acid at 0% and 32% RH was undertaken. A glass saturation chamber (Fig. 13) was constructed to treat strips of Whatman No. 40 with decanoic acid in a humid atmosphere. A saturated  $MgCl_2$  aqueous solution with a relative vapor pressure of approximately 0.3 was in the side arm of the saturation vessel. Whatman No. 40 strips were suspended in the chamber from a glass hook attached to the top of the Erlenmeyer flask. Decanoic acid was in the bottom of the Erlenmeyer flask. The system was evacuated under house vacuum prior to treatment at 85°C.

Figure 14 shows Attenuated Total Reflectance (ATR) IR spectra of Whatman No. 40 filter paper treated with decanoic acid at 0% (spectrum A) and 32% RH

(spectra B + C). ATR is an infrared spectroscopy technique for acquiring spectra of surface species by reflecting the IR beam off the surface of the sample a number of times rather than transmitting the beam through the sample. Prior to acquiring spectra B and C, the treated samples were extracted in boiling benzene to remove the physically adsorbed acid. Spectrum A is the ATR spectrum of unextracted filter paper treated at 32% RH. Of interest in spectrum B is the peak at  $1728\text{ cm}^{-1}$  (indicated by the arrow) which corresponds to the carbonyl stretch of an ester. This peak establishes that chemisorption does occur at 32% RH. In spectrum C, corresponding to 0% RH treatment, a peak at  $1728\text{ cm}^{-1}$  is not found. This indicates that the esterification reaction is inhibited when water is removed from the adsorption system. In neither spectrum B nor C is there the  $1710\text{ cm}^{-1}$  peak corresponding to the decanoic acid dimer which is evident in spectrum A. This implies that all the physically adsorbed acid was removed by the benzene extraction.

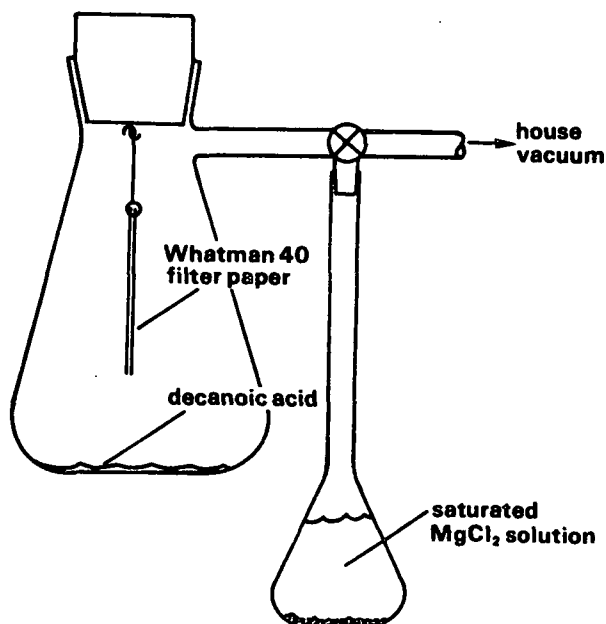


Figure 13. Glass saturation chamber.

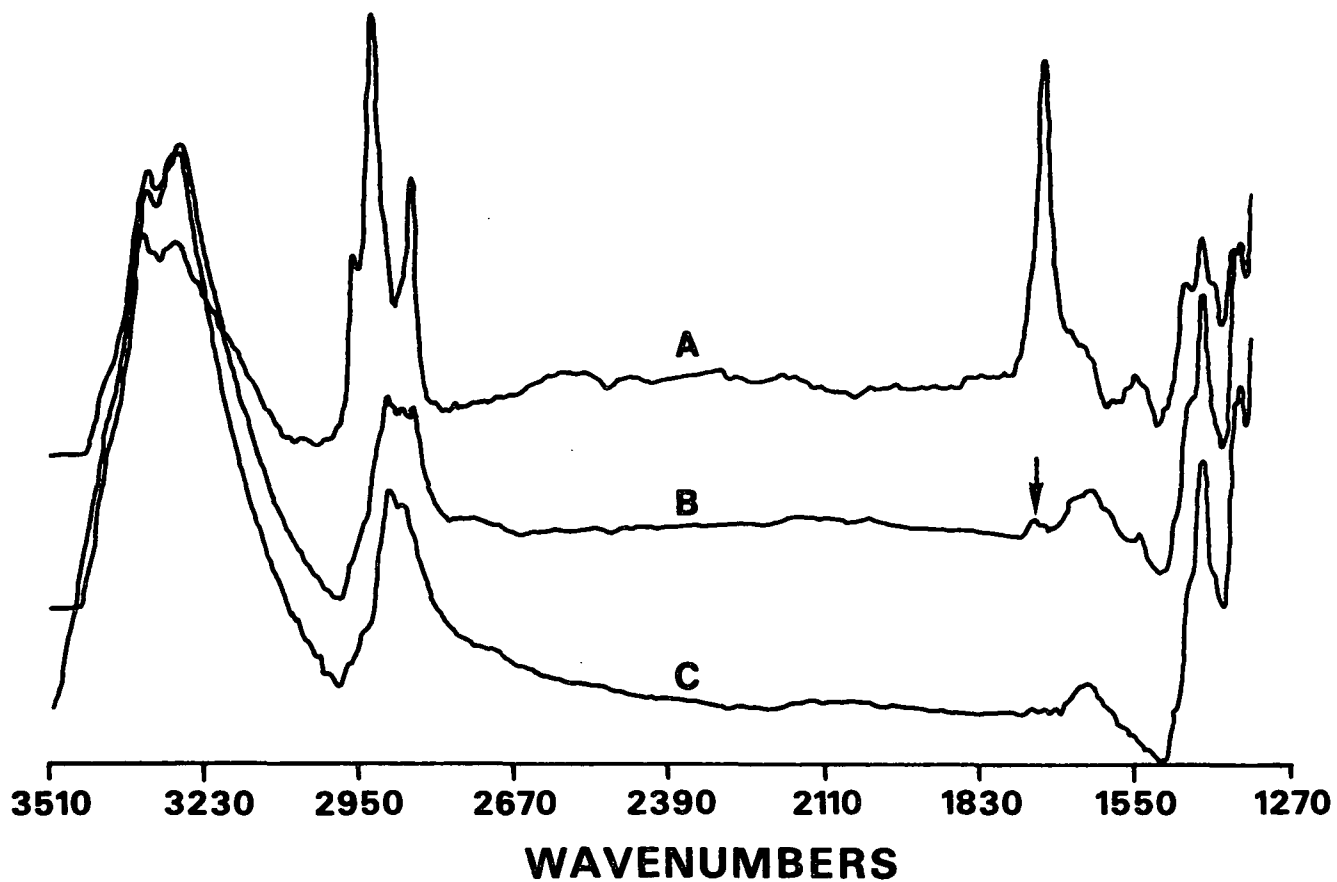


Figure 14. ATR spectra of decanoic acid treated Whatman No. 40 filter paper. (A) Unextracted with treatment at 32% RH, 46 hours at 85°C, (B) extracted with treatment at 32% RH, 46 hours at 85°C, (C) extracted with treatment at 0% RH, 70 hours at 85°C.

## ADSORPTION DATA

Decanoic acid adsorption data were collected at three temperatures: 70, 75, and 80°C. The majority of data were collected in the submonolayer region of the adsorption isotherms.

Tables V thru VII summarize the raw adsorption data and the method used to obtain that data. The sample-run column designates the sample used followed by the run number. The run number corresponds to the order in which the adsorption data were acquired. For example, sample-run 12-7 corresponds to the seventh adsorption experiment on sample 12. The acid temperature denotes the temperature of the acid reservoir for that adsorption experiment. The pressure of acid in the adsorption system is equal to the vapor pressure of the acid at the acid temperature. The actual mass of the cellulose sample is equal to the mass dial reading plus 670.4 in milligrams. The gain is the mass of acid adsorbed on the cellulose sample in micrograms. The gain is the difference between the outgassed and equilibrium weight. Experimental methods 1 and 2 are described in the Experimental section of this work.

TABLE V

## RAW ADSORPTION DATA AT 70°C

Sample-run	Acid Temp., °C	Mass Dial Reading		Weight Gain, µg	Method
		Starting Wt.	Ending Wt.		
12-17	34.7	0.68	0.831	143	1
12-18	34.8	0.64	0.780	140	1
12-19	38.6	0.64	0.813	173	2
12-20	42.5	0.64	0.842	202	2
12-21	46.4	0.64	0.886	246	2
12-22	50.3	0.64	0.974	334	2
12-23	30.9	0.63	0.740	107	1

TABLE VI

## RAW ADSORPTION DATA AT 75°C

Sample-run	Acid Temp., °C	Mass Dial Reading		Weight Gain µg	Method
		Starting Wt.	Ending Wt.		
15-5	38.8	3.715	3.844	129	1
15-6	42.1	3.715	3.889	174	2
15-7	45.3	3.715	3.922	207	2
15-8	32.5	3.668	3.758	90	1
15-9	35.4	3.668	3.782	114	2
15-10	38.6	3.668	3.805	137	2
15-11	42.0	3.625	3.793	168	1
15-12	45.2	3.625	3.831	206	2
15-13	48.0	3.625	3.856	231	2
15-14	51.8	3.625	3.924	299	2
15-15	54.6	3.598	3.920	322	1
15-16	56.7	3.598	3.951	353	2
15-17	58.6	3.598	3.984	386	2
16-7	49.8	1.700	1.970	270	1
16-8	49.9	1.682	1.949	267	1

Not all of the data acquired were used in the analysis of the adsorption isotherms. Data which were discarded were in one of the following categories:

1. Mass gains which were too high and unreproducible using a relatively clean balance
2. Adsorption experiments which did not reach an equilibrium weight gain after an excessive amount of time
3. Abnormal balance operation

All of the data which were discarded, were discarded in blocks of a number of experiments.

Upon examination of Tables V-VII, two results are evident. First, although there is variation in the outgassed weight, the variation is apparently random. There are no steady increases in the outgassed weight which would be indicative of chemisorption. Second, upon comparing adsorption experiments using methods 1

and 2, it is evident that the method has no effect on the final weight gain. This indicates that the adsorption process reached an equilibrium in both cases. Diffusion would be slower using method 2 because the system pressure was higher due to leakage and less frequent evacuation.

TABLE VII  
RAW ADSORPTION DATA AT 80°C

Sample-run	Acid Temp., °C	Mass Dial Reading		Weight Gain, µg	Method
		Starting Wt.	Ending Wt.		
13-10	47.2	9.483	9.687	204	1
13-11	47.2	9.488	9.681	193	1
13-12	52.9	9.476	9.744	268	1
13-13	55.0	9.475	9.767	292	1
13-14	59.0	9.475	9.810	335	1
13-15	62.0	9.475	9.874	399	2
13-16	65.0	9.475	9.924	449	2
13-17	68.0	9.516 <sup>a</sup>	10.014	539	1
13-18	71.4	9.516 <sup>a</sup>	10.115	640	2
13-19	75.0	9.516 <sup>a</sup>	10.291	816	2
13-20	77.0	9.516 <sup>a</sup>	10.575	1100	2
13-21	77.9	9.516 <sup>a</sup>	10.785	1310	2
12-2	34.0	0.725	0.802	77	1
12-3	35.4	0.721	0.806	85	1
12-4	35.4	0.712	0.794	82	1
12-5	38.7	0.712	0.823	111	2
12-6	38.7	0.708	0.816	108	1
12-7	42.0	0.708	0.844	136	2
12-8	39.1	0.705	0.816	111	1
12-9	45.2	0.705	0.871	166	2
12-10	48.5	0.702	0.917	215	1
12-11	34.6	0.708	0.794	86	1
12-12	38.1	0.717	0.822	105	1
12-13	40.6	0.708	0.831	123	1
12-14	46.5	0.701	0.885	184	1
12-15	50.5	0.701	0.934	233	2
12-16	41.1	0.708	0.834	126	1
24-26	46.5	7.610	7.788	178	1
24-27	51.2	7.610	7.863	253	2
30-10	34.2	3.064	3.136	72	1
30-11	42.1	3.064	3.208	144	2

<sup>a</sup>Used weight of 9.475 since this increase in weight is likely due to capillary condensation.

After the adsorption data were acquired, the acid pressure corresponding to the acid reservoir temperature was calculated from Eq. (27) or (30). The mass adsorbed was converted to mass adsorbed per gram cellulose. These data were plotted on a large sheet of graph paper and the resultant isotherms were hand-smoothed. Other than the BET analysis, all analyses of the adsorption data used data from the hand-smoothed curves.

Before using the hand-smoothed isotherms, the adsorption data were also fitted to a quadratic equation. Using the best quadratic fit, it was determined that the variance in the fit could not be explained by the variance in the data due to experimental error. Therefore, this method was not used. Higher order equations such as cubic equations were not used because fluctuations in the curves found in the higher order equations could have a significant effect on the thermodynamic analysis.

## DISCUSSION OF RESULTS

### ISOTHERM ANALYSIS

One of the fundamental methods of obtaining thermodynamic information about an adsorption system is the analysis of adsorption isotherms. From the shape of an isotherm, generalizations can be made about the adsorption process. From a series of isotherms at different temperatures, heats and entropies of adsorption as a function of surface coverage can be calculated.

#### Adsorption Isotherms - Qualitative Information

Figure 15 is an adsorption isotherm of decanoic acid on Whatman No. 40 filter paper at 80°C. The isotherm is of the common sigmoid shape (BET Type II), indicating that multimolecular adsorption is occurring. If the curve in Fig. 15 were to be extrapolated, the isotherm should asymptotically approach a relative pressure equal to 1.0, where bulk condensation begins.

It is often surmised that the first monolayer has been completed in the vicinity of the knee of the isotherm. The strength of the knee in the isotherm is indicative of the magnitude of the interaction between the adsorbate and adsorbent. In the decanoic acid adsorption isotherm the knee is indistinct, implying that the interaction between the cellulose and the adsorbed acid is not considerably stronger than the interaction of the acid with itself.

BET Type II isotherms have a linear section in the intermediate relative pressure region of the isotherm. The point at which the linear section commences, near the knee in the isotherm, is called Point B. It is often considered the point at which the first monolayer has been completed. The mass adsorbed at this point is the Point B monolayer mass and can be used to determine the

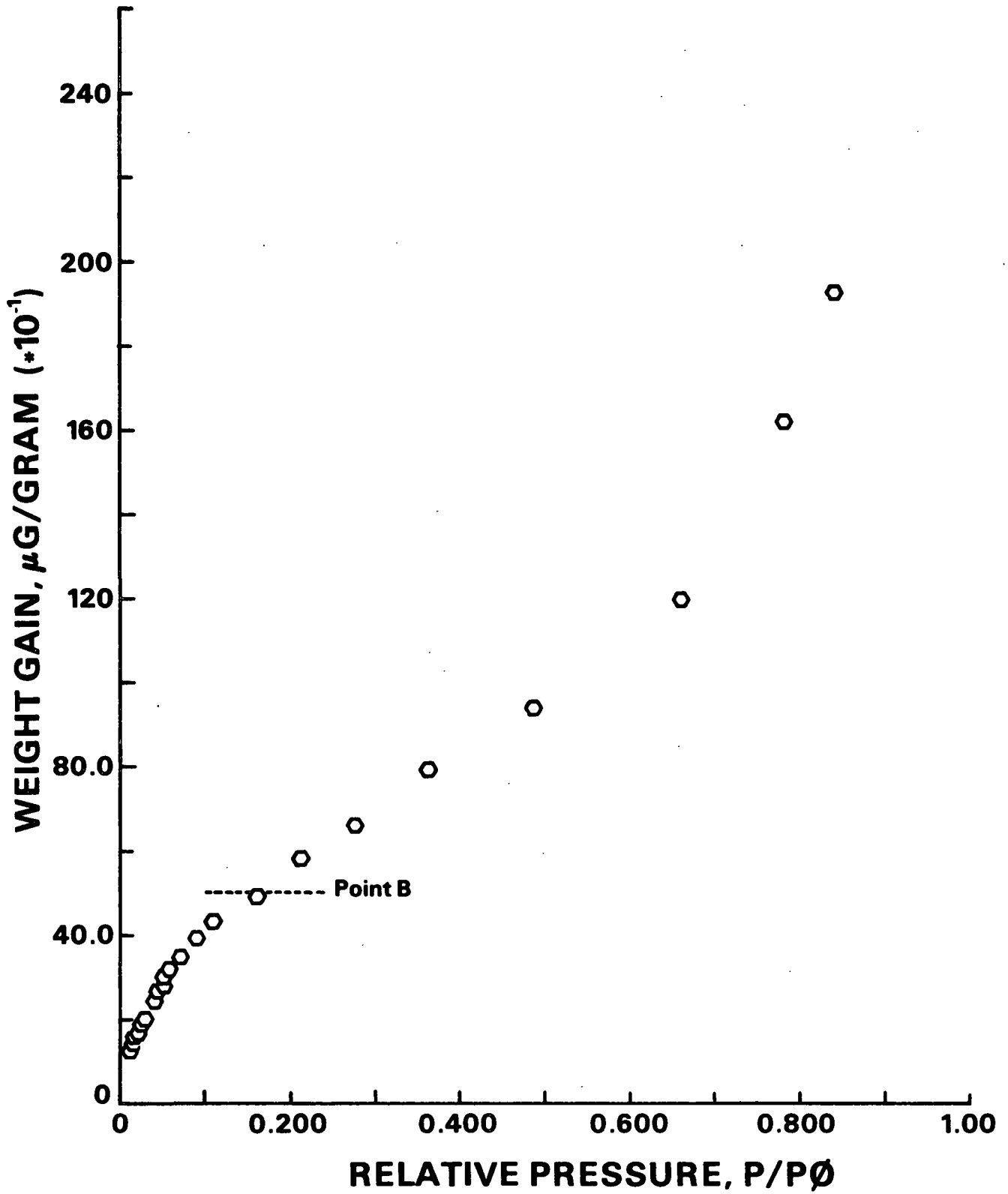


Figure 15. Adsorption isotherm of decanoic acid on Whatman No. 40 filter paper at 80°C.

adsorbent surface area. With weak kneed isotherms, such as in Fig. 15, Point B is difficult to determine accurately and is therefore an approximate value. Using the Point B method, the decanoic acid monolayer mass is approximately 500  $\mu\text{g/g}$ .

Figure 16 presents the adsorption isotherms of decanoic acid on Whatman No. 40 filter paper at 70, 75, and 80°C. The dashed line in Fig. 16 represents the BET monolayer mass. The curves in Fig. 16 were drawn to distinguish the data at the three different temperatures. They do not exactly represent the curves used in the thermodynamic analysis of the data. The curves for that analysis were drawn on a large sheet of graph paper to best fit the data.

The shape of an adsorption isotherm can provide significant information about the adsorption process. In this case, the inflection point in the 70°C isotherm suggests that two-dimensional condensation of the adsorbed acid is occurring on the cellulose surface. The inflection is weak, probably because of surface heterogeneity. Due to heterogeneity, the adsorbed acid concentration is not uniform across the cellulose surface. Therefore, two-dimensional condensation occurs over a range of relative pressures, rather than one discrete pressure. On a homogeneous surface a distinct step in the isotherm would be noticed (cf. Fig. 2).

The inflection is not as apparent at 75 and 80°C. This could be due to one of two reasons. One, the inflection in the 70°C isotherm might not be as dramatic as it appears. Considerable importance has been placed on a few points of the isotherm. However, as will be shown, adsorption isosteres show that all the adsorption data are internally consistent. Two, any step or inflection in an adsorption isotherm will diminish as the adsorption temperature is raised. Analogous to three-dimensional P-V diagrams, the step in the isotherm represents

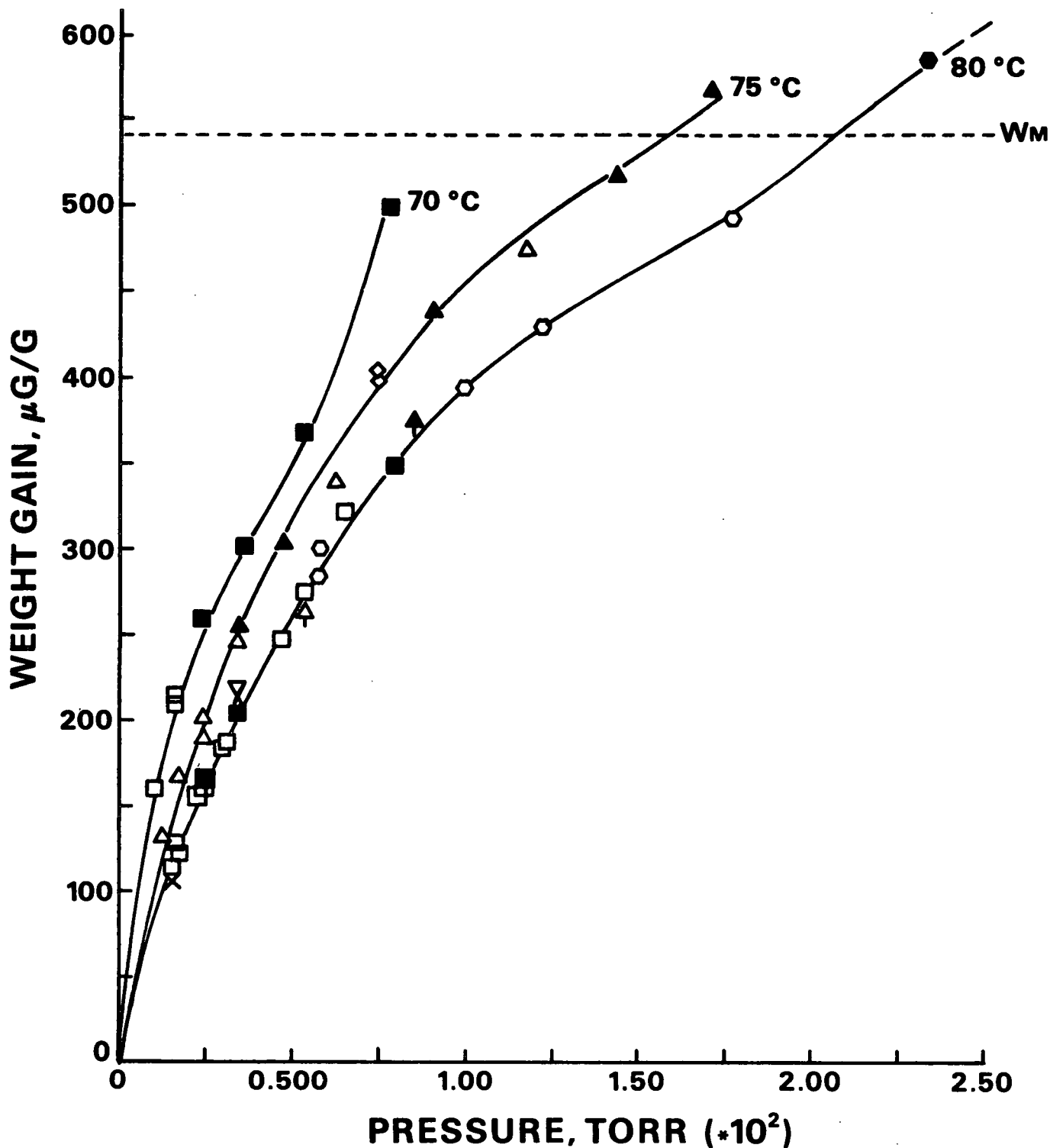


Figure 16. Adsorption isotherms of decanoic acid adsorbed on Whatman No. 40 filter paper at 70, 75, and 80°C. Dashed line represents the BET monolayer mass. Symbols represent different samples. Solid symbols represent data acquired using Method 2.

the conditions at which a "gas" and a "liquid" are in equilibrium. As the temperature is increased, the step diminishes until, at the critical temperature, two phases can no longer be distinguished.

### Thermodynamics of the Adsorption Process

Qualitatively, the adsorption isotherms suggest that two-dimensional condensation of decanoic acid is occurring on the cellulose surface in the sub-monolayer region. Interpretation of heats and entropies of adsorption as a function of surface coverage provide quantitative information about the condensation phenomenon.

#### Heat of Adsorption

One thermodynamic quantity that can be determined from adsorption data at different temperatures is the isosteric heat of adsorption. The isosteric heat is the differential heat absorbed by surroundings when an infinitesimal amount of material is adsorbed at a constant mass adsorbed. It can be calculated using the integrated form of the Clausius-Clapeyron equation:

$$\ln p = -q_{st}/RT + \text{constant} \quad (31)$$

Figure 17 presents Clausius-Clapeyron isosteres at different fractional surface coverages,  $\theta$ . A value of 540  $\mu\text{g}$  acid/g cellulose was used as the monolayer mass for the calculation of  $\theta$ . This is the BET monolayer mass calculated in a subsequent section of this work. The data for the isosteres were taken from hand-smoothed adsorption isotherms. The linearity of the isosteres is a measure of the internal consistency of the adsorption data (99).

From the slopes of the isosteres, the isosteric heat as a function of fractional surface coverage ( $\theta$ ) was calculated. These results are presented in

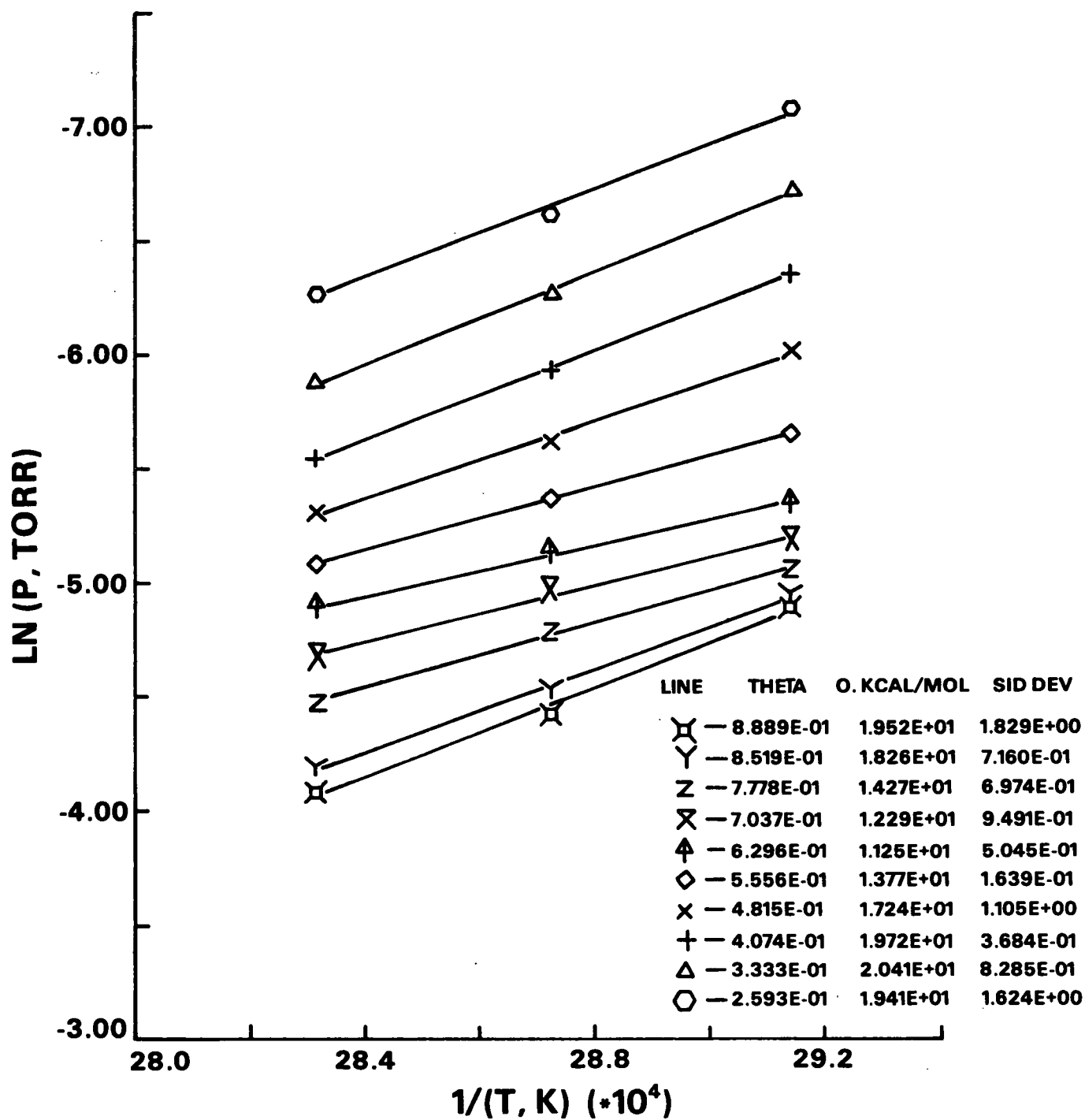


Figure 17. Clausius-Clapeyron plots of decanoic acid on Whatman No. 40 filter paper at different fractional surface coverages.

Fig. 18. The bars on the points in Fig. 18 represent the standard deviation of the isostere slope. The dashed line across the figure marks the heat of vaporization of decanoic acid at 80°C (20.2 kcal/mol).

A decrease in the heat of adsorption followed by an increase is not uncommon in adsorption systems in which two-dimensional condensation is occurring (cf. Fig. 4). However, these data are very unusual in that the heat of adsorption dips significantly below the heat of vaporization. Usually, in the submonolayer region the heat of adsorption is greater than the heat of vaporization.

The relative association of decanoic acid in the liquid and gas phases is the key to interpreting Fig. 18. In the gas phase, spectroscopic evidence has shown some association of fatty acids through the carboxyl groups (50). This is particularly evident with the lower molecular weight fatty acids. However, at pressures used in this work, decanoic acid exists predominantly as a monomer (Appendix II). In the liquid phase, the acid is highly associated through the carboxyl groups either as dimers or multimers. When decanoic acid liquefies, it not only releases heat due to van der Waals interaction with other molecules, but a significant amount of heat is released when the dimer is formed. The heat of dissociation of the dimer is approximately 14 kcal/mol (50).

At all coverages decanoic acid adsorbs on cellulose as a monomer. At lower coverages ( $\theta < 0.3$ ), the high heat of adsorption suggests that the acid probably hydrogen bonds with surface hydroxyl groups. The heat of adsorption at lower coverages is similar to the heat of vaporization. This indicates that the energy of interaction with the surface is not significantly different than its interaction in the liquid phase. The heat of vaporization involves breaking two hydrogen bonds. Most likely, the heat of adsorption involves the formation of

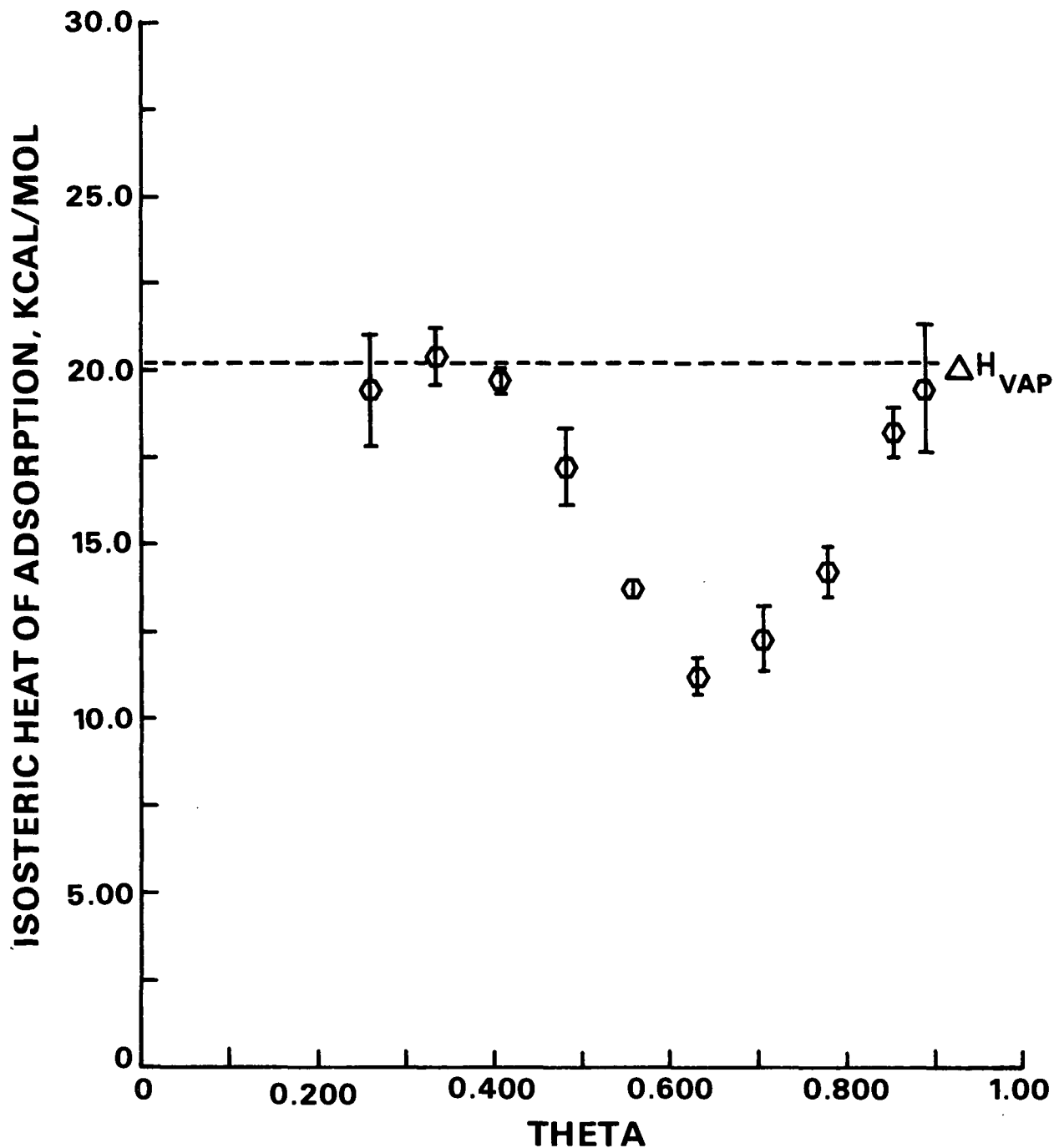


Figure 18. Isosteric heat of adsorption of decanoic acid on Whatman No. 40 filter paper. Bars on data points represent standard deviation of the slope of Clausius-Clapeyron plots. Dashed line represents heat of vaporization of decanoic acid at 80°C.

one hydrogen bond with the additional heat derived from interaction of the fatty acid tail with other surface hydroxyl groups. Surface defects, cracks and crevices will also play a role in the high heat of adsorption at low surface coverages.

As surface coverage increases, the heat of adsorption decreases. This decrease is typical of adsorption on heterogeneous surfaces, since adsorption will occur on the most active sites first, where the heat of adsorption is high. In this decreasing region the incremental acid adsorbed is less firmly attached to the surface. However, enough energy is released that a single hydrogen bond with the surface is plausible. It is also possible that the adsorbed acid is in some monomer/dimer equilibrium.

At a coverage corresponding to the minimum in the heat curve, the adsorbed film pressure on portions of the surface is high enough that two-dimensional condensation begins. The acid condenses to a state which is highly dimerized. There is a noticeable increase in the heat of adsorption upon condensation because of the heat released when the acid dimerizes. There is also additional heat released due to increased adsorbate-adsorbate van der Waals interaction of the hydrocarbon tails. This additional heat should be small relative to the heat of dimerization.

Two-dimensional condensation occurs in discrete patches across the surface at different relative pressures due to the energetic heterogeneity of the surface. Therefore, as there was not a discontinuous jump in the adsorption isotherm, the approach of the heat of adsorption to the heat of vaporization is also "smeared".

Very few systems show heats of adsorption which are less than the heat of vaporization of the adsorbate. In this system, the dip below the heat of

vaporization is reasonable. The heat curve is approaching, from above, a "heat of vaporization" for the monomer. This heat is considerably smaller than 20.2 kcal/mol, since it does not include the heat of dissociation.

As the surface coverage approaches a monolayer, the heat of adsorption approaches the heat of vaporization of the dimer. This indicates that the acid on the surface is highly dimerized at monolayer coverage.

#### Entropy of Adsorption

A second thermodynamic quantity which can be determined from adsorption data at different temperatures is the differential entropy of adsorption. It can be calculated from isosteres of the form:

$$\ln p = (s_G - \bar{s}_S) \ln T / R + \text{constant} \quad (10)$$

The differential entropy of the adsorbed phase,  $\bar{s}_S$ , is usually referenced to the liquid molar entropy,  $s_L$ , using the following equation:

$$s_L - \bar{s}_S = (s_G - \bar{s}_S) + R \ln(p/p_0) - \Delta H_{\text{vap}}/T \quad (11)$$

Figure 19 presents a number of entropy isosteres at different surface coverages. The data for the isosteres were taken from hand-smoothed adsorption isotherms. The linearity of the isosteres is a measure of the internal consistency of the adsorption data (99).

From the slopes of the isosteres, the differential entropy of adsorption as a function of fractional surface coverage ( $\theta$ ) was calculated. The differential entropy of the adsorbed phase was then referenced to the liquid molar entropy. These results are presented in Fig. 20. The bars on the points represent the standard deviation of the isostere slope. The dashed line across the

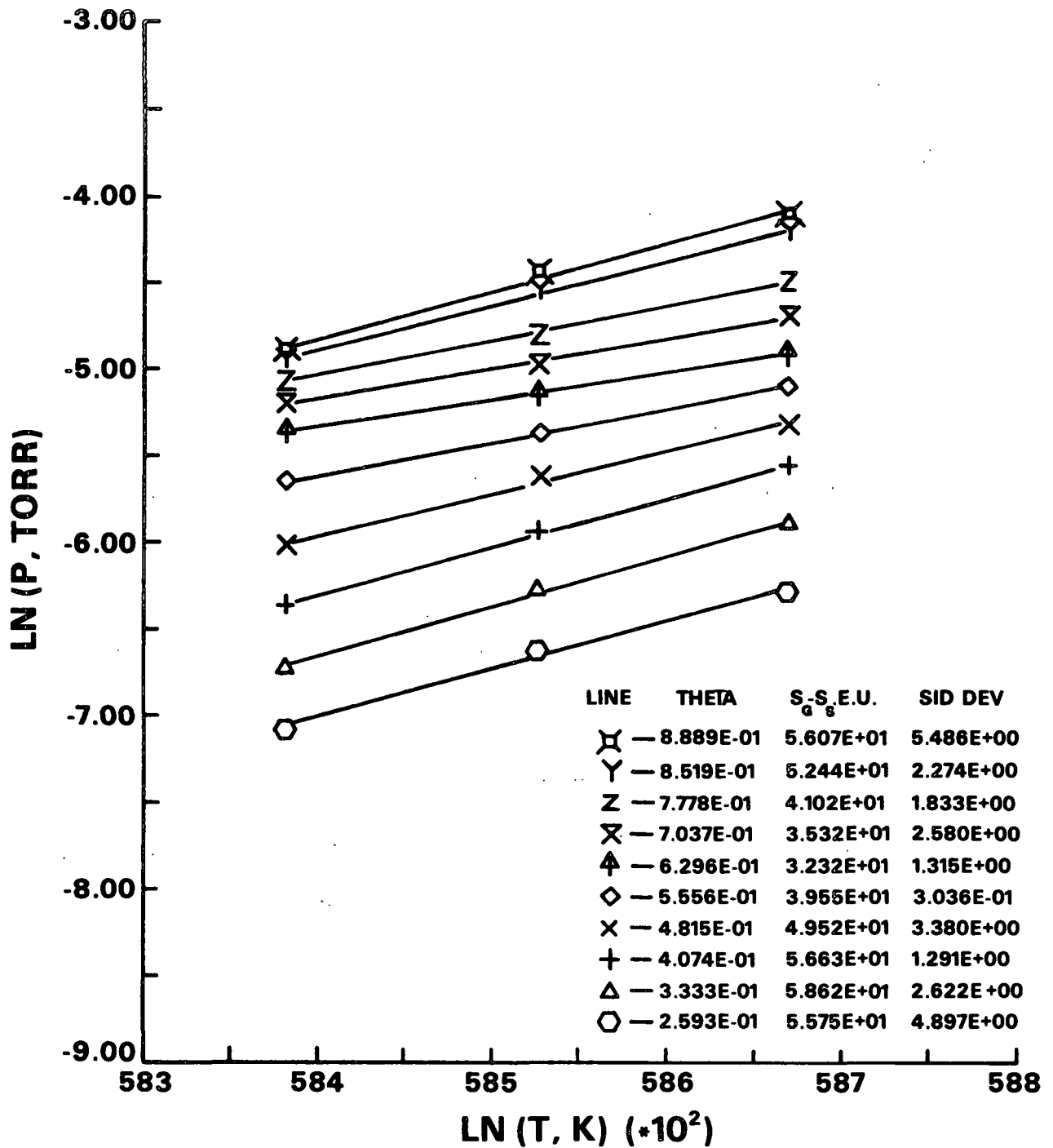


Figure 19: Adsorption isosteres for determination of differential entropy of adsorption of decanoic acid on Whatman No. 40 filter paper at different fractions of surface coverage,  $\theta$ .

figure marks the point at which the differential entropy of the adsorbed phase is equivalent to the liquid molar entropy.

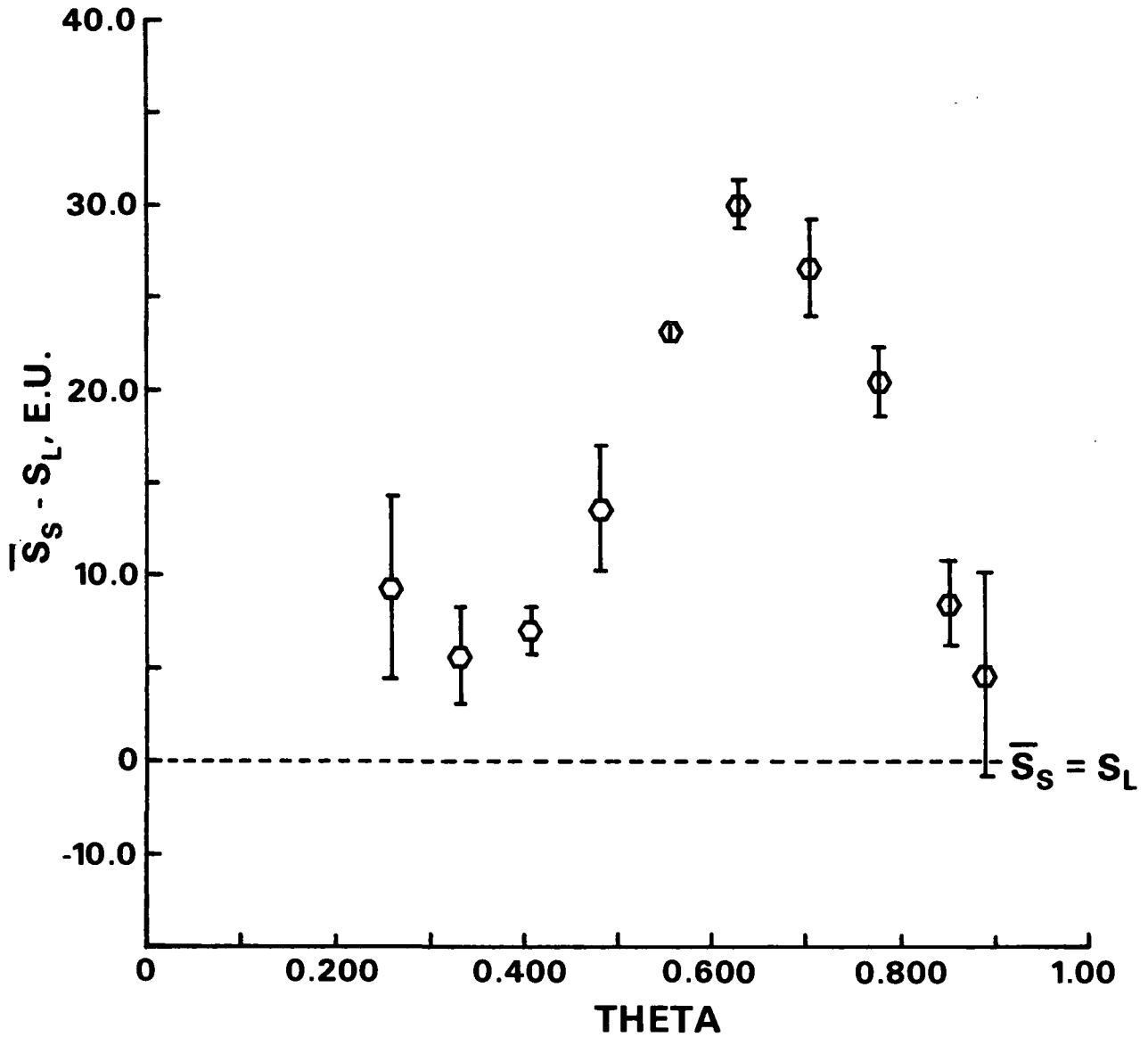


Figure 20. Differential entropy of adsorbed phase of decanoic acid on Whatman No. 40 filter paper reference to the liquid molar entropy of decanoic acid at 80°C. Bars on data points represent the standard deviation of the slope of adsorption isosteres. Dashed line represents point at which the differential entropy of the adsorbed phase is equivalent to the liquid molar entropy.

As would be expected (100), the entropy curve mirrors the heat curve (Fig. 18). The combination of these two curves results in a monotonically increasing energy plot (adsorption isotherm).

At low surface coverages ( $\theta < 0.3$ ), heat data indicate that the acid is probably hydrogen bonded to the surface. Hydrogen bonding limits the acid's mobility, implying a low entropy. As the surface coverage increases up to about  $\theta = 0.7$ , heat data show that the incremental adsorbed acid interaction with the surface weakens. This implies that the acid mobility is increasing, and thus the differential entropy of the adsorbed phase is increasing.

The coverage corresponding to the maximum in entropy signifies onset of two-dimensional condensation. At this maximum, the acid on the surface begins to dimerize in discrete patches. Statistical calculations show the change in entropy upon dimerization approximates 35 e.u. based solely upon the decrease in number of particles (50). This value has also been established experimentally (50). Therefore, the decrease in entropy upon two-dimensional condensation is due to a decrease in the number of particles on the surface when the adsorbed acid dimerizes.

As the surface coverage approaches a monolayer, the differential entropy of the adsorbed phase is approaching the liquid molar entropy. This implies that the adsorbed acid is approaching a liquidlike state which is highly dimerized.

### Two-Dimensional Condensation

Throughout this discussion the term "two-dimensional condensation" has been used without being specifically defined. It is not meant to imply that adsorbed acid condenses from a gaseous state to a liquid state. At low surface coverages, heat and entropy data indicate that the acid is probably adsorbed on specific

sites (cellulose hydroxyl groups). This is contrary to the description of a two-dimensional mobile gas. During the condensation phenomenon, there is a distinct increase in adsorbate-adsorbate interaction. The adsorbed acid is dimerizing. Therefore, at coverages less than about 0.7 monolayers the acid is unassociated or associated with the cellulose hydroxyl groups. Approaching and beyond a monolayer, the adsorbed acid is highly dimerized in a liquidlike state. Two-dimensional condensation is defined here as this distinct increase in adsorbate-adsorbate interaction.

#### ORIENTATION OF ACID ON CELLULOSE SURFACE

Of interest in this work is the orientation of decanoic acid physically adsorbed on the surface of cellulose. Knowledge of this orientation can characterize the acid interaction with the cellulose surface. R. Swanson (71) and Ferris (73) concluded that the fatty acid adsorbs with its major axis parallel to the surface of the cellulose. Mazurak (78) came to the opposite conclusion that the fatty acid is adsorbed in a "standing up" configuration.

R. Swanson (71) and Ferris (73) treated cellulose film with stearic acid and then observed how the water contact angle on the film varied as a function of the quantity of acid chemisorbed and physisorbed. They concluded that the physically adsorbed acid reclines on the surface below the chemisorbed acid/water interface, since it had no apparent effect on the contact angle. At high chemisorption levels, Swanson hypothesized that some of the physically adsorbed acid is oriented perpendicular to the surface by the high concentration of chemisorbed acid.

Mazurak (78) assumed that his fatty acid treated fibers were covered with a monolayer of stearic acid when the interaction of hexanol and decane vapors with

the treated surface was similar. When that level of adsorption was reached, the amount of acid adsorbed was much greater than would be expected if the acid reclined on the surface. He concluded that the acid must therefore be oriented perpendicular to the surface.

The orientation of decanoic acid physically adsorbed on cellulose was investigated in this work from two points of view. First, the BET theory, which assumes localized adsorption, was used to compare krypton and decanoic acid monolayer volumes. Second, the Hill Equation, which treats the adsorbed material as a two-dimensional film, was used to follow the film pressure as a function of surface coverage.

#### BET Analysis

One of the most commonly used models of adsorption isotherms is the BET equation. The BET equation can be presented in the form:

$$p/[w(p_0-p)] = 1/w_m c + [(c-1)/w_m c](p/p_0) \quad (19)$$

If the left hand side of Eq. (19) is plotted against the relative pressure,  $p/p_0$ , a straight line is usually obtained over the relative pressure range of 0.05 to 0.35. The monolayer mass,  $w_m$ , can be calculated from the slope and intercept of the BET plot. Knowing the monolayer mass and the surface area of the sample, the adsorbate molecular area can be calculated:

$$\sigma_0 = 10^{20} M \sum / w_m N \quad (31)$$

The BET plots of the adsorption data acquired at 70, 75, and 80°C are shown in Fig. 21. The isotherm data acquired at 75 and 80°C fit the BET equation over the usual range of fit. The 70°C isotherm is not modeled by the BET equation as

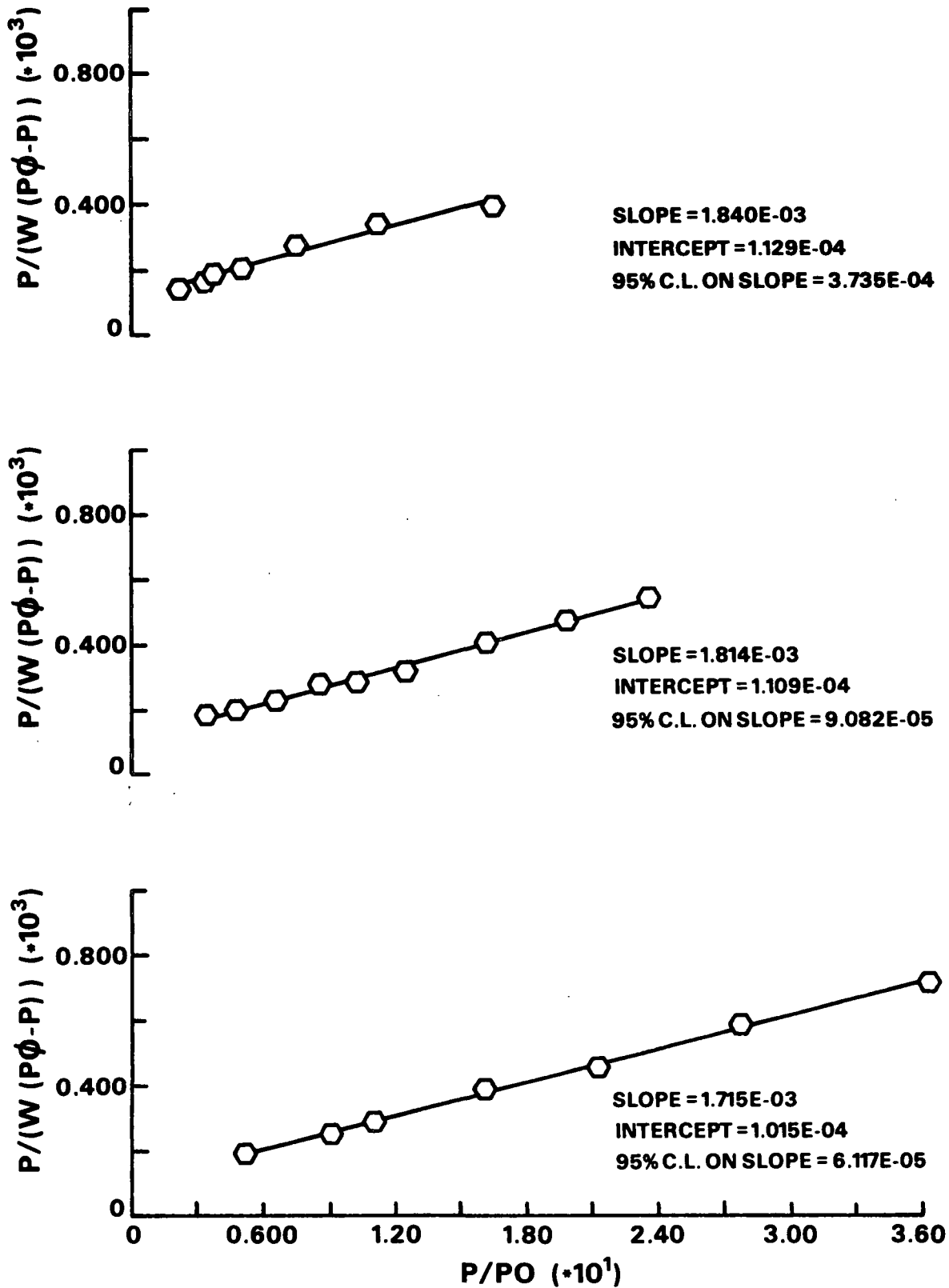


Figure 21. BET plots of decanoic acid adsorbed on Whatman No. 40 filter paper at 70°C (top), 75°C (center), 80°C (bottom).

well. The lack of fit of the 70°C isotherm can be attributed to the more dramatic step in the isotherm.

The results from the BET analysis are presented in Table VIII. The inverse variance is used as a weighting factor in determining the presented weighted average (101). The average monolayer mass compares favorably with the mass calculated using the Point B method (~ 500 µg). This is not surprising, since with a c constant of this magnitude (~ 17), the BET equation is an analytical method of determining the inflection point in the isotherm (102). The quantity  $Q_1 - Q_L$  is the difference between the heat of adsorption in the first,  $Q_1$ , and succeeding monolayers,  $Q_L$ . The heat of liquefaction,  $Q_L$ , is 20.2 kcal/mol, so, on a relative basis, the difference is not large.

TABLE VIII  
BET ANALYSIS OF DECANOIC ACID ADSORBED  
ON WHATMAN NO. 40 FILTER PAPER

Adsorption Temperature, °C	Monolayer Mass, µg	BET C constant	$Q_1 - Q_L$ kcal/mol
70.0	512 ± 82	17.3	1.94
75.0	519 ± 23	17.4	1.98
80.0	550 ± 17	17.9	2.02
Weighted av.	540 ± 22	17.5	1.98

The theoretical acid area/molecule, with its major axis oriented parallel or perpendicular to the surface, can be approximated by using the decanoic acid liquid molar volume at 80°C and the cross-sectional area of the acid determined in fatty acid monolayer studies. These calculations are presented in Appendix III and the resulting area/molecule for the two orientations is included in Table IX.

TABLE IX

MOLECULAR AREA OF DECANOIC ACID ADSORBED ON  
WHATMAN NO. 40 FILTER PAPER

Adsorption Temperature, °C	Monolayer Mass, $\mu\text{g/g}$	Molecular Area, $\text{\AA}^2$
70.0	$512 \pm 82$	$84.3 \pm 13.5$
75.0	$519 \pm 23$	$83.1 \pm 3.7$
80.0	$550 \pm 17$	$78.4 \pm 2.3$
Weighted av.	$540 \pm 22$	$79.7 \pm 3.1$
Parallel orientation (theoretical)		82.5
Perpendicular orientation (theoretical)		20.5

The BET surface area of Whatman No. 40 filter paper was determined to be  $1.51 \text{ m}^2/\text{g}$  using krypton as the adsorbate. Assuming that the same amount of surface is accessible to a decanoic acid molecule as to a krypton molecule, Eq. (31) can be used to calculate the decanoic acid molecular area. This molecular area would be equal to the surface area covered by one acid molecule. The molecular diameter of krypton is  $5.2 \text{ \AA}$  (based on a molecular area of  $21.0 \text{ \AA}^2$ ). An approximate molecular diameter for decanoic acid is  $9.8 \text{ \AA}$  (Appendix I). The only area which would not be accessible to decanoic acid but would be accessible to krypton are the pores with diameters from  $5.2$  to  $9.8 \text{ \AA}$ . Haselton (103) found that cellulose is essentially nonporous. With critical-point dried cellulose, Sommers (104) calculated that most of the surface is in pores greater than  $36 \text{ \AA}$  in diameter. Exposure to moisture and air-drying will bring about a closure of these pores (105). Since the Whatman No. 40 filter paper has been air-dried, the surface accessibility should be the same for decanoic acid and krypton.

Employing the BET surface area determined using krypton and the monolayer masses calculated from the BET plots of Fig. 21, an experimental molecular area

for decanoic acid was determined using Eq. (31). The experimental molecular areas are presented in Table IX. Upon comparison of the experimental and theoretical molecular areas it is apparent that decanoic acid is adsorbed on the Whatman No. 40 filter paper cellulose surface in the parallel orientation.

### Film Pressure - Area Analysis

The BET model of adsorption theorizes the adsorption process to be localized. An alternative procedure would be to consider the adsorbed material as a two-dimensional phase. This treatment would be analogous to the treatment of monolayers on liquid substrates. Taking this approach, Hill (24) has shown that a two-dimensional film pressure can be calculated as a function of mass adsorbed and adsorbate pressure:

$$\pi_{at p} = \frac{1000RT}{M\sum} \int_0^p w d \ln p \quad (23)$$

or

$$\pi_{at p_1} = \frac{1000RT}{M\sum} \left[ \int_{p/w \text{ as } w \rightarrow 0}^{p_1/w_1} w d \ln(p/w) + w_{at p_1} \right] \quad (24)$$

A computer program, PI, was written which calculates the film pressure,  $\pi$ , as a function of the area available per adsorbed molecule,  $\sigma$ .  $\sigma$  is inversely proportional to the mass adsorbed:

$$\sigma = \sum M(10^{20})/wN \text{ \AA}^2/\text{molec.} \quad (32)$$

The integral in Eq. (32) was evaluated by fitting a spline function to the curve of w versus  $\ln(p/w)$  and then exactly integrating the spline function. The data ( $p, w_{at p}$ ) for the curve were taken from the hand-smoothed isotherms of decanoic acid adsorbed on Whatman No. 40 filter paper. The calculations are completed only up to the BET monolayer mass, since the film pressure of multilayered

adsorbed acid would be meaningless. The film pressure-area curves for adsorption at 70°C thru 80°C are shown in Fig. 22. Program PI is on file at The Institute of Paper Chemistry Computer Center.

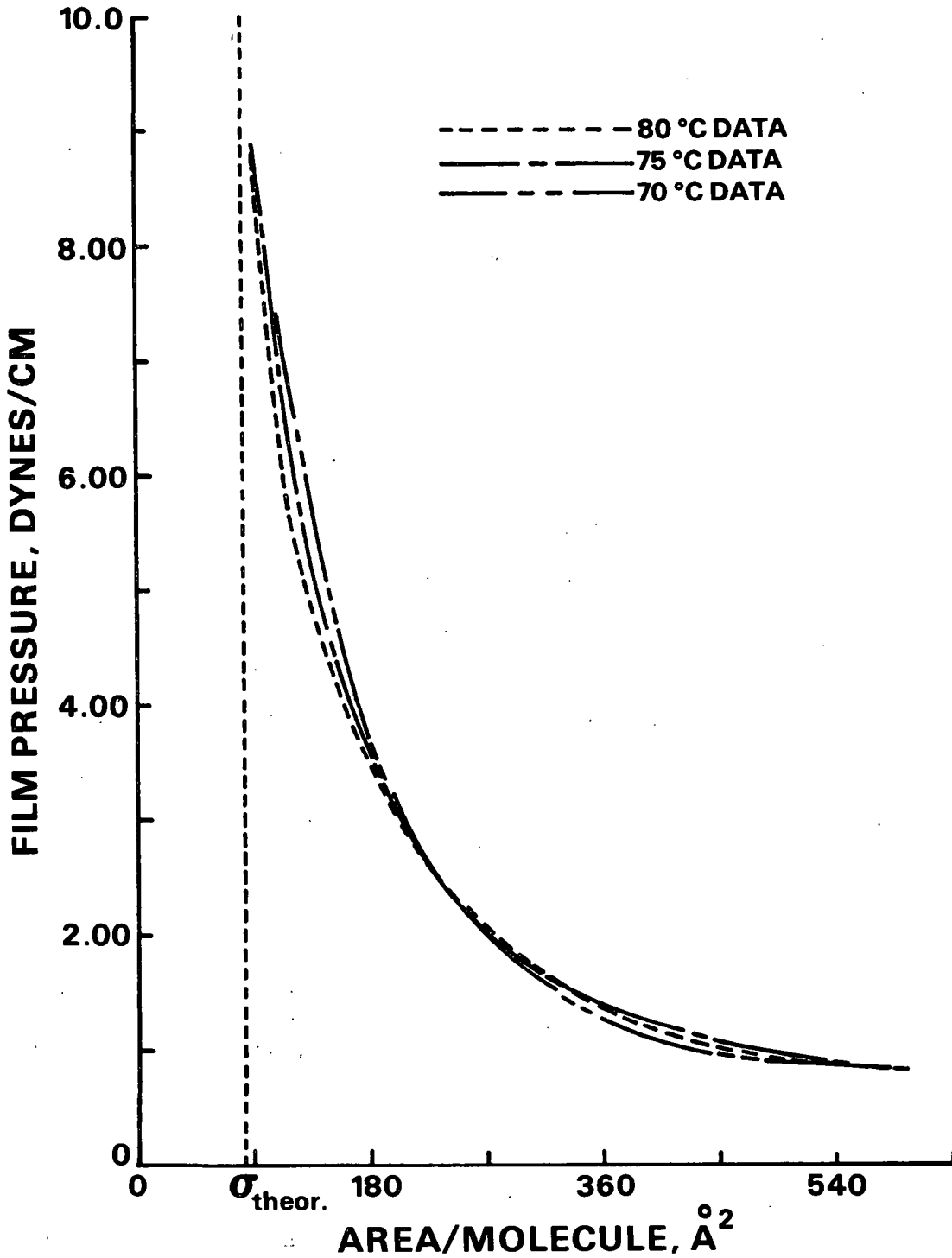


Figure 22. Surface pressure - area curves of decanoic acid on Whatman No. 40 filter paper at 70, 75, and 80°C.

The trend in the three curves does not present significant information. As expected, the area available per molecule decreases (surface coverage increases) as the film pressure increases. In studies where a step in the isotherm due to two-dimensional condensation is dramatic, a step in the film pressure-area curve is evident. This step would be analogous to that found in bulk pressure-volume curves where liquid and vapor are in equilibrium. A step is not found in the pressure-area curves of Fig. 22 because two-dimensional condensation occurs over a range of surface coverages. This points out an inherent problem in the interpretation of pressure-area curves. The interpretation of  $\pi$ - $\sigma$  curves assumes that the film pressure across the surface is constant at a given surface coverage. In an adsorption system such as decanoic acid on cellulose where the adsorbent surface is energetically heterogeneous, the film pressure will vary across the surface. The above assumption then breaks down, making it difficult to interpret the trend of the pressure-area curves.

Of particular interest in Fig. 22 is the asymptotic approach to a specific sigma value as the film pressure increases. This number would be of little interest if the approach were not asymptotic because the final sigma value is set by the computer program as corresponding to the BET monolayer mass. However, the asymptotic approach to this value indicates that when the BET monolayer mass has been reached, the film is fully compressed and the monolayer is completed. Thus, the asymptotic approach to  $\sigma_0$  indicates that the acid is oriented parallel to the cellulose surface. This approach to interpreting the adsorption isotherms confirms the results obtained using the BET analysis.

#### Conclusions on Adsorbed Acid Orientation

The conclusions drawn from BET and film pressure analysis of decanoic acid adsorbed on Whatman No. 40 filter paper are a direct determination of the

orientation of the adsorbed acid. These conclusions substantiate the hypothesis of Swanson and Ferris. R. Swanson (71) and Ferris (73) hypothesized that since physically adsorbed stearic acid has little influence on the water/cellulose film contact angle, the acid must be adsorbed with its major axis parallel to the surface of the cellulose film.

Kipling and Wright (44,45) found that stearic acid adsorbed from solution onto carbon surfaces with its major axis parallel to the surface. On oxide surfaces of electropositive elements (aluminum, titanium) stearic acid orients perpendicularly. Apparently, the perpendicular orientation was adopted on the more polar surfaces due to the ability of the acid to hydrogen bond to specific sites. However, a parallel orientation was preferred on oxides of the more electronegative silicon. They claimed that for perpendicular orientation, the heat of adsorption has to be substantial to overcome the heat of interaction of the fatty acid tail which is available in the parallel orientation. Or, the adsorption sites have to be close enough such that lateral interaction of perpendicular molecules is possible.

Applying Kipling and Wright's conclusions to the cellulose/decanoic acid system suggests that the interaction of the acid carboxyl group with the cellulose surface is not strong enough to overcome the van der Waals interaction of the fatty acid tails with the surface and other adsorbed molecules.

The evidence for parallel orientation of decanoic acid adsorbed on cellulose applies only at monolayer coverages. No direct evidence was obtained for the orientation of the fatty acid at lower coverages. However, since the parallel orientation is energetically preferred at monolayer coverage, it is proposed that the acid adsorbs in a parallel orientation at all coverages for the same reasons.

## ADSORBED ACID MOBILITY

Given that decanoic acid adsorbs on cellulose with its major axis parallel to the surface, some conclusions can be drawn about the mobility of the adsorbed acid. Gregg and Sing (107) have stated that if the experimental molecular area [using Eq. (31)] of the adsorbate is similar to that calculated assuming an adsorbed liquid phase, then the adsorbate is probably mobile on the adsorbent surface. If the adsorbed phase were localized, the molecular area of the adsorbate would be influenced by the distribution of adsorption sites.

A weak knee in the adsorption isotherm (implying a small BET  $c$  constant) also implies that the adsorbate is mobile on the surface. A small  $c$  constant indicates that the adsorbate-adsorbent interaction is not considerably stronger than the adsorbate-adsorbate interaction of the liquid phase.

The adsorbate molecular area calculated using Eq. (31) averages  $80 \text{ \AA}^2/\text{molecule}$  (Table IX). Assuming that the adsorbed phase is liquidlike with the acid molecules oriented parallel to the cellulose surface, the theoretical molecular area is  $82.5 \text{ \AA}^2/\text{molecule}$ . This calculation is in Appendix III. Also, the knee in the  $80^\circ\text{C}$  adsorption isotherm is weak and the BET  $c$  constant at all adsorption temperatures is small ( $\sim 17$ ) (Table VIII). Based on this information, it is proposed that at coverages approaching and exceeding a monolayer the adsorbed acid is mobile on the cellulose surface. At lower coverages, the adsorbed acid is probably more localized, since the high heats of adsorption indicate that some hydrogen bonding with the cellulose surface is possible.

## CHARACTERISTIC ADSORPTION CURVES

Tremaine and Gray (77) investigated the relative interaction of various adsorbates with cotton cellulose surfaces. This analysis involved the

interpretation of "characteristic adsorption curves" which are plots of  $RT\ln(p/p_0)$  versus  $\theta$ . These curves will be nearly identical for isotherms of a given adsorbate measured at different temperatures.

If gas phase ideality is assumed, the function  $RT\ln(p/p_0)$  is the difference in free energy of the adsorbate vapor at pressures  $p$  and  $p_0$  at constant temperature,  $T$ . At constant  $T$  and  $P$ , the free energies of two phases in equilibrium are equal. So, the function  $RT\ln(p/p_0)$  can also be described as the difference in free energy of a mole of adsorbate in the adsorbed phase and the liquid phase. This function can then be qualitatively related to the interaction of the adsorbate with the adsorbent surface. The more negative the function  $RT\ln(p/p_0)$ , the greater the interaction with the surface. Figure 23 is the characteristic curve for the adsorption of decanoic acid on Whatman No. 40 filter paper at 70, 75, and 80°C.

Figure 24 shows characteristic curves of adsorption on cellulose obtained by Tremaine and Gray (77) and also the present results for decanoic acid. Tremaine and Gray showed that the surface-adsorbate attraction decreased from the alkan-1-ols to dioxane to decane. This trend is expected since the alcohols can interact strongly with the cellulose hydroxyl groups. The decanoic acid adsorption data show the strongest interaction. This also could be predicted on the basis of its ability to interact with the cellulose hydroxyl groups.

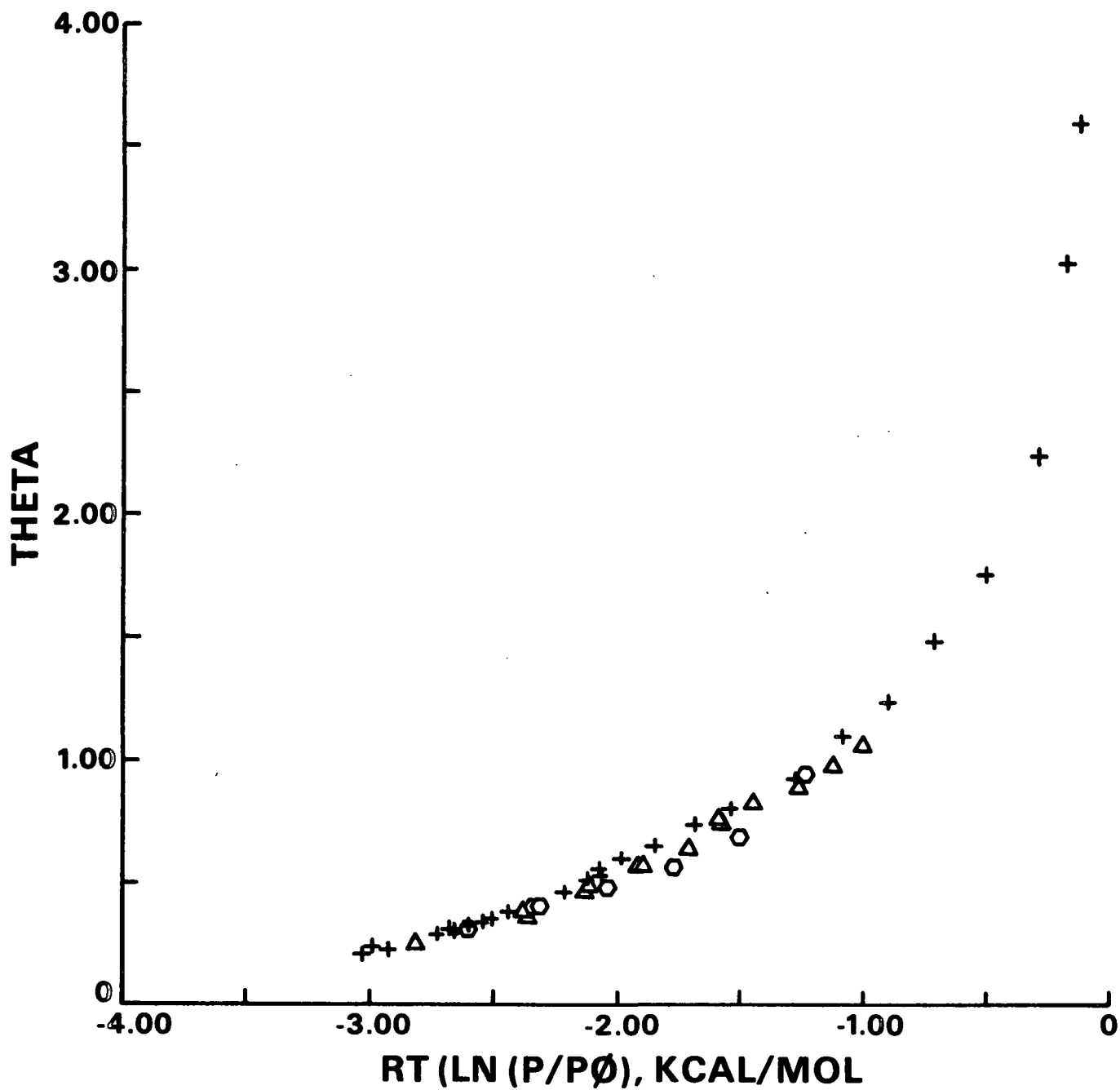


Figure 23. Characteristic curves of decanoic acid on Whatman No. 40 filter paper at: 0, 70°C;  $\Delta$ , 75°C; + 80°C.

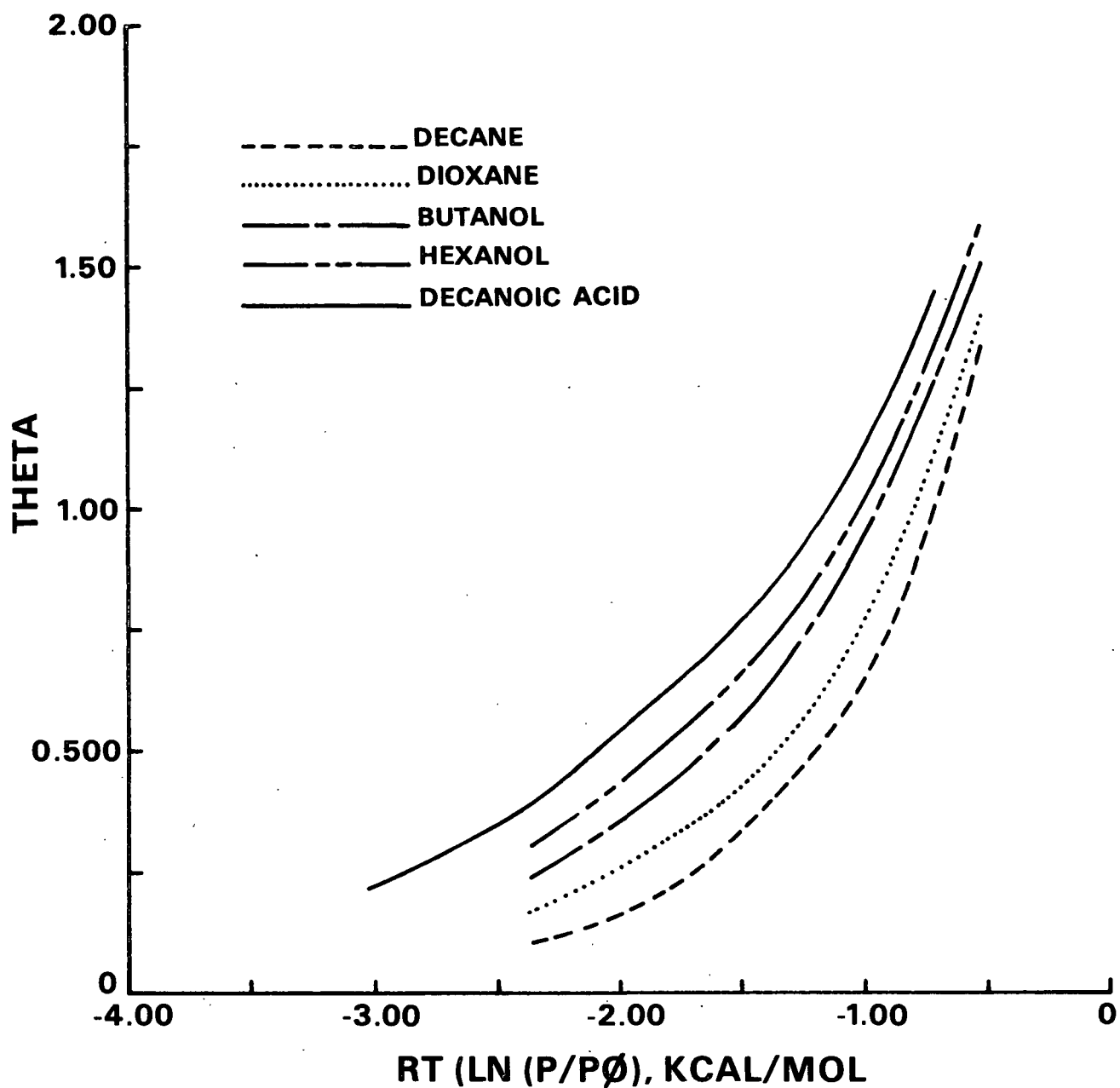


Figure 24. Characteristic curves of several adsorbates on cellulose. Decane, dioxane, butanol and hexanol data from Tremaine and Gray (77). Decanoic acid data from present work.

## SUMMARY OF CONCLUSIONS

It is known (66,71,73) that fatty acids can adsorb on the surface of cellulose from the vapor phase and chemically react with the cellulose hydroxyl groups through an esterification reaction. The objective of this study was to investigate, on a fundamental level, the physical adsorption process which precedes this chemical reaction.

An infrared analysis of cellulose treated with decanoic acid at 0% and 32% RH showed that the esterification reaction is inhibited when water is removed from the adsorption system. Also, during the acquisition of adsorption data, it was found that all adsorbed acid could be removed by evacuation. This indicated that no acid was chemically bonded to the surface. This information shows that water is needed for the chemical reaction to occur. The esterification process is probably acid catalyzed and a proton from water can act as the catalyst.

BET analysis and film-pressure area curves showed that decanoic acid adsorbs on cellulose with its major axis parallel to the surface. This conclusion supports previous work (71,73) which determined that the physically adsorbed acid reclines on the surface below the chemisorbed acid/water interface. The orientation of the fatty acid also indicates that the interaction of the acid carboxyl group with the cellulose surface is not strong enough to overcome the van der Waals interaction of the fatty acid tails with the surface and other adsorbed molecules.

The evidence for parallel orientation of decanoic acid adsorbed on cellulose applies only at coverages approaching a monolayer and beyond. No direct evidence was obtained for the orientation of the fatty acid at lower coverages. However, since the parallel orientation is energetically preferred at monolayer

coverage, it is proposed that the acid adsorbs in a parallel orientation at all coverages for the same reasons.

Adsorption data indicated that cellulose has a low surface energy. Qualitatively, it can be stated that the interaction of acid with the surface is not significantly stronger than the adsorbate-adsorbate interaction. Comparing BET surface areas obtained using krypton and decanoic acid as adsorbates shows that the molecular area of the adsorbed molecule is similar to that of the acid molecule in the liquid phase. This information suggests that the adsorbed molecules are mobile on the cellulose surface as opposed to a localized interaction.

A thermodynamic analysis of the adsorption process in the submonolayer region showed a distinct variation in the isosteric heat and differential entropy as a function of surface coverage. Decanoic acid adsorbs as a monomer. Up to a fractional coverage approximating 0.7, the acid exists on the surface as a monomer or in some monomer/dimer equilibrium. At the lowest coverages, the heat of adsorption is high enough that hydrogen bonding with the cellulose is probable. At a fractional coverage exceeding 0.7, two-dimensional condensation begins in discrete patches across the cellulose surface. At monolayer completion, the heat and entropy of adsorption indicate that the adsorbed fatty acid is highly dimerized. The adsorbed phase at monolayer completion can be approximated by the thermodynamic properties of liquid decanoic acid.

SUGGESTIONS FOR FUTURE RESEARCH

Ferris (73) proposed that a monomer of acid in the vapor phase could adsorb on cellulose, quickly dimerize, and dissociate again to the monomer in some equilibrium. Any monomer on the surface could then slowly chemisorb by esterification with the cellulose hydroxyl groups (Fig. 25). Investigation of the physical adsorption process (steps A and B) was the goal for this work. Further understanding of the entire adsorption process can lead toward development of methods of initiating sizing or inhibiting self-sizing.

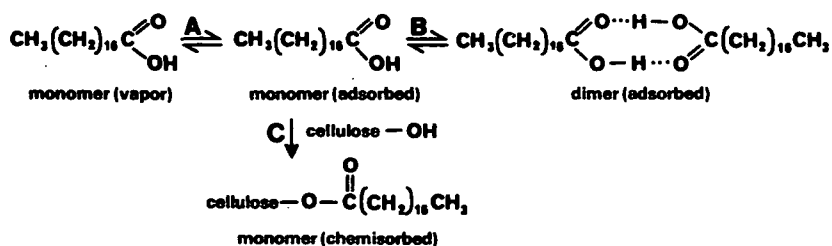


Figure 25. Proposed mechanism for the vapor phase sizing of cellulose (73).

Decanoic acid adsorption work has indicated that water has considerable influence on the esterification reaction (step C). Most likely, the esterification reaction is acid-catalyzed and water is the catalyst. However, a kinetic analysis of the effect of water on the esterification reaction should be completed to fully understand this mechanism.

This work indicates that the monomer/dimer equilibrium constant might vary with surface coverage. At coverages greater than a monolayer the adsorbed acid is highly associated, whereas at lower coverages a significant amount of acid is adsorbed on the surface as a monomer. It would seem that the rate of chemisorption could be strongly dependent upon surface coverage. A kinetic analysis of the chemisorption process as a function of surface coverage would also prove beneficial.

NOMENCLATURE

a	= adsorbate activity
A	= adsorbent surface area
Å	= Angstrom unit
c	= BET constant
$E_s$	= energy of adsorbed phase
$G_s$	= free energy of adsorbed phase
$h_G$	= molar enthalpy of adsorbate in gas phase
$h_s$	= molar enthalpy of adsorbed phase
$\bar{h}_s$	= differential molar enthalpy of adsorbed phase
$H_s$	= total enthalpy of adsorbed phase
$\Delta H_{vap}$	= heat of vaporization of adsorbate
M	= molecular weight
micron	= 0.001 mm Hg pressure
$n_a$	= number of moles of adsorbent
$n_s$	= number of moles of adsorbate in adsorbed phase
N	= Avogadro's number
p	= adsorbate vapor pressure
$p_0$	= adsorbate saturation vapor pressure
$q_d$	= calorimetric heat of adsorption
$q_{st}$	= isosteric heat of adsorption
$Q_1$	= BET heat of adsorption in first monolayer
$Q_L$	= BET heat of adsorption in 2nd and succeeding layers
R	= ideal gas constant
RH	= relative humidity
$s_G$	= molar entropy of adsorbate vapor
$s_s$	= molar entropy of adsorbed phase

$s_l$	= molar entropy of adsorbate liquid
$\bar{s}_s$	= differential molar entropy of adsorbed phase
$S$	= total entropy of adsorbed phase
$T$	= absolute temperature
torr	= 1.0 mm Hg pressure
$v_G$	= molar volume of adsorbate vapor
$\bar{v}_s$	= differential molar volume of adsorbed phase
$V_s$	= total volume of adsorbed phase
$w$	= mass adsorbed
$w_m$	= BET monolayer mass
$\gamma_0$	= surface energy of clean surface
$\gamma_s$	= surface energy of surface with adsorbate
$\theta$	= fractional surface coverage
$\mu_G$	= chemical potential of adsorbate vapor
$\mu_s$	= chemical potential of adsorbed phase
$\pi$	= two-dimensional surface pressure
$\sigma$	= surface area per adsorbed molecule
$\sigma_s$	= surface area covered by one adsorbed molecule
$\Sigma$	= specific surface area

#### ACKNOWLEDGMENTS

I wish to express my appreciation to the members of my thesis advisory committee: Dr. J. W. Swanson, the initial chairman, Dr. R. A. Stratton, the chairman over the final portion, and Dr. T. J. McDonough. These faculty members provided advice and support without which this work could not have been completed.

The overall help from faculty, staff and students has been sincerely appreciated. Special thanks go to Mr. L. J. Straub for his assistance in keeping the experimental equipment operational, and Mr. J. P. Rademacher for his assistance with the infrared spectroscopy work.

The financial support of The Institute of Paper Chemistry and its member companies enabled the completion of this work and it is gratefully acknowledged.

Finally, I wish to thank my wife, Sue, who, while on a simultaneous journey through the Institute, managed to find time to serve as an excellent sounding board and provide unending support.

LITERATURE CITED

1. Adamson, A. W. Physical chemistry of surfaces. 3rd ed. Chap. V. New York, Interscience, 1976. 698 p.
2. Langmuir, I., Met. Chem. Eng. 15:468-70(1916).
3. Zettlemyer, A. G., American Scientist 47:216-33(1959).
4. Ross, S. and Olivier, J. P. On physical adsorption. p. 8. New York, Interscience, 1964.
5. Shaw, D. J. Introduction to colloid and surface chemistry. 2nd ed. Chap. 5. London, Butterworths, 1970. 236 p.
6. Laidler, K. J. Chemisorption. In Emmetts's Catalysis. Vol. 1. Pt. 1. p. 75-118. New York, Reinhold, 1954.
7. Adamson, A. W. Physical chemistry of surfaces. 3rd ed. p. 644. New York, Interscience, 1976.
8. Brunauer, S. The adsorption of gases and vapors. Vol. 1. p. 150. Princeton, Princeton Univ. Press, 1945.
9. Clark, A. The theory of adsorption and catalysis. Chap. 1. New York, Academic Press, 1970. 418 p.
10. Aveyard, R. and Haydon, D. A. An introduction to the principles of surface chemistry. p. 182-187. Cambridge, University Press, 1973.
11. Young, D. M. and Crowell, A. D. Physical adsorption of gases. Chap. 3. London, Butterworths, 1962. 426 p.
12. Pace, E. L. Adsorption thermodynamics and experimental measurement. In Flood's The solid-gas interface. Vol. 1. New York, Marcel Dekker, 1967.
13. Brunauer, S., Emmett, P. H., and Teller, E., JACS 60:309(1938).
14. Langmuir, I., JACS 40:1361(1918).
15. Brunauer, S. Discussion, Chap. 10. In Gomer and Smith's Structure and properties of solid surfaces. p. 395. Chicago, Univ. of Chicago Press, 1953.
16. Halsey, G. D., J. Chem. Phys. 16:931(1948).
17. Halsey, G. D., Advanc. Catalys. 4:259(1952).
18. Hill, T., J. Chem. Phys. 14:263(1946).
19. Barber, H. A. The determination of the site energy distribution of surface of cellulose fibers by gas adsorption methods. Doctor's Dissertation. Appleton, Wis., The Institute of Paper Chemistry, 1968. 107 p.

20. Ross, S. and Olivier, J. P. On physical adsorption. New York, Interscience Publishers, 1964. 401 p.
21. Volmer, M., Z. Phys. Chem. 115:253(1925).
22. Harkins, W. D. and Jura, G., JACS 66:1366(1944).
23. Gibbs, J. W. The collected works of J. W. Gibbs. Vol. 1. New York, Longmans, 1931.
24. Hill, T. L., J. Chem. Phys. 17(6):520-535(1949).
25. Adamson, A. W. Physical chemistry of surfaces. 3rd ed. p. 572. New York, Interscience, 1976.
26. Fisher, B. B. and McMillan, W. G., JACS 79:2969(1957).
27. Adamson, A. W. Physical chemistry of surfaces. 3rd ed. p. 591. New York, Interscience, 1976.
28. Nagao, M., J. Phys. Chem. 75:3822(1971).
29. Kittaka, S., Kanemoto, S., and Morimoto, T., JCS Faraday I 74:676-85(1978).
30. Kittaka, S., Morishige, K., Fujimoto, T., and Morimoto, T., J. Colloid Interface Sci. 72(2):191-9(1979).
31. Kittaka, S., Nishiyama, J., Morishige, K., and Morimoto, T., Colloids Surfaces 3(1):51-60(1981).
32. Day, R. E. and Parfitt, G. D., Trans. Faraday Soc. 63:708-16(1967).
33. Dawson, P. T., J. Phys. Chem. 71:838-44(1967).
34. Morishige, K. and Kittaka, S., Surf. Sci. 120:223-38(1982).
35. Bennett, M. K. and Zisman, W. A., J. Phys. Chem. 71(7):2075-82(1967).
36. Rideal, E. and Tadayan, J., Proc. Roy. Soc. (London) A225(1162):346-56(1954).
37. Yiannos, P. N. Molecular reorientation of some fatty acids when in contact with water. Doctor's Dissertation. Appleton, Wis., The Institute of Paper Chemistry, 1960. 115 p.
38. Hasegawa, M. and Low, M. J. D., J. Colloid Interface Sci. 30(3):378-86(1969).
39. Cook, H. D. and Ries, H. E., Jr., J. Phys. Chem. 63(2):226-33(1959).
40. Young, J. E., Austral. J. Chem. 8(2):173-93(1955).
41. Smith, H. A. and Allen, K. A., J. Phys. Chem. 58(6):449-52(1954).
42. Timmons, C. O., J. Colloid Interface Sci. 43(1):1-9(1973).

43. Timmons, C. O., Patterson, R. L. and Lockhart, L. B., Jr., *J. Colloid Interface Sci.* 26:120-7(1968).
44. Kipling, J. J. and Wright, E. H. M., *JCS* 1962:855.
45. Kipling, J. J. and Wright, E. H. M., *JCS* 1963:3382.
46. Kipling, J. J. and Wright, E. H. M., *JCS* 1964:3535.
47. Rahman, M. A., Basu, S. K., Roychoudhury, A. and Ghosh, A. K., *J. Colloid Interface Sci.* 85(2):452(1982).
48. Dacre, B., Savory, B. and Wheeler, P. A., *JCS Faraday I* 77(6):1297-307 (1981).
49. Dacre, B. and Wheeler, P. A., *JCS Faraday I* 77:1285-96(1981).
50. Allen, G. and Caldren, E. F., *Quart. Rev.* 7:255-78(1953).
51. Sinclair, R. G., McKay, A. F. and Jones, R. N., *JACS* 76:2570-5(1952).
52. Harris, J. T., Jr. and Hobbs, M. E., *JACS* 76:1419(1954).
53. Gillette, R. H. and Daniels, F., *JACS* 58:1139(1936).
54. Millikan, R. C. and Pitzer, K. S., *J. Chem. Phys.* 27(6):1305-8(1957).
55. Davies, M. M. and Sutherland, G. B. B. M., *J. Chem. Phys.* 6:755-66(1938).
56. Hasegawa, M. and Low, M. J. D., *J. Colloid Interface Sci.* 29:593(1969).
57. Marshall, K. and Rochester, C. H., *JCS Faraday I* 1975:1754-61(1975).
58. Yang, R. T., Low, M. J. D., Haller, G. L. and Fenn, J., *J. Colloid Interface Sci.* 44(2):249-258(1973).
59. Jakobsen, R. J. Application of FT-IR to surface studies. In Ferraro and Basile's Fourier transform infrared spectroscopy. Vol. 2. p. 165-91. New York, Academic Press, 1979.
60. Howe, R. F. and Metcalfe, A., *JCS Faraday I* 1972:393-402(1972).
61. McManus, J. C. and Low, M. J. D., *J. Phys. Chem.* 72:2378-84(1968).
62. Rochester, C. H. and Topham, S. A., *JCS Faraday I* 75:872(1979).
63. Rochester, C. H. and Topham, S. A., *JCS Faraday I* 75:1259(1979).
64. Griffiths, D. M. and Rochester, C. H., *JCS Faraday I* 1977:1988-97(1977).
65. Kipling, J. J. and Wright, E. H. M., *J. Phys. Chem.* 67:1789(1963).
66. Swanson, J. W. and Cordingly, S., *Tappi* 42(10):812(1959).

67. Buchanan, M. A., Burson, S. L. and Springer, C. H., Tappi 44(8):576-80 (1961).
68. Sinclair, G. D., Evans, R. S. and Sallans, H. R., Pulp Paper Mag. Can. 1961:t23-27(1961).
69. Swanson, J. W., unpublished work, 1965.
70. Takeyama, S. and Gray, D. G., Cellulose Chem. Technol. 16:133-42(1982).
71. Swanson, R. E. The influence of molecular structure of vapor phase chemisorbed fatty acids present in fractional monolayer concentrations on the wettability of cellulose film. Doctor's Dissertation. Appleton, Wis., The Institute of Paper Chemistry, 1976. 153 p.
72. Swanson, R. E., Tappi 61(7):77-80(1978).
73. Ferris, J. L. The wettability of cellulose film as affected by vapor phase adsorption of amphipathic molecules. Doctor's Dissertation. Appleton, Wis., The Institute of Paper Chemistry, 1974. 154 p.
74. Becher, J. J., unpublished work, 1976.
75. Becher, J. J., unpublished work, 1977.
76. Soteland, N. and Loras, V., Svensk Papperstid. 79(7):203(1976).
77. Tremaine, P. R. and Gray, D. G., JCS Faraday I 71:2170-85(1975).
78. Mazurak, P. A. Gas chromatographic characterization of adsorbent cellulose surfaces. Doctor's Dissertation. Appleton, Wis., The Institute of Paper Chemistry, 1979. 156 p.
79. Dorris, G. M. and Gray, D. G., J. Colloid Interface Sci. 71:93(1979).
80. Katz, S. and Gray, D. G., J. Colloid Interface Sci. 82(2):318-25(1981).
81. Columbo, E. A., Immergut, E. H., J. Polymer Sci. C 31:137(1970).
82. Walker, D. C. and Ries, H. E. Advances in Chemistry Series No. 43. p. 295-301. Washington, American Chemical Society, 1964.
83. Tremaine, P. R., Mohlin, U.-B., and Gray, D. G., J. Colloid Interface Sci. 60:548(1977).
84. Dorris, G. M. and Gray, D. G., JCS Faraday I 77:725-40(1981).
85. Campbell, W. E. Proceedings of the friction and surface finish conference. p. 197. Cambridge, USA, M.I.T., 1940. Work cited in reference (40).
86. Wan, C.-Z. and Haller, G. L., J. Phys. Chem. 83(9):1154-60(1979).
87. Hirst, W. and Lancaster, J. K., Trans. Faraday Soc. 47:315(1951).
88. Ingold, C. K. Structure and mechanisms in organic chemistry. 2nd ed. Ithaca, NY, Cornell Univ. Press, 1969. 1266 p.

89. Biddle Bulletin 43b, James G. Biddle Instruments Co., p. 6.
90. Colson, N., personal communication, 1982.
91. Dorris, G. M. and Gray, D. G., JCS Faraday I 77(1):713-24(1981).
92. Micromeritics Materials Analysis Laboratory, Dec. 9, 1982.
93. Platt, W. M., Unpublished work, 1983.
94. Whalen, J. W., Vacuum Microbalance Tech. 8:121-130(1971).
95. Dushman, S. Scientific foundations of vacuum technique. p. 65. New York, John Wiley and Sons, 1949.
96. Davies, M. and Malpass, V. E., JCS 1961:1048-55.
97. Spizzichino, C., J. Recherches Centre National Recherche Sciences 34:1-24(1956).
98. De Kruif, C. G., Schaake, R. C. F., van Miltenburg, J. C., van der Klauw, K. and Blok, J. G., J. Chem. Thermodynamics 14:791-8(1982).
99. Young, D. M. and Crowell, A. D. Physical adsorption of gases. p. 4. London, Butterworths, 1962.
100. Adamson, A. W. Physical chemistry of surfaces. 3rd ed. p. 602. New York, Interscience, 1976.
101. Hoel, P. G. Introduction to Mathematical Statistics. 4th ed. p. 128-9. New York, John Wiley and Sons, Inc., 1971.
102. Gregg, S. J. and Sing, K. S. W. Adsorption, surface area and porosity. 2nd ed. p. 48. New York, Academic Press, 1982.
103. Haselton, W. R., Tappi 37(9):404-12(1954).
104. Sommers, R. A., Tappi 46(9):562-9(1963).
105. Swanson, J. W. The porous nature of pulpwood fibers. In Gregg, Sing, and Stoeckli's Characterization of porous solids. p. 339-42. London, Society of Chemical Industry, 1979.
106. Gregg, S. J. and Sing, K. S. W. Adsorption, surface area and porosity. 2nd ed. p. 70. New York, Academic Press, 1982.
107. Singleton, W. S. Solution properties. In Markley's Fatty Acids. 2nd ed. Part 1. p. 628. New York, Interscience, 1960.
108. Singleton, W. S. Properties of the liquid state. In Markley's Fatty Acids. 2nd ed. Part 1. p. 541. New York, Interscience, 1960.
109. Adamson, A. W. Physical chemistry of surfaces. 3rd ed. p. 140. New York, Interscience, 1976.

APPENDIX I

ESTIMATION OF THE MEAN FREE PATH OF DECANOIC ACID AT PRESSURES USED DURING ADSORPTION EXPERIMENTS

I. Molecular Diameter of Decanoic Acid

Assumption 1.  $\delta_1$  = molecular length = 15.95 Å [extrapolation of data from monolayer studies on C<sub>14</sub>, C<sub>18</sub>, and C<sub>22</sub> (107)].

Assumption 2. molecular volume =  $\sum$  atomic volumes.

Atom	Covalent Radius, Å	Volume, Å <sup>3</sup>	X	No. atoms	=	Total Volume, Å <sup>3</sup>
C	0.77	1.91		10		19.1
H	0.32	0.137		20		2.74
O	0.73	1.63		2		3.26
<hr/>						
C <sub>10</sub> H <sub>20</sub> O <sub>2</sub>						25.1

$$\delta_2 = 3.63 \text{ \AA}$$

Assumption 3. The actual molecular diameter is the average of  $\delta_1$  and  $\delta_2$  = 9.8 Å

II. Estimation of the Mean Free Path

From the kinetic theory of gases,

$$L = kT / (\sqrt{2}\pi P \delta^2)$$

where,

k = Boltzmann constant,  $1.381 \cdot 10^{-23}$  J/K

T = temperature, 353 K

$\delta$  = molecular diameter,  $9.8 \cdot 10^{-10}$  m

P = acid pressure, Pa

The decanoic acid adsorption experiments were performed over an adsorbate pressure range of 0.001 to 0.100 torr (0.133 to 13.3 Pa). Using Eq. (1), the

mean free path in this pressure range will vary between 0.086 and 8.6 mm. This mean free path range is less than the average diameter of the glass tubing in the adsorption apparatus (12 mm), inferring that the equilibrium pressure in the sample chamber will be equal to the vapor pressure of the acid in the acid reservoir (95). The actual mean free path will probably be even smaller due to other gases within the adsorption system.

APPENDIX II

DECANOIC ACID MONOMER/DIMER EQUILIBRIUM IN VAPOR PHASE AT 70°C

From the thermodynamic relationship:

$$-RT \ln K_{eq} = \Delta G = \Delta H - T\Delta S \quad (33)$$

the monomer/dimer equilibrium constant can be determined, given  $\Delta H$  and  $\Delta S$ .

Allen and Caldvin (50) have calculated  $\Delta H$  and  $\Delta S$  for the lower molecular weight fatty acids ( $C_1-C_4$ ). With reference to a standard atmosphere:

$$\Delta H = 14 \text{ kcal/mol}$$

$$\Delta S = 35 \text{ cal/K mol}$$

There is no apparent change in these quantities with varying chain length.

Using these values and Eq. (33), the equilibrium constant,  $K_{eq}$ , at 70°C is:

$$K_{eq} = 0.0535$$

At equilibrium,

$$(p_m)^2 = K_{eq}(p_d) \quad (34)$$

where,  $p_m$  and  $p_d$  are the partial pressures of the monomer and dimer in atmospheres.

Since  $p_m + p_d = p_o$  ( $p_o$  = acid vapor pressure), Eq. (34) can be rewritten:

$$p_m^2 + K_{eq}p_m - K_{eq}p_o = 0 \quad (35)$$

As two examples, consider acid vapor at 0.001 and 0.100 torr at 70°C. This would correspond to relative pressures of 0.021 and 2.1. Substituting the appropriate values for the pressure (atmospheres) and equilibrium constant (0.0535) into Eq. (35) yields:

0.001 torr : 0.0024% dimer

0.100 torr : 0.24% dimer

APPENDIX III

DECANOIC ACID MOLECULAR AREA

The following are calculations for the molecular area of decanoic acid when it assumes a parallel orientation on an adsorbent surface. Assumptions in this calculation are

1. The density of the adsorbed layer is equivalent to the liquid molar density at 80°C.
2. The adsorbed acid can be approximated by a cylinder of length equal to the molecular length determined from acid/water monolayer studies.
3. The molecular area is equal to the projected area of the adsorbed cylinder.

liquid molar volume, $V_m$ (108)	201.80 cm <sup>3</sup> /mol
molecular volume, $v_m = (V_m/N) \times 10^{20}$	335 Å <sup>3</sup> /molecule
molecular length, h [extrapolation of data from monolayer studies on C <sub>14</sub> , C <sub>18</sub> , and C <sub>22</sub> (107)]	15.95 Å
molecular diameter, $\delta = \sqrt{4v_m/\pi h}$	5.17 Å
adsorbate molecular area	
parallel orientation	82.5 Å
perpendicular orientation (109)	20.5 Å

APPENDIX IV

PROGRAM BET

C-  
C-  
C- USING THE MICROMERITICS ACCUSORB GAS ADSORPTION INSTRUMENT,  
C- ADSORPTION DATA IS PLOTTED ON THE CALCOMP 1012 PLOTTER IN THE  
C- FORM OF THE BET ISOTHERM. A LEAST SQUARES LINE IS CALCULATED  
C- ON THE CHOSEN PORTION OF THE DATA AND THE BET SURFACE AREA AND  
C- C CONSTANT ARE CALCULATED. FOR MORE INFORMATION ON THE  
C- CALCULATIONS SEE THE MICROMERITICS MANUAL. SUBROUTINE  
C- "AXES" (LISTED AT END OF THIS PROGRAM) IS NEEDED FOR  
C- OPERATION OF THIS PROGRAM. THE VARIABLES IN THE PROGRAM  
C- DEFINED AS FOLLOWS:

C-  
C-       ADS: ADSORBATE (KRYPTON OR NITROGEN)  
C-       ALPH: CORRECTION FOR THE IDEAL GAS LAW  
C-       BOR: L(ARGE) IF LARGE BORE SAMPLE TUBES WERE USED  
C-       C1: THE BET C CONSTANT, RELATED TO HEAT OF ADSORPTION  
C-       H1: INITIAL HE PRESSURE FOR DEAD SPACE ANALYSIS, TORR  
C-       H2: FSIS  
C-       P1(I): INITIAL PRESSURE DURING EXPERIMENT  
C-       P2(I): FINAL PRESSURE DURING EXPERIMENT  
C-       PE: EQUILIBRIUM PRESSURE  
C-       PS: ADSORBATE SATURATION PRESSURE, TORR  
C-       S: ADSORBATE MOLECULAR CROSS-SECTIONAL AREA  
C-       SW: SURFACE AREA, M2/G  
C-       TI: INTERMEDIATE TEMPERATURE, K  
C-       TS: ADSORPTION TEMPERATURE, K  
C-       V(I): VOLUME ADSORBED ML AT STP  
C-       VS: DEAD SPACE, ML AT STP  
C-       W1: WEIGHT OF SAMPLE AND SAMPLE TUBE, G  
C-       W2: WEIGHT OF SAMPLE TUBE, G  
C-       WS: WEIGHT OF SAMPLE, G  
C-       X1: EXTRA VOLUME, ML  
C-       XV: Y(ES) IF EXTRA VOLUME WAS USED  
C-       X(I): BET X VARIABLE, P/PO  
C-       Y(I): BET Y VARIABLE, P/(V(PO/P))

C-  
C- \$RESET FREE  
C- FILE 5(KIND=DISK,TITLE="BET/DATA",FILETYPE=7)  
C- FILE 7(KIND=REMOTE,MAXRECSIZE=321,MYUSE=IO)  
C- FILE 6(KIND=PRINTER)  
C- \$INCLUDE "CALCOMP/1012"  
C- \$INCLUDE "AXES"  
C-       DIMENSION X(30),Y(30),XCALC(30),YCALC(30),P1(30),P2(30),V(30)  
C-       DIMENSION SW(2),C1(2)  
C-       REAL INT  
C-       INTEGER DESIG(5),DATE(2),READY  
C-       INTEGER Z/'N'/,K/'K'/,L/'L'/

C-  
C- SCREEN FORMATTING CODES

IFF=12  
ILF=10  
IBV=26  
IHC=20  
IRV=14  
IETX=3  
ILEFT=31  
ILEFTR=29  
IRIGHT=30  
IDC2=18

C-  
C- SCREEN FORMATTING AND READING OF INPUT VARIABLES  
C-

28 WRITE(7,1000) IFF, ILEFT, IRIGHT, ILEFT, IRIGHT, ILEFT, IRIGHT,  
\* ILEFT, IRIGHT, ILEFT, IRIGHT, ILEFT, IRIGHT,  
\* ILEFT, IRIGHT, ILEFT, IRIGHT, ILEFT, IRIGHT  
WRITE(7,1001) IDC2, IETX  
READ(7,1002) ADS, W1, W2, H1, H2, TS, XV, BOR, N  
WRITE(7,1003) IFF, ILF, IETX  
WRITE(7,1004) IBV, ILF, ILF  
DO 25 I=1, N  
25 WRITE(7,1005) IBV, ILEFT, IRIGHT, ILEFT, IRIGHT, ILF  
WRITE(7,1006) ILF, ILEFT, IRIGHT  
WRITE(7,1007) IDC2, IETX  
READ(7,1008) (P1(I), P2(I), I=2, N+1)

C-  
IF (ADS.EQ.K) GO TO 4

C-  
C- SETUP OF PARAMETERS FOR NITROGEN ADSORPTION  
C-

PS=EXP(-694/TS + 15.61)  
ALPH=0.000066  
S=16.2  
GO TO 7

C-  
C- SETUP OF PARAMETERS FOR KRYPTON ADSORPTION  
C-

4 PS = EXP(-1336/TS +18.18)  
ALPH=0.000030  
S=21.0

C-  
C- CALCULATION OF INTERMEDIATE VOLUME AND TEMPERATURE  
C-

7 TI=(307.2+TS)/2  
IF (BOR.EQ.L) GO TO 5  
VI=3.65  
GO TO 8  
5 VI=6.99

C-  
C- CALCULATION OF DEAD SPACE

```
C-
8 VS=(TS/H2)*((28.99*(H1-H2)/307.2)-(VI*H2/TI))
  IF (XV.EQ.Z) GO TO 9
  X1=131.3
  GO TO 6
9 X1=0.0
```

```
C-
C-          CALCULATION OF BET VARIABLES
C-
```

```
6 WS = W1-W2
  V(1)=0.0
  P2(1)=0.0
  A=0.001169*(28.99+X1)/WS
  B=((0.3593*VS)/(TS*WS))+(.359*VI/(TI*WS))
  C=(0.3593*VS*ALPH)/(WS*TS)
  DO 3 I=2,N+1
    PE=P2(I-1)
    D=P1(I)-P2(I)
    E=P2(I)-PE
    F=P2(I)**2-PE**2
    G=A*D
    H=B*E
    DLJ=C*F
    DLK=G-H-DLJ
    V(I)=V(I-1)+DLK
    X(I)=P2(I)/PS
  3 Y(I)=X(I)/(V(I)*(1.0-X(I)))
  NF=1
  NL=N
  DO 10 I=1,N
    X(I)=X(I+1)
    V(I)=V(I+1)
10 Y(I)=Y(I+1)
```

```
C-
C-          REGRESSION ANALYSIS
C-
```

```
55 NX=NL-NF+1
  SUMX=0
  SUMY=0
  SUMXY=0
  SUMXSQ=0
  DO 11 I=NF,NL
    SUMX=SUMX+X(I)
    SUMY=SUMY+Y(I)
    SUMXY=SUMXY+X(I)*Y(I)
11 SUMXSQ=SUMXSQ+X(I)**2
  SLOPE=((NX*SUMXY)-(SUMX*SUMY))/((SUMXSQ*NX)-(SUMX**2))
  INT=(SUMY-SUMX*SLOPE)/NX
  DO 20 I = 1,NX
    XCALC(I)=X(I-1+NF)
20 YCALC(I)=INT+SLOPE*X(I-1+NF)
```

```
C-
C-          CALCULATING SURF. AREA AND BET C CONSTANT
```

C-

```
SW1=(0.2687*S)/(SLOPE+INT)
C1(1)=.2687*S/(SW1*INT)
E1=1.987*TS*ALOG(C1(1))
WRITE(7,1009)IFF,SW1
WRITE(SW,1043)SW1
WRITE(SW,1044)SW
WRITE(C1,1043)C1(1)
WRITE(C1,1044)C1
```

C-

PLOT ALTERNATIVE

C-

C-

```
WRITE(7,1010)ILEFTR,IRIGHT,IDC2,IETX
READ(7,1011)PLO
IF (PLO.EQ.Z) GO TO 29
WRITE(7,1041)IFF,IBV,ILF,ILF,ILF,ILF,ILF,ILEFTR,IRIGHT,
*IDC2,IETX
READ(7,1042)READY
CALL GRAF(X,Y,XCALC,YCALC,N,SW,NF,NL,NX,C1,NPLOT)
```

C-

REGRESSION RANGE ALTERNATIVE

C-

C-

```
29 WRITE(7,1012)IFF,ILF,ILEFTR,IRIGHT,IDC2,IETX
READ(7,1013)NFNL
IF (NFNL.EQ.Z) GO TO 60
WRITE(7,1014)IFF,ILEFTR,IRIGHT,ILF
WRITE(7,1015)ILEFTR,IRIGHT,ILF
WRITE(7,1016)ILEFTR,IRIGHT,IDC2,IETX
READ(7,1017)NF,NL
GO TO 55
```

C-

HARD COPY ALTERNATIVE

C-

C-

```
60 WRITE(7,1020)IFF,ILF,IETX
WRITE(7,1021)ILEFT,IRIGHT,IDC2,IETX
READ(7,1022)HC
IF (HC.EQ.Z) GO TO 41
WRITE(7,1023)IFF,ILF,IETX
WRITE(7,1024)ILEFT,IRIGHT,ILF
WRITE(7,1025)ILEFTR,IRIGHT,IDC2,IETX
READ(7,1026)DESIG,DATE
WRITE(6,1027)DESIG,DATE
WRITE(6,1028)WS
IF (ADS.EQ.K) GO TO 32
WRITE(6,1029)
GO TO 33
32 WRITE(6,1030)
33 WRITE(6,1031) TS
WRITE(6,1032) VS
IF (XV.EQ.Z) GO TO 34
WRITE(6,1033)
GO TO 35
34 WRITE(6,1034)
```

```
35 WRITE(6,1035) SW1
   WRITE(6,1045) E1
   WRITE(6,1038)SLOPE
   WRITE(6,1039)INT
   WRITE(6,1036)
   DO 36 I = 1,N
36 WRITE(6,1037) X(I),V(I),Y(I)
   WRITE(6,1040)NF,NL
1043 FORMAT(1PE9.3)
1044 FORMAT(2A6)
1045 FORMAT(5X,'E1 - EL = ',1PE9.3,' CAL/MOL',/)
C-
C-          RUN AGAIN ALTERNATIVE
C-
41 WRITE(7,1018)IFF,ILEFTR,IRIGHT,IDC2,IETX
   READ (7,1019) RERUN
   IF (RERUN.EQ.Z) GO TO 31
   GO TO 28
31 IF (NPLOTT) 43,43,42
42 CONTINUE
   CALL PLOT(0.0,0.0,999)
43 STOP
C-
C-
1000 FORMAT(1X,C1,30X,'PROGRAM BET',
  *133X,'KRYPTON OR NITROGEN ADSORPTION, K OR N',4X,C1,1X,C1,
  *115X,'WEIGHT OF SAMPLE AND TUBE, W1',6X,C1,8X,C1,
  *115X,'WEIGHT OF SAMPLE TUBE, W2',10X,C1,8X,C1,
  *115X,'INITIAL HE PRESSURE, H1',12X,C1,8X,C1,
  *115X,'FINAL HE PRESSURE, H2',14X,C1,8X,C1,
  *115X,'ADSORPTION TEMPERATURE, TS',9X,C1,8X,C1,
  *115X,'EXTRA VOLUME USED, Y OR N',10X,C1,1X,C1,
  *122X,'BORE OF SAMPLE TUBE, L OR S',8X,C1,1X,C1,
  *122X,'NUMBER OF DATA SETS',16X,C1,2X,C1)
1001 FORMAT(1X,2C1)
1002 FORMAT(A1,5E8.4,2A1,I2)
1003 FORMAT(1X,3C1)
1004 FORMAT(28X,2C1,'P1',16X,'P2',2C1)
1005 FORMAT(25X,2C1,6X,C1,10X,C1,6X,2C1)
1006 FORMAT(/,25X,C1,'TRANSMIT FROM HERE 'C1,1X,C1)
1007 FORMAT(1X,2C1)
1008 FORMAT(40F6.4)
1009 FORMAT(1X,C1,'SURFACE AREA = ',F8.4,' M2/G',/)
1010 FORMAT(1X,'DO YOU WISH TO PLOT THE DATA (Y OR N)?',C1,1X,3C1)
1011 FORMAT(A1)
1012 FORMAT(1X,2C1,'CHANGE THE REGRESSION ANALYSIS RANGE (Y OR N)?'
  *C1,1X,3C1)
1013 FORMAT(A1)
1014 FORMAT(2X,C1,'FIRST DATA SET NUMBER IN REGRESSION 'C1,2X,2C1)
1015 FORMAT(1X,'LAST DATA SET NUMBER IN REGRESSION ' C1,2X,2C1,/)
1016 FORMAT(13X,'TRANSMIT FROM HERE 'C1,1X,3C1)
1017 FORMAT(2I2)
1018 FORMAT(1X,C1,'DO YOU WISH TO RUN PROGRAM AGAIN (Y OR N)? '
```

```
*C1,1X,3C1)
1019 FORMAT(A1)
1020 FORMAT(1X,3C1)
1021 FORMAT(1X,'HARDCOPY OF RESULTS (Y OR N)? ',C1,1X,3C1)
1022 FORMAT(A1)
1023 FORMAT(1X,3C1)
1024 FORMAT(1X,'SAMPLE DESIGNATION ',C1,30X,2C1)
1025 FORMAT(15X,'DATE ',C1,12X,3C1)
1026 FORMAT(7A6)
1027 FORMAT('1',/,/,/,10X,5A6,10X,2A6,/,/)
1028 FORMAT(5X,'SAMPLE WEIGHT = ',F8.4,' GRAMS')
1029 FORMAT(5X,'ADSORBATE = NITROGEN')
1030 FORMAT(5X,'ADSORBATE = KRYPTON')
1031 FORMAT(5X,'ADSORPTION TEMPERATURE = ',F5.2,' K')
1032 FORMAT(5X,'DEAD SPACE = ',F8.4,' ML AT STP')
1033 FORMAT(5X,'EXTRA VOLUME = 131.3 ML',/)
1034 FORMAT(5X,'EXTRA VOLUME WAS NOT USED',/)
1035 FORMAT(5X,'SURFACE AREA = ',1PE9.3,' M2/G')
1036 FORMAT(1X,'RELATIVE PRESSURE, MM HG',5X,'VOLUME ADSORBED, ML AT
*STP',10X,'Y',/)
1037 FORMAT(5X,F8.4,21X,F8.4,19X,F8.4)
1038 FORMAT(9X,'SLOPE = ',F8.4)
1039 FORMAT(9X,'INTERCEPT = ',F8.4,/,/)
1040 FORMAT(/,1X,'REGRESSION BETWEEN POINTS',I3,' AND',I3,)
1041 FORMAT(1X,7C1,'READY PLOTTER WITH THE PEN OVER PERFORATION INTE'
*'RSECTION ON THE RIGHT SIDE, THEN TRANSMIT',C1,1X,3C1)
1042 FORMAT(I1)
END
```

C-  
C-

```
SUBROUTINE GRAF(X,Y,XCALC,YCALC,N,SW,NF,NL,NX,C1,NPLOT)
DIMENSION X(30),Y(30),XCALC(30),YCALC(30),SW(2),C1(2)
INTEGER HEAD1(5),HEAD2(5),NUM
```

C-  
C-

SCREEN FORMATTING CODES

```
ILF=10
ILEFTR=29
IRIGHT=30
IDC2=18
IETX=3
IFF=12
ILEFT=31
```

C-  
C-  
C-

SETTING UP PLOT TITLE AND FIGURE NUMBER

```
WRITE(7,1003)IFF,ILF,IETX
WRITE(7,1000)ILEFT,IRIGHT
WRITE(7,1001)ILEFT,IRIGHT
WRITE(7,1004)ILEFTR,IRIGHT,IDC2,IETX
READ(7,1002)HEAD1,HEAD2,NUM
```

C-  
C-  
C-

PLOTTING ROUTINE

```
IF (NPLOT) 10,10,20
10 NPLOT = 1
CALL PLOTS(0,0,99)
20 CALL PLOT(1.0,1.0,-3)
CALL SCALE(X,7.0,N,1)
CALL SCALE(Y,9.0,N,1)
CALL AXES(0.0,0.0,4HP/PO,-4,7.0,0.0,X(N+1),X(N+2),0.12)
CALL AXES(0.0,0.0,11HP/(V(PO-P)),11,9.0,90.0,Y(N+1),Y(N+2),0.12)
XCALC(NX+1)=X(N+1)
XCALC(NX+2)=X(N+2)
YCALC(NX+1)=Y(N+1)
YCALC(NX+2)=Y(N+2)
WRITE(SW,1005)SW
WRITE(C1,1005)C1
CALL LINE(X,Y,N,1,-1,1)
CALL LINE(XCALC,YCALC,NX,1,0,5)
CALL SYMBOL(1.0,8.2,.10,7HFIGURE ,0.0,7)
CALL NUMBER(999,8.2,.10,NUM,0.0,0)
CALL SYMBOL(2.10,8.2,.10,19HB.E.T. SURFACE AREA,0.0,19)
CALL SYMBOL(1.0,8.0,.10,HEAD1,0.0,30)
CALL SYMBOL(1.0,7.8,.10,HEAD2,0.0,30)
CALL SYMBOL(1.0,7.6,.10,15HSURFACE AREA = ,0.0,15)
CALL SYMBOL(999.0,7.6,.10,SW,0.0,10)
CALL SYMBOL(999,7.6,.10,1HM,0.0,1)
CALL SYMBOL(999.,7.7,.07,1H2,0.0,1)
CALL SYMBOL(999.,7.6,.10,2H/G,0.0,2)
CALL SYMBOL(1.0,7.4,.10,4HC = ,0.0,4)
CALL SYMBOL(999.0,7.4,.10,C1,0.0,9)
C-
C-      SETUP FOR MARKING 1ST AND LAST POINTS IN REGRESSION
C-
XMARKF=(X(NF)-X(N+1))/X(N+2)
XMARKL=(X(NL)-X(N+1))/X(N+2)
YMARKF=(Y(NF)-Y(N+1))/Y(N+2)+.1
YMARKL=(Y(NL)-Y(N+1))/Y(N+2)+.1
CALL SYMBOL(XMARKF,YMARKF,.07,2HS ,0.0,2)
CALL SYMBOL(XMARKL,YMARKL,.07,2HF ,0.0,2)
CALL SYMBOL(5.,.5,.07,26HREGRESSION BETWEEN S AND F,0.,26)
CALL PLOT(7.5,-1.0,-3)
RETURN
C-
C-
1000 FORMAT(1X,'TITLE OF PLOT',1X,C1,30X,C1)
1001 FORMAT(15X,C1,30X,C1)
1002 FORMAT(5A6,5A6,I2)
1003 FORMAT(1X,3C1)
1004 FORMAT(1X,'FIGURE NUMBER 'C1,2X,3C1)
1005 FORMAT(2A6)
END
```

```
C-
C-          SUBROUTINE AXES - A MODIFIED VERSION OF THE
C-          CALCOMP/1012 SUBROUTINE AXIS
C-
SUBROUTINE AXES(XPAGE,YPAGE,IBCD,NCHAR,AXLEN,ANGLE,FIRSTV,
IDELTAV,AXHT)
DIMENSION IBCD(2)
KN=NCHAR
A = 1.0
IF (KN) 1,2,2
1 A = -A
KN = -KN
2 EX = 0.0

C-
C-          SET EXPONENT SUCH THAT DELTAV LIES BETWEEN 0.1 AND 100.0
C-
ADX=ABS(DELTAV)
IF (ADX) 3,7,3
3 IF (ADX-99.0) 6,4,4
4   ADX=ADX/10.0
   EX=EX+1.0
   GO TO 3
5   ADX=ADX*10.0
   EX=EX-1.0
6 IF (ADX-0.1) 5,7,7
7 ADX=10.0**(-EX) %SET ADX = AXIS VALUE CONVERSION FACTOR

C-
STH=ANGLE*0.0174533 %CONVERT ANGLE OF AXIS TO RADIANS
XVAL=FIRSTV*ADX %CONVERT INITIAL AXIS VALUE TO EXPONENT FORM
CALL SIGFI(XVAL,NSIG) %DETERMINE SIGFIG FOR INITIAL AXIS VALUE
ADX=DELTAV*ADX %DETERMINE DELTAV IN EXPONENTIAL FORM
CTH=COS(STH) %CTH = COSINE OF ANGLE OF ROTATION
STH=SIN(STH) %STH = SINE OF ANGLE OF ROTATION
DXB=-AXHT %AXHT = AXIS HEIGHT IN INCHES
DYB=(1.00*A-0.5)*0.8*AXHT %DETERMINE AXIS HEIGHT FOR Y-COMPONEN
XN=XPAGE-DYB*STH %POSITION OF XVAL ON PLOT, X-DIRECTION
YN=YPAGE+DYB*CTH %POSITION OF XVAL ON PLOT, Y-DIRECTION
NTIC=AXLEN+1.0 %NUMBER OF TIC MARKS ON AXIS
NT=NTIC/2
DO 20 I=1,NTIC
IF (I-ISTEP*2) 70,71,70 %CALL NUMBER FOR EVERY OTHER AXIS VALUE
70 ISTEP = ISTEP + 1
CALL NUMBER(XN,YN,AXHT*0.8,XVAL,ANGLE,NSIG)
71 XVAL=XVAL+ADX %CALCULATE NEXT AXIS VALUE
CALL SIGFI(XVAL,NSIG) %DETERMINE SIGFIG FOR NEXT AXIS VALUE
XN=XN+CTH %CALCULATE NEW PEN POSITION FOR NEXT AXIS VALUE
YN=YN+STH
IF (NT)20,11,20
11 Z=XN
IF (EX) 12,13,12 %GO TO 12 IF THERE IS AN EXPONENT
C-          ASSOCIATED WITH THE AXIS VALUE
12 DXB = AXLEN*0.5-(KN/2)*AXHT-AXHT*3 %X-COMPONENT FOR AXIS
C-          TITLE WITH EXPONENT
GO TO 15
```

```
13 DXB = AXLEN*0.5-(KN/2)*AXHT %AXIS TITLE X-COMPONENT WHEN THER
C- IS NO EXPONENT WITH AXIS VALUE
15 DYB=(2.7*A-0.5)*AXHT %AXIS TITLE Y-COMPONENT
XT=XPAGE+DXB*CTH-DYB*STH %X AND Y POSITION FOR AXIS TITLE
YT=YPAGE+DYB*CTH+DXB*STH
CALL SYMBOL(XT,YT,AXHT,IBCD(1),ANGLE,KN)
C-
C- IF AXIS VALUE HAS AN EXPONENT, PRINT EXPONENT IN AXIS TITLE
C-
IF (EX) 14,20,14
14 Z=KN+2
XT=XT+Z*CTH*AXHT
YT=YT+Z*STH*AXHT
CALL SYMBOL(XT,YT,AXHT,4H(*10,ANGLE,4)
XT=XT+(4.0*CTH-0.6*STH)*AXHT
YT=YT+(4.0*STH+0.6*CTH)*AXHT
CALL NUMBER(XT,YT,0.66*AXHT,-EX,ANGLE,-1)
XT = 999*CTH + 0.6*STH*AXHT + XT*STH
YT = 999*STH - 0.6*CTH*AXHT + YT*CTH
CALL SYMBOL(XT,YT,AXHT,2H) ,ANGLE,2)
20 NT=NT-1
C-
C- DRAW AXIS ROUTINE
C-
CALL PLOT(XPAGE+AXLEN*CTH,YPAGE+AXLEN*STH,3) %FIND AXIS ORIGIN
DXB=-AXHT*0.66*A*STH %X-COMPONENT OF TIC MARK HEIGHT
DYB=AXHT*0.66*A*CTH %Y-COMPONENT OF TIC MARK HEIGHT
A=NTIC-1
XN=XPAGE+A*CTH
YN=YPAGE+A*STH
DO 30 I=1,NTIC
CALL PLOT(XN,YN,2)
CALL PLOT(XN-DXB,YN-DYB,2)
CALL PLOT(XN,YN,2)
XN=XN-CTH
YN=YN-STH
30 CONTINUE
RETURN
END
```

```
C-
C- SUBROUTINE SIGFI - DETERMINATION OF SIGNIFICANT
C- FIGURES FOR AXIS VALUES
C-
SUBROUTINE SIGFI(XVAL,NSIG)
XVAL1 = ABS(XVAL)
IF (XVAL1-100.00) 1,2,2 %IF XVAL > OR = 100, THEN NO DECIMAL PT
2 NSIG = -1
GO TO 7
1 IF (XVAL1-10.0) 3,4,4 %IF XVAL > OR = 10, THEN ONE SIGFIG
4 NSIG=1
GO TO 7
3 IF (XVAL1-1.0) 5,6,6 %IF XVAL > OR = 1.0, THEN TWO SIGFIG
6 NSIG=2
```

```
GO TO 7
5 IF (XVAL1) 8,9,8      %IF XVAL = ZERO, THEN NO DECIMAL PT.
9 NSIG = -1
GO TO 7
8 NSIG=3
7 CONTINUE
RETURN
END
%END.
```